ROLE OF PROTEIN KINASE C-GAMMA IN THE REGULATION OF LENS GAP JUNCTIONS

by

SATYABRATA DAS

M.Sc., Orissa University of Agriculture and Technology, Orissa, India, 2002

AN ABSTRACT OF A DISSERTATION

submitted in partial fulfillment of the requirements for the degree

DOCTOR OF PHILOSOPHY

Department of Biochemistry
College of Arts and Sciences

KANSAS STATE UNIVERSITY
Manhattan, Kansas

2009

Abstract

The avascular lens tissue depends on the gap junction channels to facilitate intercellular communication for supplying cells deep within the lens with nutrients and removing waste products of cellular metabolism. In the absence of the protein synthesis machinery in the inner lens fiber cells, the proper regulation of gap junction channels becomes extremely important as disturbance of the lens homeostasis can lead to cataract development. Phosphorylation of gap junction subunit connexin proteins has been shown to play an important channel-modulating role in a variety of tissue. Protein kinase C-γ (PKCγ) has been implicated in the phosphorylation of connexins in the lens. Here the role of PKCγ in the regulation of gap junction coupling in the mouse lens has been investigated. We have compared the properties of coupling in lenses from wild type (WT) and PKCγ knockout (KO) mice. Western blotting, confocal immunofluorescence microscopy, immunoprecipitation, RT-PCR and quantitative real time PCR were used to study gap junction protein and message expression; gap junction coupling conductance and pH gating were measured in intact lenses using impedance studies. PKCγ was found to regulate the amount and distribution of Cx43 in the lens. Gap junction coupling conductance in the differentiating fibers (DF) of PKCγ KO lenses was 34% larger than that of WT. In the mature fiber (MF), the effect was much larger with the KO lenses having an 82% increase in coupling over WT. Absence of PKCγ in the KO mice also caused abnormal persistence of nuclei in the typical nucleus-free region in the DF. These results suggest a major role for PKCγ in the regulation of gap junction expression and coupling in the normal lens mediated by phosphorylation of the lens connexins. This becomes very vital in the diabetic lenses which contain a depleted amout of PKCγ and people suffering from spinocerebellar ataxia type-14 (SCA14) who have a mutated inactive form of PKCγ. Prolonged exposure of lenses to oxidative stress in these patients can lead to cataract formation.

In cultured human lens epithelial cells (HLECs), 12-*O*-tetradecanoylphorbol-13-acetate (TPA) stimulated the depletion of Cx43 protein level via PKC-mediated phosphorylation of Cx43. At the same time Cx46 protein and message levels were upregulated in response to TPA treatment. So, the PKC activator regulates Cx43 and Cx46 in opposing ways. The possible mitochondria localization of Cx46 reported here could help in finding the non-junctional roles for Cx46.

ROLE OF PROTEIN KINASE C-GAMMA IN THE REGULATION OF LENS GAP JUNCTIONS

by

SATYABRATA DAS

M.Sc., Orissa University of Agriculture and Technology, Orissa, India, 2002

A DISSERTATION

submitted in partial fulfillment of the requirements for the degree

DOCTOR OF PHILOSOPHY

Department of Biochemistry
College of Arts and Sciences

KANSAS STATE UNIVERSITY
Manhattan, Kansas

2009

Approved by:

Major Professor

Dolores J. Takemoto

Abstract

The avascular lens tissue depends on the gap junction channels to facilitate intercellular communication for supplying cells deep within the lens with nutrients and removing waste products of cellular metabolism. In the absence of the protein synthesis machinery in the inner lens fiber cells, the proper regulation of gap junction channels becomes extremely important as disturbance of the lens homeostasis can lead to cataract development. Phosphorylation of gap junction subunit connexin proteins has been shown to play an important channel-modulating role in a variety of tissue. Protein kinase C-γ (PKCγ) has been implicated in the phosphorylation of connexins in the lens. Here the role of PKCγ in the regulation of gap junction coupling in the mouse lens has been investigated. We have compared the properties of coupling in lenses from wild type (WT) and PKCγ knockout (KO) mice. Western blotting, confocal immunofluorescence microscopy, immunoprecipitation, RT-PCR and quantitative real time PCR were used to study gap junction protein and message expression; gap junction coupling conductance and pH gating were measured in intact lenses using impedance studies. PKCγ was found to regulate the amount and distribution of Cx43 in the lens. Gap junction coupling conductance in the differentiating fibers (DF) of PKCγ KO lenses was 34% larger than that of WT. In the mature fiber (MF), the effect was much larger with the KO lenses having an 82% increase in coupling over WT. Absence of PKCγ in the KO mice also caused abnormal persistence of nuclei in the typical nucleus-free region in the DF. These results suggest a major role for PKCγ in the regulation of gap junction expression and coupling in the normal lens mediated by phosphorylation of the lens connexins. This becomes very vital in the diabetic lenses which contain a depleted amout of PKCγ and people suffering from spinocerebellar ataxia type-14 (SCA14) who have a mutated inactive form of PKCγ. Prolonged exposure of lenses to oxidative stress in these patients can lead to cataract formation.

In cultured human lens epithelial cells (HLECs), 12-*O*-tetradecanoylphorbol-13-acetate (TPA) stimulated the depletion of Cx43 protein level via PKC-mediated phosphorylation of Cx43. At the same time Cx46 protein and message levels were upregulated in response to TPA treatment. So, the PKC activator regulates Cx43 and Cx46 in opposing ways. The possible mitochondria localization of Cx46 reported here could help in finding the non-junctional roles for Cx46.

Table of Contents

List of Figures

List of Tables

Acknowledgements

It's a great pleasure to thank the many individuals who have made this thesis possible. I would like to express my deepest gratitude and appreciation for my advisor, Dr. Dolores J. Takemoto, for her continuous guidance, support, and advice. Her enthusiasm and encouragement has helped me push my research in the right direction especially at times of uncertainty and doubt. During the time I have spent in her lab, I have had the opportunity to learn so much from her that I will forever remain indebted to her.

I would like to extend my gratitude to my committee members, Dr. Subbarat Muthukrishnan, Dr. Larry J. Takemoto and Dr. Michal Zolkiewski for agreeing to be on my committee. Their sincere suggestions and valuable insights about my work have been instrumental in significantly strengthening my work (improving the quality of my work).

I am grateful to Dr. Vladimir Akoyev, Dr. Michael Barnett and Dr. Dingbo Lin, past post-doctoral fellows in Dr. Takemoto's lab, my good friends and respected colleague for teaching me that with patience and perseverance, one can make anything work. It has been a wonderful experience working with Willard Lloyd and I'm grateful to him for helping me with the microscopy techniques.

I am thankful to Dr. Philine Wangemann and Joel D. Sanneman for letting me use the COBRE core confocal facility and the technical assistance provided in acquiring the confocal images.

I have had the pleasure to collaborate with individuals outside my lab and I would like to thank Dr. Richard T. Mathias of SUNY, New York for the fruitful results. I am also grateful to Dr. Duy Hua, Dept. of Chemistry, KSU for the collaborative work leading to the identification of a novel gap junction inhibitor.

Working in the Takemoto's lab has been a pleasure and also a lot of fun, thanks to my wonderful colleagues (past and present) who made this experience a very memorable one and one that I will cherish for a long time. In particular, I would like to thank Sushanth Gudlur for all his help and standing through thick and thin during stay at KSU.

To my wife, Snehalata, your patience, love and encouragement are few among many reasons that have kept me going. Most of all, thanks for being so understanding, especially

during the times when I spent more time in front of the computer or in the lab than with you. Finally, I wish to thank my parents for their constant love and support. I am grateful to them for having faith and confidence in me to carry out my doctoral research.

Dedication

To my beloved Parents.

Declaration

Unless otherwise mentioned in the figure legends, all figures are drawn/generated and experiments are performed by me.

Chapter 1 - Introduction and Literature Review

1.1. Introduction

The intricate needs of the mammalian body are achieved by a complex network of cells forming tissues and organs, which work in a coordinated way to perform specific functions required at specific parts in a specific time. These coordinated activities in the body help achieving the tissue homeostasis. Homeostasis, in the multi-cellular organism, is managed by three major communication processes: extracellular communications by hormones, growth factors, neurotransmitters and cytokines lead to intra-cellular communication via changes in the levels of second messages and activated signal transduction system eventually modulating intercellular communication mediated by gap junction channels (Trosko and Ruch, 1998). Intercellular communication is vital for the coordination of different cell types within a specific tissue and perhaps gap junctions, being membrane channels linking cytoplasms of adjacent cells, mediate the most direct form of intercellular communication. Gap junctions play critical roles in embryonic development, differentiation, growth, co-ordinated contraction of excitable cells, and diffusional feeding (Goodenough, 1996; Solan and Lampe, 2009). The ocular lens has been at the forefront of gap junction research as gap junction mediated communication has been shown to be essential for maintaining transparency in the avascular lens. Here I document my research trying to understand the regulation of gap junctions in the lens. In this section I review the lens structure and function, role played by the gap junctions in the lens, and finally the regulation of gap junction proteins by protein kinases in the lens.

1.2. The Eye: Anatomy and Function

The coordinating activity of the eye and brain together enables us to detect and interpret the information and surroundings from the visible light range reaching the eye; resulting in the perception called the sight or vision. Among all the senses known, sight is arguably the most important one as it provides the information for coordinating movement and creating a tangible representation of the world around us. Vision is a complicated process that requires the translation of the incoming external light into a form that can be interpreted by our brains by the complex and amazing organ of sight known as the eye.

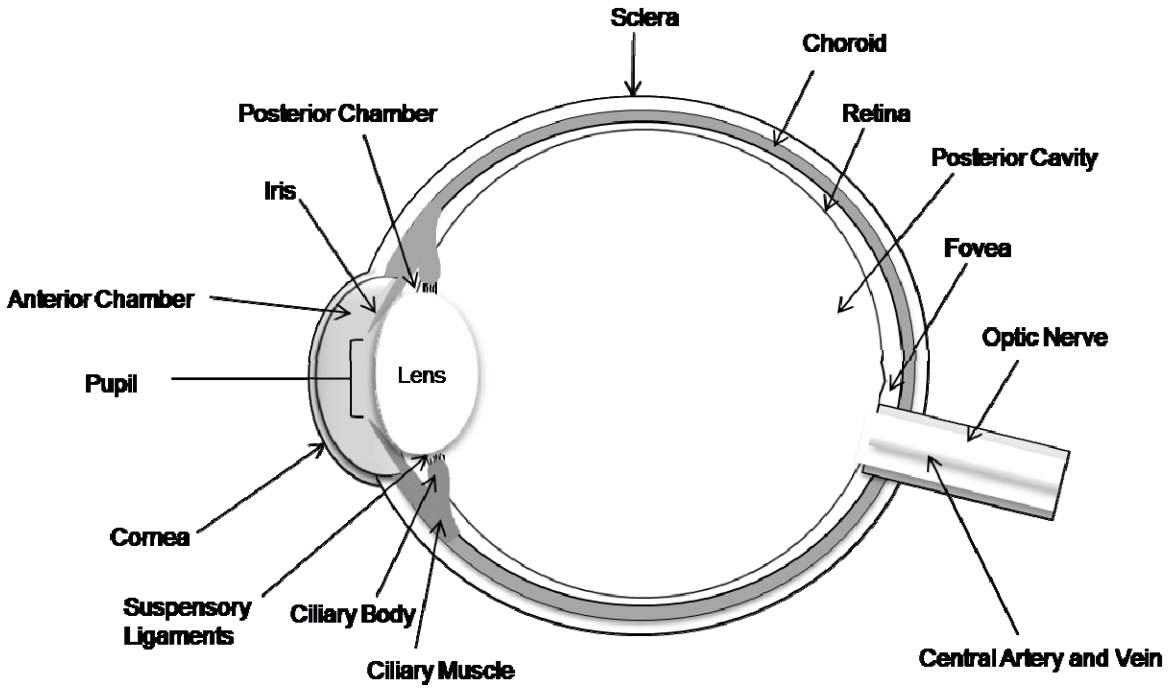

Figure 1.1 Structural Organization of the Eye

The spherical-shaped eye is often compared to a camera as both gather light and transform it into a picture. The eye is divided into anterior and posterior cavities separated by the lens and the surrounding suspensory ligaments (Figure 1.1). The outermost coat of the eye is composed of the sclera and cornea. Both tissues consist mainly of a densely woven collagen fiber which makes the tissues rigid and acts as a protective cover for the more delicate inner layers. Whereas the white sclera is opaque, the transparent dome-shaped cornea covers the front of the eye. The cornea is the eye's principal refractive element owing its transparency to the regularity of its structural organization and an absence of vasculature.

The colored part of the eye is called the iris and the round opening in the center of the iris is called the pupil. The iris regulates the amount of light entering the eye like the aperture of a camera. The anterior cavity of the eye is further subdivided into the anterior and posterior chambers by the iris. The anterior cavity is filled with the watery aqueous fluid called the aqueous humor, whereas the posterior cavity is filled with the vitreous humor. Adjacent to the periphery of the iris is the ciliary body, consisting primarily of a circular ring of muscle called

the ciliary muscle. The ciliary body is continuous with the choroid, the main components of which are blood vessels.

The eye's innermost layer is the retina, performing the role of the photosensitive film of a camera for the eye. The retina captures the light rays that enter the eye and the resulting signals are transmitted to brain via the optic nerve. But the ocular structure is incomplete without the lens, which lies about a third way between the front and the back of the eye. Functionally, the lens provides about a third of the eye's total refractive power and also serves the purpose of altering focal distance via accommodation. As lens is the major organ of interest in this thesis, a more comprehensive description of the lens structure and function is discussed in the next section.

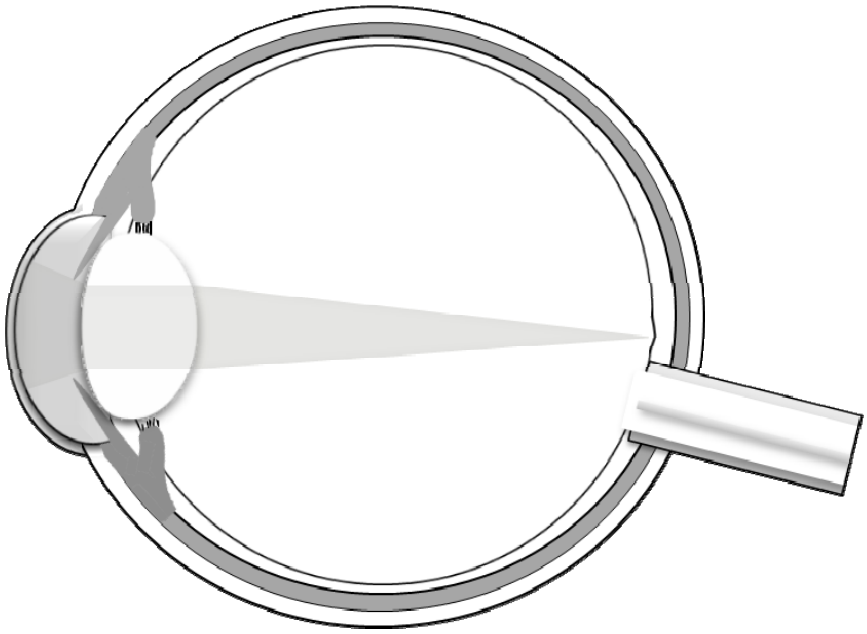

Figure 1.2 The Visual Light Path. Light, reflected from objects, enters the eye through the cornea. Refractive properties of the cornea, lens and vitreous humor bring the light rays to a sharp focus on the retina. At the retina, the light rays get converted to electrical impulses and get transmitted to the brain through the optic nerve. Images reach the retina upside down and are inverted and interpreted in an upright position by the brain.

1.2.1. The Path of Light through the Eye

The major function of the eye is to focus light onto the retina, where the light rays are converted to electrical impulses and transmitted to the brain via the optic nerve. Focusing light onto the

retina is a multistep process and starts when light rays reflected, from the object being looked at, onto the cornea. The light rays are bent, refracted and focused by the cornea, lens, and vitreous (Figure 1.2).

The lens' job is to make sure the rays come to a sharp focus on the retina and facilitate dynamic changes in focus. The focusing power of the lens is facilitated by the over-expression of the crystalline proteins and the ability to change shape and optical power to a certain extent in response to forces imposed on it by the ciliary muscle. This deformation of the lens is called accommodation.

1.3. The Structure of the Lens

The native structure of the lens is truly unique being a compact disc-shaped mass of protein-filled cells of a single lineage except for a solitary layer of cells. The lens resides in an exceptional habitat suspended in a watery fluid, the aqueous humor from the anterior side and the vitreous humor from the posterior side, and permanently deprived of contact with any other cell. The shape and size of the more commonly used lenses in research are asymmetrical, oblate, spheroids (Kuszak et al., 2004). The mouse lenses are the most spherical among the lenses studied, or the least asymmetrical, with the anterior half approximating one-half of a 45° spheroid and the posterior half approximating one-half of a 55° spheroid (Kuszak et al., 2004). However, the human lenses are more asymmetrical spheroids, with anterior and posterior halves approximating halves of a 15° and a 30° spheroid respectively (Albert and Jakobiec, 1994). The cellular parts of the lens are enclosed by the acellular lens capsule, which is tough yet porous and contains collagen fibrils (Figure 1.3A).

The anterior-posterior dimension of the lens is smaller than either its vertical or horizontal diameters. The lens can be described as having anterior and posterior surfaces separated by the equator. The geometric centers of the anterior and posterior surfaces are known as the anterior and posterior poles of the lens respectively (Oyster, 1999). The lens is composed of only two distinct types of cells: a monolayer of epithelial cells covering the anterior surface of the lens and a core of elongated, crystalline-rich fiber cells comprising the rest of the lens (Le and Musil, 1998). While the single layer of anterior epithelium covers the anterior surface of the lens, the posterior epithelium has disappeared early in the formation of the lens (Figure 1.3A).

1.3.1. The Epithelial Cells of the Lens

Although the lens is composed of only two types of cells, the lens can be divided into three broad regions based on the cellular organization: anterior epithelium, cortex and nucleus (Figure 1.3A). The anterior epithelium is the only source of new cells for the lens. The epithelial cells divide at the equator, elongate and differentiate into fiber cells in a region called the transitional zone or the bow region. The morphology of the epithelial cells differs from one location of the epithelium to another and the morphological variation is also associated with functional variation.

The Central Epithelium

The majority of epithelial cells, constituting the central zone or central epithelium, are present around the anterior pole. These cells are flattened and hexagonal in outline with their basal surface in contact with the capsule and the apical surface in contact with the fiber cells in the cortex (Oyster, 1999). The association of the epithelial cell apical surfaces with the apical surface of fiber cells extending from the posterior cells forms the epithelial-fiber interface (Zampighi et al., 2000; Kuszak, 1995). The central epithelial cells are usually non-proliferative, but can participate in the repair mechanism when the epithelium is damaged.

The Germinative Zone

Surrounding the central epithelium is an annulus of epithelial cells which are proliferative and differentiating known as the germinative zone. Cells in this zone are columnar in shape with their apical-basal axis being approximately five times longer than the lateral axis. Here the cells start to differentiate and begin to produce some of the crystallins (Oyster, 1999; Zampighi et al., 2000). This set of epithelial cells generates new cells for the lens, but they do not pile up more than one layer of cell which indicates that the cells continually migrate towards the equator (Oyster, 1999).

The Transitional Zone

The germinative zone is surrounded by an annulus of elongated cells called the transitional zone. Here the epithelial cells not only elongate and differentiate but also rotate so that their axes become parallel to the surface of the lens. These elongated cells go through cytodifferentiation,

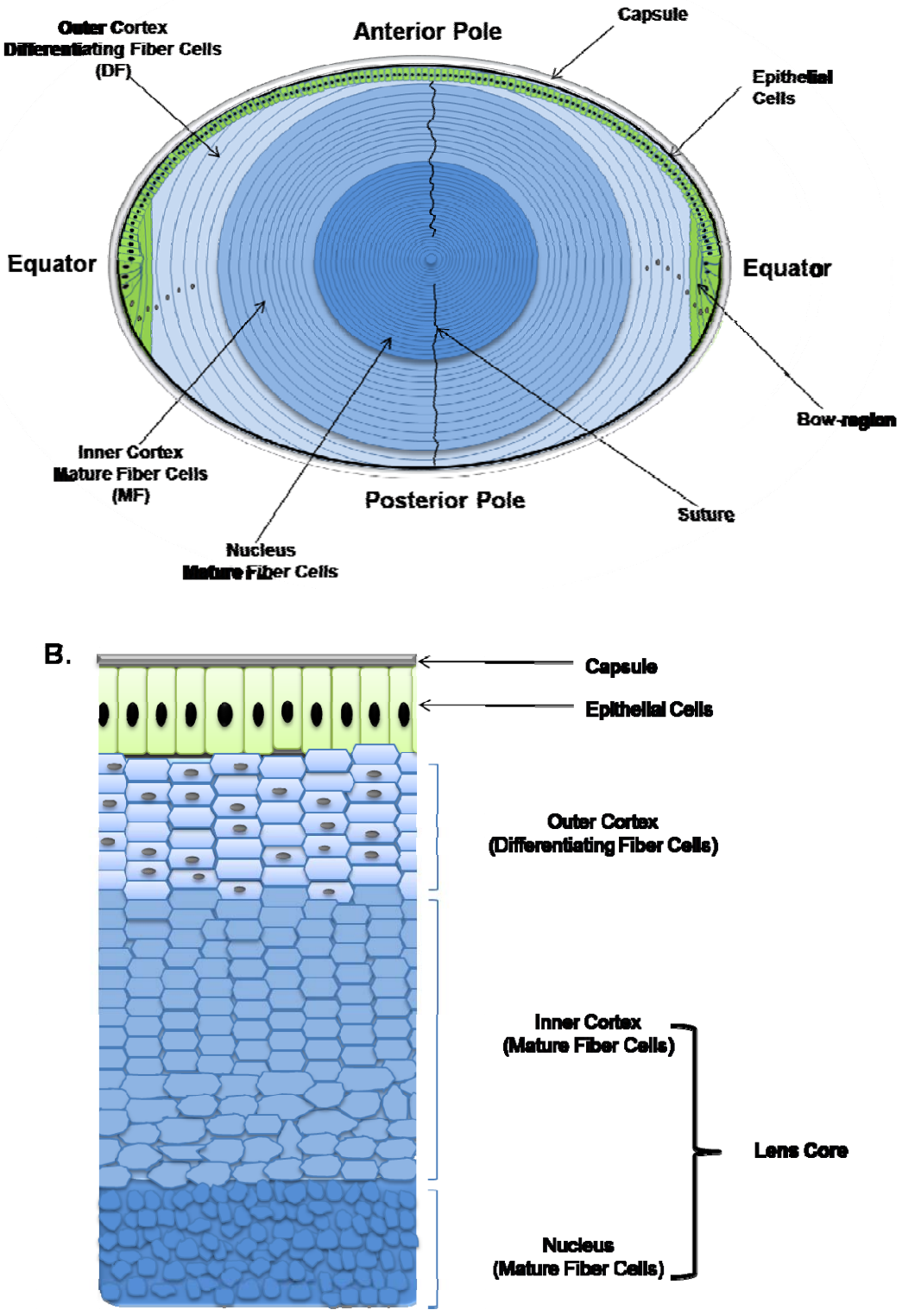

Figure 1.3 Cellular Organization of the Lens. A. Axial cross-section; **B.** Equatorial cross-section showing hexagonal fiber cells arranged into columns. (Based on a figure from Sisley, 2007)

which includes massive synthesis of crystallins and the degradation of the cellular organelles including nuclei (Kuszak, 1995; Oyster, 1999).

1.3.2. Lens Fiber Cells

Other than the one layer of epithelial cells on the anterior side, the rest of the lens is constructed of a series of concentric shells composed of long, thin fiber cells giving the lens an onion-like structure in its longitudinal section (Figure 1.3A). The lens grows inside out, adding new shells onto the existing structure resulting in the onion-like structure (Oyster, 1999). The fiber cells have a long flattened ribbon-like shape with a hexagonal cross-sectional profile. The lens fiber cells can be divided into two distinct regions: the nucleus and the cortex (Duke-Elder and Wyber, 1961). Lens fibers do not reach from pole to pole and meet along lines called lens sutures.

The Cortex

Although there is no anatomical division, roughly the outer third of the lens is considered as the cortex (Oyster, 1999). The cortex is the younger part of the lens, formed after sexual maturation, comprising of secondary fiber cells (Kuszak et al., 1988). The cortex can be further subdivided into outer cortex and inner cortex (Figure 1.3). The cortex consists of both the young differentiating fibers (DF) and the fully differentiated mature fibers (MF). The fiber cells at the posterior of the lens are the longest fiber cells of the lens with the apical and basal ends containing organelles (Zampighi et al., 2000). DF cells lose their nuclei, mitochondria, endoplasmic reticulum, golgi apparatus, and other organelles to become MF cells through the differentiation process (Bassnette and Beebe, 1992; and Bassnett, 1995).

The Nucleus

The inner, central part of the lens is the nucleus of the lens. This is also the oldest part of the lens and contains both primary fiber cells (the first group of cells to be transformed into fiber cells during embryological lens development) and secondary fiber cells (the germinative zone epithelial cells recruited to terminally differentiate into fiber cells) (Albert and Jakobiec, 1994; Kuszak, 1995). The nucleus can be subdivided into three separate parts: (1) the innermost embryonal nucleus (formed during the first three months of gestation) consisting solely of primer fiber cells; (2) the fetal nucleus (portion added until birth) consisting of the embryonic nucleus and all secondary fiber cells; and (3) the adult nucleus (portion added postnatally) consisting of

the embryonic and fetal nucleus along with secondary fiber cells arrayed in growth shells added onto the embryonic and fetal fiber cells until sexual maturation (Albert and Jakobiec, 1994; Oyster, 1999). So, some of the nuclear fiber cells, especially the primary fiber cells are as old as the human body. The nuclear fiber cells are the MF lacking membranous organelles and filled with crystallins. As the fiber cells age they begin to lose the hexagonal cross-sectional profile associated with the younger fiber cells and become more rounded (Figure 1.3B).

Another unique feature of the lens is that the size of the lens and the number of lens fibers continue to grow throughout life adding younger differentiating fiber cells on top of existing older fiber cells. Primate lenses measure ~6 mm in equatorial diameter at birth, and in 70+ years old human lenses this diameter increases to ~9.5 mm (Kuszak, 1995). In humans at birth there are ~1.7 million fiber cells and by the age of 20, this number grows to ~3.0 million fiber cells (Jaffe and Horwitz, 1992; Harding, 1997; Kuszak and Brown, 1994).

1.3.3. Lens Transparency

Transparency is the most important necessity for the lens to efficiently perform the role of focusing the light rays onto the retina at the back of the eye. Several structural and functional adaptations enable the lens in achieving its goal of bringing the light rays into a clear focus. An absence of vasculature, nerves, and a programmed loss of cellular organelles in the fiber cell differentiation process helps in the reduction of light scattering by the lens (Bassnett and Beebe, 1992; Bassnett, 1995). The loss of nuclei and the other organelles renders the inner cortex and nuclear cells transcriptionally inactive, making them rely on exceptionally stable proteins produced during the early stages of development and differentiation for the rest of their existence; rather than having mRNA with unusually long half-lives (Faulkner-Jones et al., 2003). A relatively high concentration protein (90% percent of the lens is protein, a higher percentage than any other tissue) helps the lens in achieving the necessary refractive power for the lens [lens contributes about one-third (~ 18 dioptres) of the eye's total dioptric power of ~ 60 dioptres)] (Oyster, 1999). Typical protein concentrations in the center of the lens are 450 mg/ml (Jaffe and Horwitz, 1992). At low protein concentrations, light scattering is proportional to the protein concentration, but when the protein concentration in the lens fibers is greater than ~10%, light scattering decreases dramatically with increase in protein concentration (Delaye and Tardieu, 1983; Bettelheim and Siew, 1983; Tardieu, 1998). The crystallin proteins comprise 90% of the

total lens protein mass (Hoehenwarter et al., 2006). Among the soluble protein fraction in the lens, a very high percent are the crystallins. The solubility and the compact globular structure of the crystallins permit their dense and uniform packing within the lens cells. This arrangement plays a significant role in lens transparency (Oyster, 1999). The thin long shape of the fiber cells with a hexagonal cross sectional profile facilitates the close packing of the cells into a columnar array that creates extracellular spaces smaller than the wavelength of light, further helping the unscattered passage of light through the lens.

Denatured and unfolded proteins tend to aggregate, and uncontrolled aggregation of proteins in the lens leads to light scattering. Among the crystallins, α-crystalline acting as a molecular chaperone recognizes and binds to the denatured proteins, and prevents the non-specific aggregation of proteins in the lens (Horwitz, 1992; Jakob et al., 1993; Derham and Harding, 1999; Bloemendal et al., 2004).

So, a combination of a variety of factors works in coordination to maintain the lens transparency. However, any compromise in the lens transparency, either due to change in refractive properties caused by lens cell swelling or shrinking or due to opacification of the lens cells caused by accumulation of protein aggregates (Hanson et al., 2000; Jacob, 1999), results in cataract or clouding of the lens. Cataract is the leading cause of blindness today. According to the World Health Organization report, the cause for 65% of the 45 million blind people in the world in 2000 was cataract, or other treatable refractive errors (World Health Organization, 2005).

A large number of factors can cause cataracts, including UV light (Davies and Truscott, 2001), oxygen, glycation as well as posttranslational modifications (Derham and Harding, 1999), poor nutrition (Taylor and Hobbs, 2001), diabetes (Kyselova et al., 2004), smoking (DeBlack, 2003), alcohol (Morris et al., 2004), radiation exposure (Ferrufino-Ponce and Henderson, 2006), certain chemicals (Kruse et al., 2005), and inherited gene mutations. However, ageing is the most common factor contributing to cataract (Hejtmancik and Kantorow, 2004; Truscott, 2005).

Fortunately, implantation of artificial lenses by surgery can be used to treat cataract. Although the surgery is relatively cheap and straightforward, huge numbers of people, particularly in developing countries, have to wait for the surgery, or might not even receive the opportunity. Therefore, finding non-surgical cheaper ways to prevent cataract could help in the

restoration of sight in many more people. To develop such methods, the lens physiology and homeostasis must be understood completely.

1.4. The Lens Circulation Model

There were doubts about lens being a 'living' tissue until the 1970s when intracellular microelectrode studies revealed a resting voltage and input resistance suggesting a spark of life (Rae et al., 1970; Rae, 1973; Eisenberg and Rae, 1976). Unlike the known lens cellular structure of today; in the past some speculated it to be a single giant cell (Duncan, 1969), while some others considered it to be a simple epithelium with anterior-posterior polarity (Kinsey and Reddy, 1965; Candia et al. 1970; and 1971). As already discussed in the lens structure section now we know that lens is a complex structure comprising of different types of cells and it is also an avascular organ as vasculature would interfere with the transparency and subsequently the focusing power of the lens. But this adaptation creates the unique problem of providing sufficient nutrients to the inner fiber cells and removing the metabolic waste to sustain the lens homeostasis. Diffusion alone would not be able to fulfill the requirements of the lens as mathematical modeling has predicted that it would take many hours for metabolites like glucose to reach the central fiber cells and glucose would only be able to reach the outer 8-10% of rat and rabbit lenses by diffusion before being metabolically depleted (Fischbarg et al. 1999).

Although the question of maintaining the lens homeostasis is far from settled and a universally accepted model is yet to emerge, work from several groups has helped in the development of a hypothesis establishing an internal circulatory system for the lens. This circulation hypothesis is developed treating the lens as an electrical model of a spherical syncytium (Eisenberg et al., 1979) and incorporates the contributions of surface and inner cell membranes, extracellular spaces, ion channels, Na/K pump, water channels as well as gap junctions (Mathias et al., 1997; Mathias and Rae, 2004).

Studies using impedance techniques lent support to the spherical syncytium model (Mathias et al., 1979; Rae et al., 1982). The membrane conductance of the fiber cells was found to be small but fairly uniform throughout the lens, and the fiber cell membranes were found to have higher resistance than the surface membranes. The reason for the lower conductance of the fiber cell membranes appeared to be the significantly less K^+-conductance in comparison to the K^+-conductance of the surface cells (Mathias et al., 1985). A large number of studies also

reported the localization of the majority of Na/K ATPase activity to the anterior epithelial cells and the rest to the outer DF (Fournier and Patterson, 1971; Mathias et al., 1997).

In the same time period, Robinson and Patterson measured the current around the lens using the vibrating probe (a technology that uses a small voltage recording electrode, which is rapidly moved back and forth over a short distance), (Robinson and Patterson, 1982-1983). This study showed the existence of a circulating current in the lens with inward currents at the poles, stronger at the anterior pole and to a lesser degree at the posterior pole, and strong outward currents at the equator. They concluded that the current is dependent on the electrochemical gradients generated by the Na/K pump, and sodium and potassium, therefore, to be the ionic components of the current.

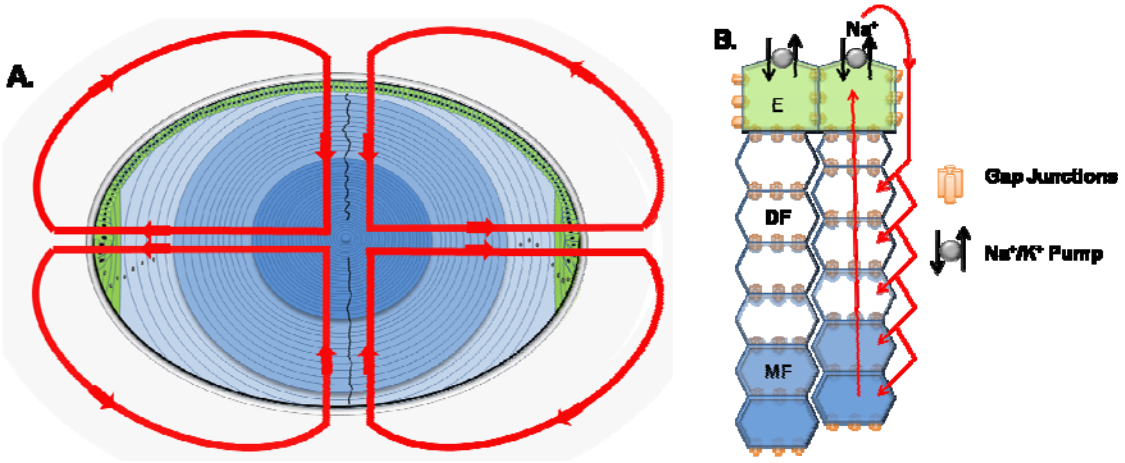

Figure 1.4 The Lens Circulation Model. A. In an intact lens, current flows in the pattern indicated by the arrows. **B.** Representative cross-section taken through the lens equator. The major ion carrier of the circulating current appears to be Na^+, which enters the lens along the extracellular spaces between cells, then moves down its electrochemical gradient into fiber cells, where it returns to the surface via gap junctions. The pattern of gap junction coupling in the differentiating fibers directs the intracellular current flow to the lens equator, where the epithelial cells transport it out of the lens using Na^+/K^+-ATPase activity. (Based on a figure from Donaldson et al., 2001)

Continuing with their impedance studies, the Mathias group observed a stepwise change in membrane conductance, decreasing from the anterior surface epithelial cells to the posterior surface differentiating fiber cells (Mathias et al., 1985). They incorporated an intercellular pathway of current flow mediated by gap junction channels into the lens circulatory model, and

reported a smooth and symmetrical change in gap junction coupling conductance of the DF from the equator to poles with the maximum conductance at the equator and falling to near zero at the poles (Baldo and Mathias, 1992). The cell to cell coupling conductance in the MF was about half the average value in the DF (Mathias et al., 1981). The other observed difference between the DF and MF was that a drop in pH caused reversible uncoupling of the DF gap junction channels, whereas it had no effect on the MF gap junctions (Mathias et al., 1991). This suggested that the DF (20% of total fiber cells) gap junctional coupling conductance, which is concentrated at the equator, could be physiologically regulated, whereas the MF (80% of total fiber cells) gap junction channels have lost the capacity for regulation. However, these studies did not answer the question of whether the observed higher equatorial conductance was because of the mere presence of higher number of gap junctions in the equatorial region, or a higher number of open gap junctions in the equator in comparison to the poles. Dye transfer studies demonstrated extensive passage of dye between the lens epithelial cells, whereas the dye coupling between epithelial to fiber cells was about one in ten suggesting that the preferential direction of current flow for the anterior epithelial cells is towards the equator rather than towards the lens center (Rae et al., 1996).

Incorporating the available properties of lens physiology till then, Mathias et al. presented a model for lens circulation in 1997 (Mathias et al., 1997). The model suggests that Na^+ enters extracellularly into the lens everywhere at the surface locations and moves inward along the pervading extracellular spaces. As the Na^+ moves inward, it continuously crosses into the fiber cells driven by the transmembrane electrochemical gradient (Figure 1.4). Once inside the fiber cell, the current generated by the gap junctions drives the Na^+ flow through cell to cell towards the lens surface. As the DF gap junction coupling conductance is concentrated in the equatorial region, the intracellular current drives the intracellular current towards the equatorial surface epithelial cells, thus bringing the Na^+ out of the lens and completing the circulation of current. Gap junction plaques are found on the broadsides of the fiber cells in the outer cortex (Paul et al., 1991; Kuszak et al., 1995; Jacobs et al., 2004). This helps in driving the net outward Na^+ movement towards the equator where the total Na/K pump current per area of lens surface is predicted to be about 20 times greater than the anterior pole (Gao et al., 2000). So, the Na/K pump activity and the gap junction channels establish a steady current which is outward at the

equator and inward at the pole. This circulating current also generates a water flow which carries the nutrients and anti-oxidants into the fiber cells where they can be used for homeostasis.

This hypothesis got support from Candia and Zamudio's measurements of Na^+ and K^+ currents in different regions of the rabbit lens (Candia and Zamudio, 2002). Using ouabain and $BaCl_2$, inhibitor of Na/K pumps and blocker of K^+ channel respectively, this study was able to distinguish between currents mediated by Na/K pumps and K^+ channels. At the equator, the outward current was found to be composed of both the Na/K pump current and the diffusion of K^+. At the posterior surface, a relatively uniform inward Na^+ current was observed that was unaffected by ouabain and $BaCl_2$. At the anterior and posterior polar region, an inward Na^+ current was detected which was not affected by ouabain suggesting an absence of Na/K pump activity. These findings suggested that all three currents (Na/K pump, passive Na^+ diffusion and passive K^+ diffusion) may coexist and the relative contributions from each establish the net current between the equator and the anterior pole. Similar pattern of Na/K pump current pattern were found in porcine lenses with most of the Na/K pump current concentrated at the equator (Tamiya et al., 2003).

Taken together these results show that the Na/K pumps at the equator and the anterior surface, except around the anterior pole, create an outward Na^+ current that circulates around the lens surface and re-enters across the posterior surface and the anterior pole. The K^+ flux is also translocated into the lens by the Na/K pump and leaves the lens principally at the equator and just anterior to the equator. These observations support the hypothesis that the circulating current inside the lens is carried by Na^+ and is directed to the equatorial surface cells by the gap junction conductance where the Na/K pumps help in transporting it out.

Functional water channels constituted of aquaporins (AQP) have been identified in the lens, with AQP1 being expressed in the surface epithelial cells whereas in DF AQP1 is degraded and AQP0 is expressed (Mathias et al., 1997, Chandy et al. 1997). The circulation model assumes that epithelial and fiber cell membrane water permeabilities are high enough for an essentially isotonic solution to follow the circulating Na^+-flux. The water permeability of lens epithelial cells is 3- to 4-fold greater than that of fiber cell membranes (Varadaraj et al., 1999). These quantitative water permeability values are consistent with the assumption and it is predicted that the solutions within the intracellular and extracellular spaces inside the lens will be within 0.1% of isotonic (Mathias and Rae, 2004).

The model also predicts that fiber cells should have the functional transporters to accumulate the nutrients brought to them by the circulating current and water flow. Molecular experiments have identified a variety of membrane transporters in the fiber cells including glucose transporters (Merriman-Smith et al., 1999; 2003), glutamate transporters (Lim et al., 2005 and 2006), glycine transporters (Lim et al., 2006), cysteine/glutamate exchanger (Lim et al. 2005) and vitamin C transporter (Kannan et al., 2001). These membrane transporters are also expressed in a differentiation-dependent manner which helps in establishing the spatial differences in the transport properties critical for the generation of the circulation system. In case of the glucose transporters; the epithelial cells express the facilitative glucose transporter GLUT1, whereas the fiber cells express the higher affinity GLUT3 and sodium-dependent glucose transporter SGLT2 involved in glucose uptake by the secondary active transport mechanism. This differential expression of glucose transporters establishes an affinity gradient, which increase the chances of deeper fiber cells to extract a diminishing supply of glucose from the extracellular space. Expression of SGLT2 in the lens nucleus indicates that the mature fiber cells can utilize the energy stored in the sodium gradient, established by the lens circulation, to accumulate glucose above its concentration gradient, where it can be used for anaerobic metabolism.

Although evidence, supporting the hypothesized lens circulation system, is mounting by the day, it is still not a fully proven and universally accepted model. But one conclusive reality is that the gap junctional conductance plays an important role in the lens internal circulation system. The mechanism of the gap junctional coupling in the lens is a complex process and the role played by the gap junctional intercellular communication (GJIC) in lens homeostasis and cataract formation needs further investigation. The structure and function of gap junctions is further discussed in the next section.

1.5. Gap Junctions and Intercellular Communication

Cells of multicellular organisms need to communicate with each other to maintain the cell homeostasis and regulate the patterns of growth and differentiation. This communication is achieved by the linking of the cells together by different junctions like the tight, adherens, desmosomes and gap junctions. But among all the junctions, gap junctions provide the most direct form of communication between adjacent cells.

1.5.1. Gap Junctions: Structure and Function

Gap junctions are transmembrane aqueous channels that connect the cytoplasm of neighboring cells and allow the passage of molecules up to the size of 1 kDa between the connected cells (Harris 2001; Goldberg et al., 2004; Weber et al., 2004). Much of the early structural studies on gap junctions were done using electron microscopy and this revealed a narrow gap between membranes of apposed cell membranes, hence the term gap junction (Revel and Karnovsky, 1967). SDS-polyacrylamide gel electrophoresis (SDS-PAGE) separation of gap junctions isolated from mouse hepatocytes led to the hypothesis that gap junctions were composed of subunits termed "connexins" (Goodenough, 1974). The term connexin was proposed as the protein forms the connection between adjacent cells in the gap junction. Around the same time Goodenough also proposed the term "connexon" for the hexagonal subunits comprising the gap junctions observed in isolated liver gap junction vesicles (Goodenough, 1976).

Today the structural unit of the gap junction is known as the connexon or the hemi-channel. Each connexon is a hexameric subunit consisting of six connexin proteins, oriented roughly perpendicular to the membrane plane, forming an aqueous pore that spans a single plasma membrane. To form a functional gap junction one connexon from one cell docks or associates with a corresponding connexon from an adjacent cell (Figure 1.5B). The maximal functional pore size of gap junction channel has been suggested to be about 1.5 nm in diameter in mammalian cells (Oyamada et al., 1998). Several hundreds of gap junctions, in turn cluster to aggregate in the in the contact regions of the adjacent cells to form gap junctional plaques (Werner, 1998). It has also been showed that the formation of gap junctional plaques is a prerequisite for the functional gap junctions (Bukausas et al., 2000). Connexons are ~65 Å in diameter and are arranged on a hexagonal lattice. Two connexons associate to form a tight seal with a 20-30 Å gap between the apposing cell membranes. This structure creates a hydrophilic pathway of ~15 Å wide and ~180 Å long (Sosinsky, 1996). Gap junction channels have been shown to be permeable to a variety of metabolites and signaling molecules such as ions like K^+ and Ca^{2+}, amino acids, nucleotides, small peptides, sugars, cAMP, and inositol triphosphate (Alexander and Goldberg, 2003, Harris and Locke, 2009).

1.5.2. Structure and Arrangement of Connexins

Connexin proteins are the principal structural components of the gap junctions (Kumar and Gilula, 1996). Each connexin consists of four hydrophobic transmembrane domains (M1 to M4), two extracellular loops (E1 and E2), each containing three conserved cysteine residues, a cytoplasmic loop and cytoplasmic N- and C-termini (Solan and Lampe, 2009). The most conserved regions in the connexin are localized to the extracellular loops followed by less conserved region of four membrane-spanning domains. Connexins differ markedly from each other in sequence and length mainly based on their C-termini and the cytoplasmic loop (Hertzberg, 2000), which allows unique functional or regulatory properties for channels formed by different connexins.

Gap junctional intercellular communication (GJIC) is essential for a variety of processes in the cell. Increasing numbers of inheritable genetic diseases are being reported to be caused by mutations to the connexin genes (White and Paul, 1999). Cells can also adjust the permeability and gating properties of their gap junction channels (Valiunas et al., 2002; Goldberg et al., 2004), as well as their ability to communicate with other cells by expressing multiple connexin isoforms (Goodenough et al., 1996; Simon et al., 1998). This means that each connexon can be homomeric (composed of the same connexin isoform) or heteromeric (composed of different connexin isoforms) (Figure 1.5B). The gap junction channel in turn can be homomeric-homotypic, homomeric-heterotypic or heteromeric-heterotypic (Kumar and Gilula, 1996).

20 connexin family members in the mouse and 21 family members in the humans have already been reported, which makes the expression and distribution of gap junctions almost ubiquitous (Laird, 2006). Connexins have molecular masses ranging between 25 to 62 kDa and this size is used for the nomenclature of the proteins (Evans et al., 2006). In some instances, a prefix including the species name is added while describing the protein. For example, the most abundant and prominent connexin in rat heart is a 43,036 Da protein, hence called rat Cx43. The finding that two or more connexins have the same molecular mass has lead to a decimal point to distinguish them, for example mouse Cx30.3 or mouse Cx31.1 (Saez et al., 2003). Another, less commonly used, nomenclature is based on the degree of relatedness of different connexins. The analysis for the sequence relation and phylogeny of connexin polypeptide sequences categorize connexins into two groups: α and, β. The α-group includes Cx33, Cx37, Cx38, Cx40, Cx43,

Cx45, Cx46, Cx50, and Cx56; while the β-group consists of Cx26, Cx30, Cx30.3, Cx31.1, and Cx32(Kumar and Gilula, 1992; Hertzberg, 2000).

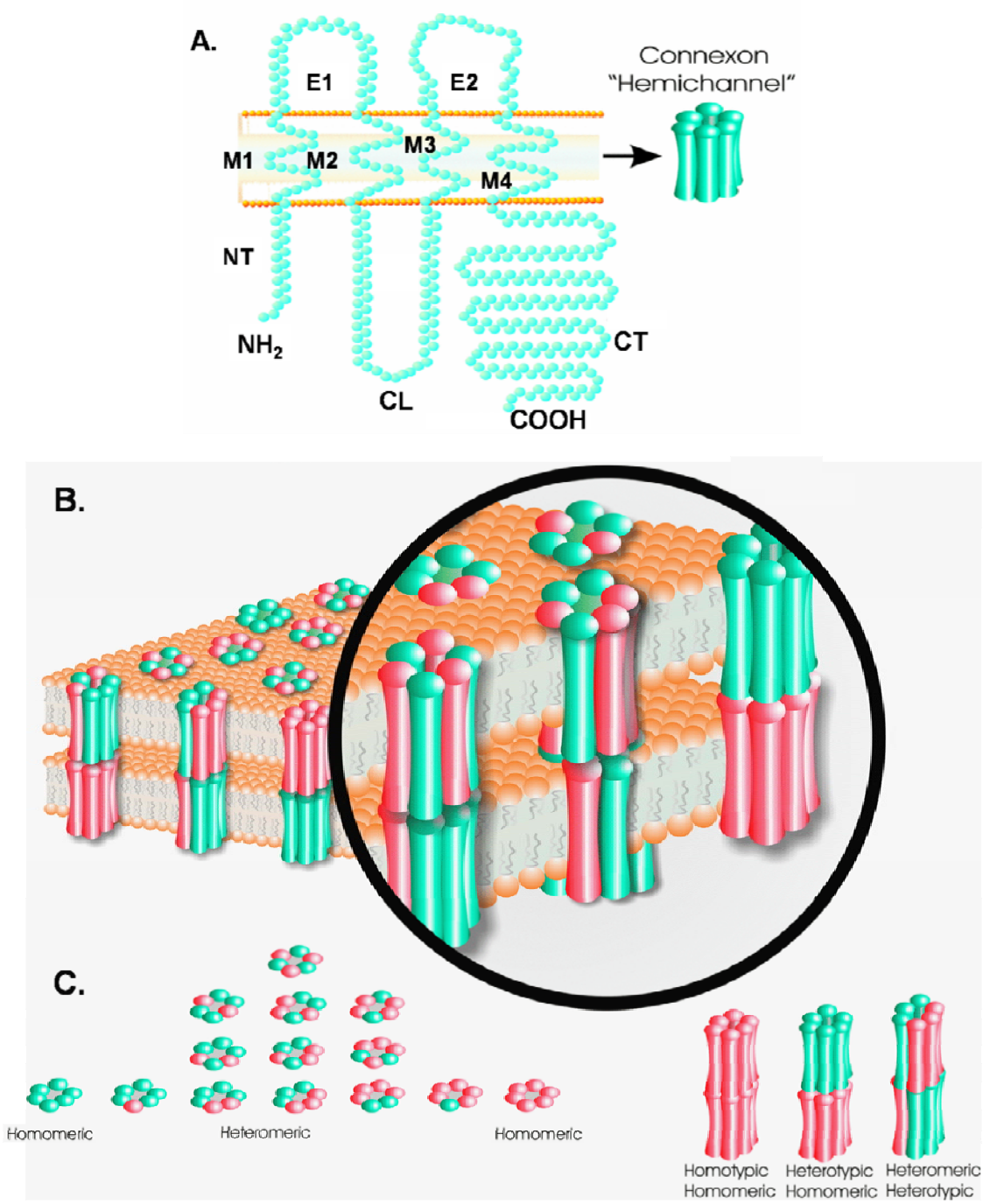

Figure 1.5 Different Levels of Structural Organization of the Gap Junction. A. One connexin molecule, the basic unit of gap junction, which has four transmembrane domains (M1 to M4), two extracellular loop domains (E1 and E2), a cytoplasmic loop domain (CL) and cytoplasmic N-terminal (NT) and C-terminal (CT) tails. Six connexin molecules form a

connexon or hemichannel. **B.** Each cell contributes one membrane-spanning connexon to form the cell-to-cell gap junction channel. **C.** Potential gap junction configurations: Homomeric connexons = Identical connexin subunit isoforms; Heteromeric = Mixed connexin subunit isoforms; Homotypic gap junctions = Identical connexons, Heterotypic gap junctions = Mixed connexons. [Modified figure reproduced with kind permission from Laird, 2006, Biochem. J. 394 (527–543) © the Biochemical Society (http://www.biochemj.org)]

1.5.3. Tissue specific expression of connexins

In vertebrates, gap junctions are found in all cell types except a few such as red blood cells, some neurons, spermatozoa, and skeletal muscle fibers. However different connexins are expressed in different tissues and most cells express two or more connexins (Saez et al., 2003). Presence of different connexins in different tissues suggests specific roles of different connexins. For example, keratinocytes express at least Cx26, Cx30, Cx30.3, Cx31, Cx31.1, and Cx43. Cardiomyocytes express Cx43, Cx40, and Cx45 and hepatocytes express Cx26 and Cx32 (Table 1.1) (Laird, 2006). The expression of multiple connexin isoforms within the same cell type and their different structural combinations provide exquisite functional tuning for this unique family of membrane channels (Laird, 2006; Harris and Locke, 2009). Gap junctions composed of different connexins do show variable and selective permeability (Steinberg et al., 1994; Harris and Locke, 2009).

Table 1.1 Representative tissues and cell types distribution of mouse Connexin family members (Modified from Laird, 2006)

Cxs	Representative Tissue/Organ	Representative Cell Type
Cx23	–	–
Cx26	Liver, skin, cochlea	Hepatocytes, keratinocytes, epithelial cells
Cx29	Brain	Oligodendrocytes
Cx30	Skin, cochlea	Keratinocytes, epithelial cells
Cx30.2	Testis	Smooth-muscle cells
Cx30.3	Skin	Keratinocytes
Cx31	Skin	Keratinocytes
Cx31.1	Skin	Keratinocytes
Cx32	Liver, nervous	Hepatocytes, Schwann cells
Cx33	Testes	Sertoli cells
Cx36	Retina, nervous	Neurons
Cx37	Blood vessels	Endothelial cells
Cx39	Developing muscle	Myocytes
Cx40	Heart, skin	Cardiamyocytes, keratinocytes
Cx43	Heart, skin, Lens	Cardiomyocytes, keratinocytes, Lens epithelial cells
Cx45	Heart, skin	Cardiomyocytes, keratinocytes
Cx46	Lens	Lens fiber cells
Cx47	Nervous	Oligodendrocytes
Cx50	Lens	Lens epithelial and fiber cells
Cx57	Retina, Nervous	Horizontal cells

1.5.4. Gap Junction Intercellular Communication (GJIC) in the Lens

Although much of the early work on gap junctions was carried out in heart, liver, and brain (Revel and Karnovsky, 1967; Benedetti and Emmelot, 1968; Brightman and Reese, 1969; Goodenough and Revel, 1970), the lens soon followed as a model tissue for gap junction

research and has played a vital role in the progress of gap junction studies over more than 30 years (Bloemendal et al., 1972 and 1977; Benedetti et al., 1976). The initial confusion, regarding whether the junctions observed in the lens cell membranes are gap or tight junctions, was resolved by Nonaka et al. in 1976 confirming them as gap junctions (Nonaka et al., 1976). Soon the potential role for gap junctions in the lens metabolism started to emerge (Goodenough et al., 1979 and 1980). The importance of gap junction intercellular communication in the avascular lens circulation has already been discussed. Different arrangements of gap junctions exist between the different regions of epithelial cells, between the fiber cells, and between the epithelial and fiber cells (Berthoud and Beyer, 2009). Only the outermost differentiating fibers make direct contact with the epithelial cells (Bassnett et al., 1994).

Epithelia- to-Epithelial Cells Gap Junction Communication

The epithelium is the only layer of cells in the lens having direct contact with the aqueous humor of the eye regulating the passage of ions and metabolites between the aqueous humor and the fiber cells (Kinsey and Reddy, 1965). High density of gap junctional complexes between epithelial cells have been reported in calf lenses (Benedetti et al., 1974), frog lenses (Rae and Kuszak, 1983), rabbit, rat and human lenses (Lo and Harding, 1986; Lo 1987), and in lens cell cultures (Menko et al., 1987). Whereas small gap junctional plaques are observed in the central epithelial cells, the epithelial cells in the germinative zone and the equator are connected through an extensive network of gap junctions (Zampighi et al., 2000).

Epithelial-to-Fiber Cell Gap Junction Communication

Lens fiber cells get their metabolites by a network of gap junctions from the overlaying epithelium as the fiber cell membranes have no active transport channels (Goodenough, 1992). The coupling of epithelial and fiber cells by functional gap junctions have been determined by dye transfer studies in rat, rabbit and embryonic chick lenses (Rae et al., 1996).

Fiber-to-Fiber Cells Gap Junction Coupling

One of the most highly ordered arrangements of gap junction plaques are found in the lens fiber cells (Gruijters et al., 1987; Jacobs et al., 2001). The fiber cell gap junction channels are composed of a novel set of gap junction channels which can be maintained throughout the lifetime of an individual in the absence of the protein synthesis machinery and remain open

under conditions where other gap junction channels would show strong gating or regulation by rapid turnover (Goodenough, 1992). Gap junctions are found in much higher density in the lens bow region than in the anterior or posterior pole regions in the lens fibers (Brown et al., 1990). Gap junction plaques are located at the apical ends of cortical fiber cells forming the interface, but not in the lateral surfaces (Zampighi et al., 2000).

1.6. Connexins in the Lens

Biochemical and molecular studies have identified three different connexins in the lens with some overlapping expression pattern. Cx43 and Cx50 are expressed in the epithelial cells, but the expression of Cx43 is turned off when the epithelial cells start to differentiate into fiber cells in the equatorial region (Musil et al., 1990; Dahm et al., 1999). Cx46 and Cx50 along with Cx43 share an overlapping distribution in the bow region of the lens, where the new fibers differentiate (Paul et al., 1991; White et al., 1992; Le and Musil, 1998). Cx46 and Cx50 become abundantly expressed in the differentiating and mature fiber cells (Paul et al., 1991; White et al., 1992). Cx46 and Cx50 co-localize at gap junctional plaques and form heteromeric connexons in the fiber cells (Paul et al., 1991; Jiang and Goodenough, 1996). The fiber-epithelial junctions may be a heterotypic channel composed of Cx43 and Cx46 (Mathias et al., 1997). Another Connexin transcript, Cx23, has recently been detected in the zebrafish embryo lens (Iovine et al., 2008) and in the mouse lens (Puk et al., 2008). However, the structural and functional role of this new connexin isoform has not yet been completely characterized. The expression of Cx43, CX46 and Cx50 in the lens has been detected in a number of species (Table 1.2).

Table 1.2 Lens Connexin Isoforms in Different Species

Species	Generic Name	Connexin Name
Human	Cx43	hCx43
	Cx46	hCx46
	Cx50	hCx50
Sheep	Cx43	oCx43
	Cx46	oCx44
	Cx50	oCx49
Mouse	Cx43	mCx43
	Cx46	mCx46
	Cx50	mCx50
Rat	Cx43	rCx43
	Cx46	rCx46
	Cx50	rCx50
Chicken	Cx43	cCx43
	Cx46	cCx56
	Cx50	cCx45.6

Cx43 gap junctions play a vital role in maintaining the osmotic balance of the lens as mice lenses lacking the expression of Cx43 develop space dilations and intracellular vacuoles (Gao and Spray, 1998). Cx46 was found to be localized to large broadside and small narrowside gap junctional plaques of the cortical fiber cells (Paul et al., 1991; Jacobs et al., 2004). Cx46 is important for maintaining the Ca^{2+} homeostasis in the lens (Gao et al., 2004). Cx46 was first implicated in human inherited cataract in 1999 (Mackay et al., 1999), and since then several Cx46 mutations causing inherited cataract have been found (Table 1.3).

Table 1.3 Cx46 Human Gene Mutations (Modified from Guleria et al., 2007, and Sisley, 2007)

Mutations	Phenotype/Morphology	Mutation Position
A->G = missense (N63S)	Early onset zonular pulverulent cataract (CZP3). Fully penetrant Autosomal Dominant Congenital Cataract (ADCC)	Extracellular loop 1 (E1)
C insertion = Frameshift (S380fs)	Early onset CZP3. Fully penetrant ADCC	C-terminal tail
C->T = Missense (P187L)	Fully penetrant ADCC	Extracellular loop 2 (E2)
C->A = missense (F32L)	Nuclear zonular pulverulent cataract. ADCC	Transmembrane domain 1 (M1)
G->A = missense (R76H)	CZP3. Incomplete penetrant ADCC	Boundary of E1 and M2
C->T = missense (P59L)	ADCC nuclear punctuate cataracts	E1
G->T = missense (D3Y)	ADCC zonular pulverulent cataract	N-terminal domain
T->C = missense (L11S)	Lamellar “ant-egg” congenital cataract	N-terminal domain

Table 1.4 Cx50 Human Gene Mutations (Modified from Sisley, 2007)

Mutation	Phenotype/Morphology	Mutation Position	Reference
C->T = missense (P88S)	ADCC zonular pulverulent cataract (CZP1)	Transmembrane domain 2 (M2)	Shiels et al., 1998
G->A = missense (E48K)	ADCC zonular nuclear pulverulent cataract (CZNP)	Extracellular loop 1 (E1)	Berry et al., 1999
T->G = missense (I247M)	ADCC zonular pulverulent cataract	C-terminal tail	Polyakov et al., 2001
G->C = missense (R23T)	ADCC progressive nuclear cataract	N- terminal domain	Willoughby et al., 2003
C->T = missense (P88Q)	ADCC lamellar pulverulent cataract	M2	Arora et al., 2006

Like Cx46, Cx50 also appears as large broadside and small narrowside plaques embedded in the lens cortical fiber cell membranes (Gruijters et al., 1987). Several mutations in the Cx50 gene have been shown in human inherited cataract phenotypes (See Table 1.4). Cx50 has been implicated in the lens growth (White et al., 1998 and 2002; Martinez-Wittinghan et al., 2003). Both the Cx46 and Cx50 C-terminal tails undergo differentiation dependent cleavage (Jacobs et al., 2004; Lin et al., 1998). Cx50 is more pH sensitive than Cx46 in the lens fiber cells (White et al., 1994; Eckert, 2002).

1.7. Mouse models of Gap Junction Function in the Lens

Development of genetically altered mice has provided excellent animal models to study the role of connexin genes in lens intercellular communication in vivo. Prenatal lens development was largely normal in Cx43 knockout (KO) mice, but further investigations were hampered because of neonatal lethality (Gao and Spray, 1998; White et al., 2001). Severe, senile-type cataracts were observed in Cx46KO mice with normal ocular development and growth (Gong et al., 1997). Absence of Cx46 in the lens resulted in the accumulation of intracellular Ca^{2+} in the fiber cells leading to the activation Ca^{2+}-activated calpain protease Lp82 (Baruch et al., 2001; Gao et al., 2004). This activation of Lp82 resulted in the cleavage and precipitation of γ-crystallins in

the nuclear region of the lens forming nuclear cataracts. Deletion of Cx50 caused significant reduction in lens growth (microphthalmia) but only mild nuclear cataracts (White et al., 1998; Rong et al., 2002, White 2002). Fewer fiber cells result in the smaller lens whereas precipitation of crystallins causes the nuclear cataract. In the Cx50KICx46 (targeted replacement of Cx50 with Cx46) mouse model, the lenses maintained clarity but continued to display growth deficits confirming the requirement of Cx50 for proper lens growth (White 2002; Sellitto et al., 2004). Double knockout of Cx46 and Cx50 produced additive effects of severe cataract and reduced lens size (Xia et al., 2006). These mouse models suggested variable roles for Cx46 and Cx50 connexins in maintaining lens transparency and proper lens growth.

1.8. Regulation of Gap Junction Intercellular Communication (GJIC)

Gap junctions respond to a variety of factors, including Ca^{2+} levels, voltage (both transjunctional and transmembrane), pH and phosphorylation events. GJIC can be regulated at many levels ranging from gating at the plasma membrane, connexin gene regulation, and gap junction assembly and degradation. Although connexin sensitivity to transjuctional voltage (V_j) varies widely, this variance is partially responsible for rendering functional diversity and permeation selectivity in GJIC (Mathias et al., 1997). There are two distinct voltage-gating mechanisms that can close gap junction channels and hemichannels. One, the fast-gating mechanism, is sensitive to V_j and leads to the closure of channels and hemichannels to a subconductance state. The fast-gating mechanism has the molecular components of its voltage sensor localized to the N-terminal domain (Saez et al., 2003; Harris and Locke, 2009). The other, loop or slow-gating mechanism, is sensitive to both V_j and inside-out or transmembrane voltage (V_{i-o} or V_m) and to channel closure by chemical agents. The slow-gating mechanism completely closes gap junction channels and hemichannels leaving no residual conductance and the molecular components of this form of gating may be located at the extracellular end of the hemichannels because of strong sensitivity to extracellular Ca^{2+}. Many studies have shown that lens epithelial cells uncouple in response to elevated levels of Ca^{2+} in the cytoplasm (Cooper et al., 1991, Crow et al., 1994).

Acidification of cytoplasm, as observed in the lens cortex, leads to the closure of gap junction channels composed of most connexin isoforms (Mathias et al., 1997, Sosinsky and Nicholson, 2005). Mutation mapping studies have predicted that the regulatory sites for pH and other chemical gating processes are located at the carboxyl terminus and within the second half

of the intracellular loop structure (at the transmembrane 2 (TM2) cytoplasmic loop interface) of the connexin molecule. This pH gating mechanism has been termed a "ball-and-chain" type scheme in which the carboxyl terminus acting as the gating particle binds to a separate receptor region of the protein to close the channel (Sosinsky and Nicholson, 2005). In lens, Cx46 and Cx50 get cleaved at the C-terminus in the DF to MF transition zone and these truncated connexins lose their ability to respond to a drop in pH in the nuclear fibers and remain open (Eckert, 2002). Possibly the Cx46 cleavage serves to initiate plaque remodeling, the large broad-side and small narrow-side plaque arrangement in the DF is lost in the MF as the plaques disperse and decrease in size. This precise connexin processing modifies gap junction structure and plaque arrangement to create functional specializations in subregions of the lens, which allow the maintenance of lens circulation, homeostasis and transparency (Jacobs et al., 2004).

Whereas junctional conductance is likely to be affected by Ca^{2+}, pH and transjunctional voltage only in pathological conditions; phosphorylation events may have a direct role in normal physiological regulation (Mathias et al., 1997). Phosphorylation of connexin proteins leads to both increase and decrease in GJIC depending on the residue phosphorylated (Table 1.5). Phosphorylation in the connexin proteins has been widely studied and most connexin family members are phosphoproteins (Solan and Lampe, 2005; Laird, 2005). Most of the phosphorylation events in the connexin isoforms have been reported in the C-termini, whereas phosphorylation of the cytoplasmically located N-terminal region is not reported (Lampe and Lau, 2000). Cx43 has been the most studied connexin isoform in terms of phosphorylation by many kinases (Pahujaa et al., 2007, Solan and Lampe, 2009). Connexin phosphorylation results in differential regulation of GJIC through a number of mechanisms, including connexin biosynthesis, trafficking, assembly, membrane insertion, channel gating, internalization and degradation. Several kinases have been implicated in the phosphorylation of connexins, including Src, MAPK, CDC2, CK1, PKA and PKC (Pahujaa et al., 2007, Solan and Lampe, 2009). Many studies describe the changes in the state of phosphorylation of Cx43 by PKC-dependent pathways. Ser-368 of Cx43 appears to be an important site since mutation of Ser-368 partially prevents the cellular uncoupling induced by phosphorylation caused by PKC in the presence of phorbol ester (TPA) (Liu and Johnson, 1999; Lampe et al., 2000). Since my research involves the phosphorylation of lens connexins by PKCγ, the structural and functional aspects of the protein kinase C (PKC) class of enzymes are discussed next.

Table 1.5 Cx43 phosphorylation events that affect GJIC (Modified from Pahujaa et al., 2007)

Cx43 amino acid residue	Kinase	Event result
Y247	Src	Decrease communication
S255	MAPK, CDC2	
S262	CDC2, PKC	
Y265	Src	
S279	MAPK	
S282	MAPK	
S368	PKC	
S372	PKC	
S325	CK1	Increase communication
S328	CK1	
S330	CK1	
S364	PKA	
S365	PKA	
S369	PKA	
S373	PKA	

1.9. Protein Kinase C

Protein kinase C (PKC), a member of the larger superfamily of AGC (PKA, PKG, PKC) kinases, comprises a multigene family of related serine/threonie (Ser/Thr) kinases sitting at the cross-roads of many signal transduction pathways (Spitaler and Cantrell, 2004). Initially thought as a single protein, this enzyme was first identified in bovine cerebellum by Nishizuka and co-workers in 1977 (Takai et al., 1977; Inoue et al., 1977). With the identification that it is activated by the tumor-promoting phorbol esters like phorbol 12-myristate 13-acetate (TPA/PMA) in the

1980s, PKCs rocketed to the forefront of signal transduction and cancer research (Griner and Kazanietz, 2007). PKCs have been implicated in processes like development (Otte et al., 1991), differentiation (Cutler et al., 1993), memory (Alkon, 1989), proliferation (Murray et al., 1993), carcinogenesis (Ashendel, 1985) and immune responses (Tan and Parker, 2003). The cloning of PKC in the mid-1980s unveiled a family of kinases having the common features: the presence of a cysteine-rich motif, the C1 domain and a carboxy terminal kinase domain (Coussens et al., 1986). This enzyme multiplicity, together with abundant and variable cellular and tissue distribution explains the variety of signal transduction functions attributed to this family of kinases.

Traditionally, PKCs have been viewed as lipid-sensitive enzymes that are activated by growth factor receptors that stimulate phospholipase C (PLC), an active PLC in turn hydrolyzing phosphatidylinositol 4,5-bisphosphate (PIP2) to generate the second messengers, diacylglycerol (DAG) and inositoltrisphosphate (IP3), which mobilizes intracellular calcium (Newton, 1995; Steinberg, 2008,). The released intracellular calcium and membrane bound DAG result in the recruitment of the inactive cytosolic PKCs to the membrane where they become allosterically activated. However, before the allosteric activation step the PKC isozymes must be processed by a series of phosphorylation events that converts an immature form of the PKC into a catalytically competent one (Newton, 1997 and 2003; Parekh et al., 2000). Research from Mochly-Rosen laboratory identified the receptors for activated C Kinases (RACKs), a family of membrane-associated PKC anchoring scaffold proteins, which localize individual PKCs to distinct membrane microdomains bringing them closer to their allosteric activators and unique intracellular substrates (Schechtman and Mochly-Rosen, 2001; and Mackay and Mochly-Rosen, 2001). Unique RACK proteins specific for each PKC isoform have been proposed to be expressed in the cells, which help in isoform-specific cellular activities of individual PKC enzymes. Recent studies have proposed new mechanisms like: 1) caspases can cleave PKCs generating a catalytically active kinase domain and a freed regulatory domain fragment which can act both as an inhitbitor of the full-length enzyme as well as a kinase-independent activator of certain signaling responses; 2) Less traditional lipid cofactors such as ceramide or arachidonic acid can activate PKCs; and 3) PKCs can also be activated by lipid-independent mechanisms like oxidative modifications or tyrosine nitration which renders PKC signaling throughout the cell and not just at the DAG-containing membranes (Violin and Newton, 2003; Steinberg, 2008).

1.9.1. PKC Family Members

PKC isoforms comprise a family of protein kinases sharing two basic structural features: 1) a highly conserved kinase domain required for the ATP/substrate binding and catalysis; 2) a regulatory domain required for maintaining the enzyme in an inactive conformation. The regulatory domains exist in the N-terminus of the protein, whereas the catalytic domains reside in the C-terminus end. The regulatory domains contain an autoinhibitory pseudosubstrate domain and two discrete membrane targeting domains; C1 and C2, each comes either in a form that binds to the ligand or in a form lacking the determinants that allow ligand binding (Hurley and Misra, 2000; Cho, 2001). PKC isoenzymes are broadly grouped into three subclasses on the basis of domain composition of the regulatory moiety, termed conventional, novel and atypical PKCs (Figure 1.6). The co-factor dependence of the isoenzymes is dictated by this domain composition (Newton, 2001). The C1 domain is the DAG-/TPA-binding motif and the C2 domain is the Ca^{2+} sensor. Conventional PKCs contain functional C1 and C2 domains and respond to both DAG/TPA and Ca^{2+} signals. Novel PKCs also contain both C1 and C2 domains, but the ordering of the two domains is switched relative to the conventional PKCs. The C2 domain of novel PKCs lack the critical calcium-coordinating aspartate residues; thus the novel PKCs respond to DAG/TPA, but not to Ca^{2+} signals. Atypical PKCs lack the C2 domain and have a non-ligand-binding C1 domain. The C1 domain of the atypical PKCs is different in the sense that, they contain only one cysteine-rich membrane targeting structure unlike the conventional and novel PKC C1 domains containing two cysteine-rich repeats termed C1A and C1B. Because of the non-ligand binding nature of the C1 domain and the absence of C2 domain, the atypical PKCs do not respond to either DAG/TPA or Ca^{2+}; though still require phosphatidylserine as a co-factor (Newton, 1995; Steinberg, 2008).

There are 10 mammalian PKCs (Figure 1.6): four conventional isoenzymes (α, βI and the alternatively spliced βII which differ only in the last 43 residues at the C-terminus, and γ), four novel PKCs (δ, θ, ε and η), and two atypical PKCs (ζ and ι/λ; an alternative transcript exists for ζ that encodes only the catalytic domain and referred to as PKM ζ (Marshall et al., 2000)) (Mellor and Parker, 1998; Newton, 2003; Steinberg, 2008). Novel PKCs can be further subdivided based on structural features into the related δ/θ, and ε/η isoforms. In addition to these 10 isozymes, PKC μ and ν are considered by some to constitute a fourth class and by others to comprise a distinct family called protein kinase D (Mellor and Parker, 1998; Newton 2001).

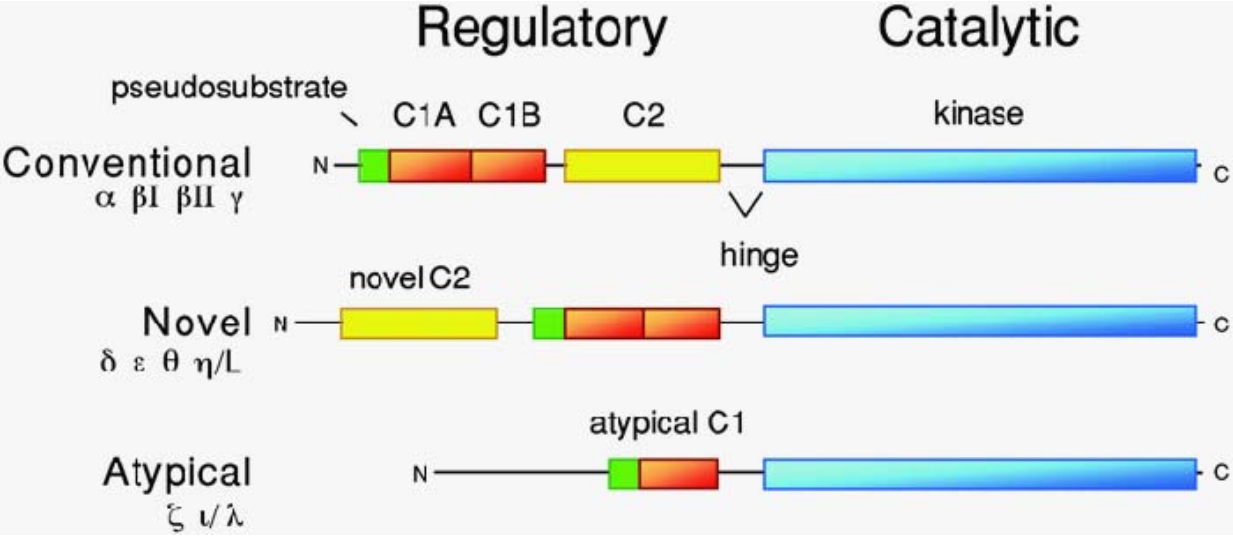

Figure 1.6 Schematic showing the domain structure of the conventional, novel, and atypical subclasses of PKC. Indicated are the pseudosubstrate, C1 and C2 domains in the regulatory moiety, and the carboxyl-terminal kinase domain. (Reproduced with kind permission of Springer Science+Business Media and Newton AC from Newton, 2003b *Methods Mol. Biol.* 233:3-7, Figure 1)

Although some PKC isoforms are expressed in a tissue specific manner, like PKCθ is primarily expressed in skeletal muscle, lymphoid organs, hematopoietic cell lines and PKCγ is expressed mainly in the neuronal tissues, most PKC isozymes are ubiquitous and multiple PKC isoforms are expressed together many cells (Steinberg, 2008).

1.9.2. Domain Structure

The multidomain PKC isozymes are under acute conformational regulation. Both phosphorylation and co-factor binding induce conformational changes that regulate interdomain interactions, of which the most important is the autoinhibitory pseudosubstrate binding to the substrate-binding cavity of the kinase domain. The regulatory and the kinase domains are connected by a proteolytically labile 'hinge' region (Figure 1.6). Cleavage at the hinge region turns the kinase domain constitutively active (Newton, 2001).

Pseudosubstrate

The pseudosubstrate of PKC lies N-terminal to the C1 domain. This peptide sequence contains an alanine in place of the serine/threonine phosphoacceptor site, but otherwise

resembles a PKC substrate, and occupies the substrate-binding cavity of the PKC in its inactive state (House and Kemp, 1987). Peptides based on this sequence were found to be effective competitive inhibitors of PKC and peptides having a serine at the putative phosphoacceptor position were found to be relatively good substrates of the enzyme (House and Kemp, 1987). Using protease as conformational probes, it was established that activation of PKC is accompanied by release of the pseudosubstrate sequence from the kinase core (Orr et al., 1992). This unmasking of the pseudosubstrate occurs independently of PKC activation mechanism: whether by binding its cofactors or by anomalous mechanisms such as by binding cofactor-independent substrates (Orr and Newton, 1994). In the closed autoinhibited conformation, PKC is relatively resistant to proteolysis (Dutil and Newton, 2000). In conventional PKCs, the engagement of the membrane-targeting C1 and C2 domains to the membranes drives the release of pseudosubstrate, and the high-affinity binding of the C1 and C2 domains provides energy to release the pseudosubstrate from the substrate-binding cavity (Johnson et al., 2000; Cho, 2001).

Membrane-Targeting C1 and C2 Domains

Many signaling enzymes take advantage of having two membrane-targeting modules, each module binds membranes with low affinity and tight-membrane binding is achieved only when both the domains engage on the membrane. When the affinity of one domain is dependent on stimulus dependent changes in membrane composition, like generation of lipid second messengers, or protein structure like phosphorylation, the interaction with the membrane is reversibly regulated. This helps in regulating the spatial distribution of the enzyme reversibly. PKC has been as a model for the reversible regulation of membrane location by the concerted action of two membrane-targeting modules (Newton and Johnson, 1998; Hurley and Misra, 2000).

The C1 Domain

C1 domains were first recognized as highly conserved DAG/TPA binding sites in PKCs with a characteristic cysteine-rich $HX_{12}CX_2CX_nCX_2CX_4HX_2CX_7C$ motif (approximately 50 residues), where H is histidine, C is cysteine, X is any other amino acid, and n is 13 or 14 (Hurley et al., 1997; Steinberg, 2008). While this motif is duplicated in tandem in conventional and novel PKCs termed as C1A and C1B ((Hurley et al., 1997), the atypical PKCs contain a single copy of the domain which lack the structural determinants for DAG/TPA binding. A

growing family of proteins is being reported that contain either typical or atypical C1 domains that lack the kinase domains (Kazanietz, 2002 and 2002). High resolution crystal and solution NMR structures of PKCα, PKCγ, and PKCδ C1B domains complexed with phorbol esters have shown that these C1 domains adopt a similar globular structure and function as hydrophobic switches to anchor PKCs to membranes (Hommel et al., 1994; Zhang et al., 1995; Xu et al., 1997). Two Zn^{2+} atoms are coordinated by histidine and cysteine residues at opposite ends of the primary sequence which help in proper folding and stabilization of the domain. Ligand binding to the C1 domain does not cause significant change in the domain conformation. Lipid cofactors such as TPA or DAG cap the hydrophilic ligand-binding pocket of the C1 domain so that the top third of the C1 domain presents a continuous hydrophobic surface. Thus the lipid cofactors act as "molecular glue" and change the surface properties of the module to increase membrane affinity (Cho, 2001; Hurley and Misra, 2000). While the C1A and C1B domains of PKCγ and PKCε bind both DAG and phorbol esters with high affinity and contribute to membrane anchoring; the C1A and C1B domains of other isoforms have opposite intrinsic affinities for DAG and phorbol esters. For example, in PKCα and PKCδ the C1A domains have high affinity for DAG and the C1B domains have high affinity for phorbol ester (Ananthanarayanan et al., 2003; Stahelin et al., 2005a and 2005b). In addition to binding DAG and phorbol esters, the C1 domain also specifically binds to anionic membrane phospholipid, phosphatidylserine (PS) (Johnson et al., 2000).

The C2 Domain

The C2 domain is an independent membrane-targeting module found not only in conventional and novel PKCs, but also in a large number of proteins unrelated to PKC (Nalefski and Falke, 1996). C2 domains were first identified as ~130 residue sequences that function as Ca^{2+}-dependent membrane-binding modules in the regulatory domain of conventional PKCs. However, the C2 domain found in the novel PKCs is second messenger-independent and do not bind Ca^{2+}; and probably plays a role in protein-protein interactions (Cho and Stahelin, 2006). The C2 domains share a common tertiary structure comprised of eight anti-parallel β-strands connected by variable loops formed by sequences at the opposite ends of the primary structure to form a pocket (Sutton et al., 1995). Broadly, the C2 domains share more structural homology in the core β-sandwich portion (which plays a more structural scaffolding role) than in the loop

sequences (which are more divergent and dictate functional specificity). Structural studies of the conventional isozyme PKCα suggest that 2-3 Ca^{2+} ions (3 in the case of PKCβ C2 domains) bind in a highly cooperative manner to several highly conserved aspartate residues in the calcium-binding loops (Medkova and Cho, 1998; Sutton and Sprang., 1998).

Binding of Ca^{2+} in the C2 domain of conventional PKCs causes a dramatic increase in the affinity of PKC for anionic membranes. This membrane interaction shows little selectivity for phospholipid headgroup, beyond the requirement for negative charge. Ca^{2+} binding effectively neutralizes the high negative electrostatic potential at the Ca^{2+}-binding site. However, mutation of the acidic residues in the Ca^{2+}-binding site revealed that this charge neutralization is not sufficient to effect membrane binding (Edwards and Newton, 1997). Also, novel C2 domains which are lacking key aspartic acid residues do not bind anionic membranes constitutively. But, the actual coordination of Ca^{2+} is required for membrane binding, suggesting that Ca^{2+} acts as a bridge between the C2 domain and phospholipid headgroups (Verdaguer et al., 1999).

The Kinase Domain

The kinase core of the PKCs and two other AGC family members, protein kinase A (PKA) and protein kinase B (PKB)/Akt, are highly conserved with more than 40% sequence similarity, with most of the residues that are invariant across the AGC kinase family members clustering at sites of nucleotide binding or catalysis and differing primarily in the C-terminal tail (Orr and Newton, 1994; Gould and Newton, 2008, Steinberg, 2008). This tail contains vital conserved regions that make key contacts with the kinase domain which is critical for the catalytic activity (Knighton et al., 1991). With the recent publication of crystal structures of several phosphorylated PKC catalytic domains bound to ATP-competitive inhibitors ((PKCβII complexed with 2-methyl-1*H*-indol-3yl-BIM-1, PKCθ bound to staurosporine, and PKCι complexed with BIM-1, i.e, a PKC isoform representative of each subfamily), many of the early assumptions have been validated (Grodsky et al., 2006; Messerschmidt et al., 2005; Xu et al., 2004). Like other AGC kinases, the PKC kinase domain is a bilobal structure with a cleft between the two lobes (Johnson and Lewis, 2001). The smaller N-terminal lobe is composed primarily of β-sheets and contains the characteristic glycine-rich ATP-binding loop with the consensus GXGXXG sequence (a structural hallmark of protein kinases and nucleotide binding proteins) and an invariant lysine which structures the enzyme for phosphoryl-transfer. The C-

terminal lobe is predominantly α-helical and contains the activation loop segment that positions magnesium and peptide substrates (Steinberg, 2008). A "gatekeeper" residue (a conserved as a large hydrophobic amino acid in the human kinome) connects the two lobes of the kinase domain and control access to a preexisting cavity in the ATP binding pocket.

The sequence of PKA terminates with a phenylalanine that tucks into the protein. All PKC isozymes have this phenylalanine which is immediately followed by a conserved phosphorylation site named the hydrophobic phosphorylation motif. This phosphorylation motif is then followed by a short sequence unique to each isozyme. This carboxyl-terminal sequence is critical to the regulation of PKC as it forms the docking site for the upstream kinase, PDK1, and, as such, is essential for the function of the enzyme (Su et al., 1993).

1.9.3. Regulation of the PKC Signal Propagation

The multidomain PKC is under acute structural and spatial regulation. PKC must be properly primed and located to effectively transduce the extracellular signals to downstream targets and achieve optimal signaling for its physiological function. Perturbation of the phosphorylation state, conformation, or localization can impair the desired signaling events.

Regulation by Phosphorylation

To gain catalytic competence and correct intracellular localization, the PKC enzyme must first be properly processed by a series of three ordered phosphorylations in the catalytic domain (Newton, 2001). Unphosphorylated forms accumulate in the detergent-insoluble fraction of cells and are catalytically inactive (Keranen et al., 1995).

The purification (Alessi et al., 1997a; Stokoe et al., 1997) and subsequent cloning (Alessi et al., 1997b; Stephens et al., 1998) of the activation segment kinase for PKB/Akt provided a major advance in cell signaling, as it soon became apparent that this novel kinase, named phosphoinsitide-dependent kinase 1 (PDK1), provided the priming phosphorylation for many other key members of the AGC protein kinase superfamily. In particular, PDK1 was quickly shown to be the upstream kinase for conventional (Dutil et al. 1998), novel (Le Good et al., 1998; Cenni et al., 2002) and atypical (Le Good et al., 1998; Chou et al., 1998) PKC family members.

The three phosphorylation positions are conserved among the AGC superfamily of kinases including the PKC family members. The first phosphorylation occurs on a loop near the

entrance to the catalytic site, called the activation loop; the second position occurs at the apex of a turn and has been named the turn motif; the third is flanked by hydrophobic residues and is referred to as the hydrophobic motif (Newton, 2001).

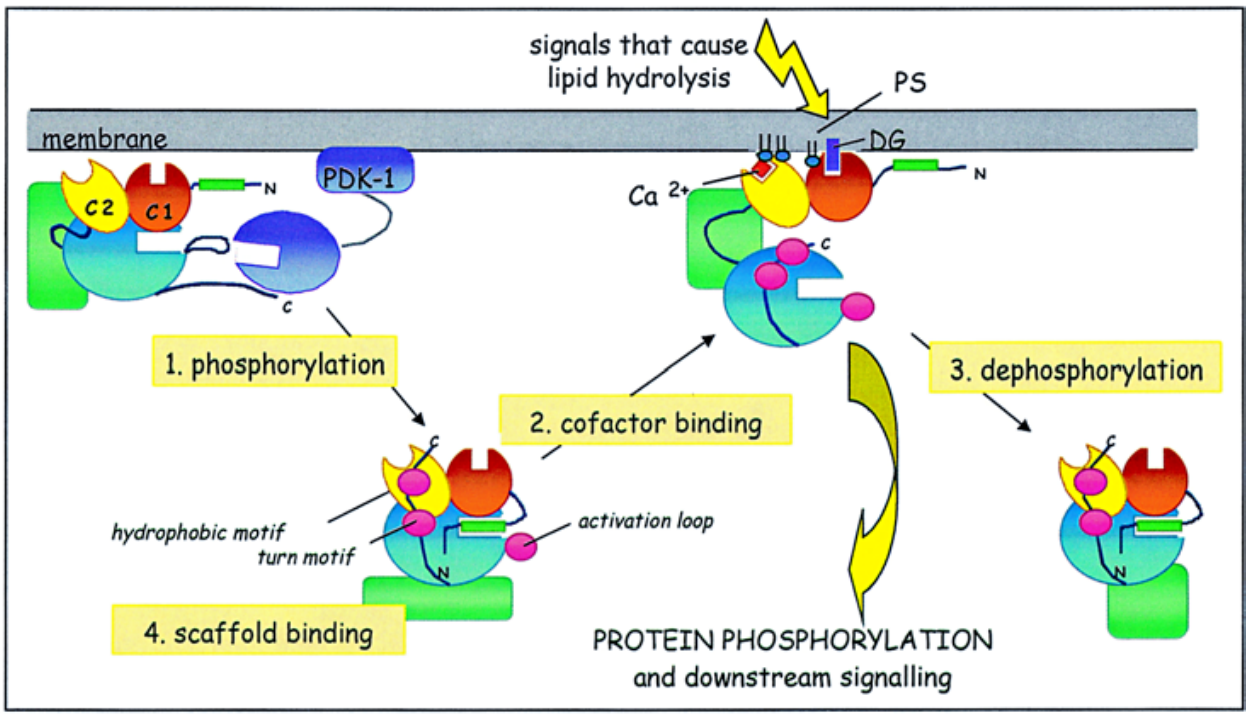

Figure 1.7 Model illustrating how the function and subcellular location of PKC is under the coordinated regulation. 1. phosphorylation mechanisms, **2.** Cofactor binding, **3.** activation-dependent dephosphorylation mechanisms, and **4.** binding to scaffold proteins. Pink circles represent phosphorylation sites. The upstream kinase, PDK1, is shown in purple. Shaded green boxes represent scaffold proteins for the various activation states of protein kinase C. Note that engaging the C2 (yellow) and C1 (orange) domains on the membrane locks PKC in the active conformation. In this conformation, the pseudosubstrate (green rectangle) is removed from the substrate-binding cavity in the kinase domain (blue circle) allowing substrate phosphorylation and down-stream signaling. (Reproduced with kind permission of Springer Science+Business Media and Newton AC from Newton, 2003b *Methods Mol. Biol.* 233:3-7, Figure 2)

Activation loop Phosphorylation

Newly synthesized PKCs are believed to be loosely tethered to the membrane in an open conformation in which the pseudosubstrate is out of the active site with the activation loop site

exposed and accessible by PDK1 (Figure 1.7; Dutil et al., 1998; Dutil and Newton 2000). PDK1 docks to the C-terminal tail of PKC and phosphorylates at a threonine residue in the activation loop. This phosphorylation introduces a negative charge that aligns residues in the catalytic pocket and stabilizes the active conformation of the enzyme. This is critical for the maturation of PKC as it allows for autophosphorylation at the C-terminus and reveals access to the binding site (Nolen et al., 2004; Orr and Newton 1994b). Once the activation loop is phosphorylated, phosphate at this site becomes dispensable for activity (Newton, 2001). Thus, phosphorylation at the activation loop is just a primer for the subsequent phosphorylations at the turn and hydrophobic motif, but this is the rate limiting step in the processing of PKC. Unphosphorylated or dephosphorylated species of PKC are rapidly degraded. Thus in cells deficient in PDK1 have grossly reduced PKC levels (Balendran et al. 2000).

Turn motif Phosphorylation

Once PKC is phosphorylated by PDK1 at the activation loop, the enzyme undergoes rapid phosphorylation at the turn motif site (threonine residues for conventional PKCs) (Newton 2001). This is an autophosphorylation reaction for the conventional PKCs. In the PKCβII structure, this phosphorylation forms ionic contacts with basic residues on opposing β strands (Grodsky et al., 2006). Phosphorylation of the turn motif is indispensable to maintain catalytic competence as dephosphorylation at this position abolishes activity (Edwards et al., 1999; Bornancin and Parker, 1996). Phosphate on the turn motif locks PKC in a thermally stable conformation in the inactive state which is relatively resistant to phosphatases (Newton, 2001). Additionally, the turn motif may serve as a docking site for protein-protein interactions particularly with 14-3-3 proteins (Yaffe et al., 1997).

Hydrophobic Motif Phosphorylation

The final step in the maturation and processing of PKC is autophosphorylation at the C-terminal hydrophobic FXXFS/TF/Y motif (a serine/threonine flanked by hydrophobic residues), with an intramolecular mechanism shown for PKCβII (Behn-Krappa and Newton, 1999). Functionally, phosphorylation at the hydrophobic motif is not required; however biochemical studies have revealed that phosphorylation of this site increases thermal stability and phosphatase resistance, and affects subcellular localization (Edwards and Newton, 1997b; Bornancin and Parker, 1997). The hydrophobic motif also provides docking site for PDK (Newton, 2003).

Agonist-Evoked Autophosphorylations and Tyrosine Phosphorylations

Other than the processing autophosphorylations, novel autophosphorylation sites have been identified in PKCs in response to agonist-evoked autophosphorylation (Gould and Newton, 2008). These additional autophosphorylation sites are isozyme-specific and mark activated PKC. These autophosphorylations can fine-tune the differences and functional roles of each isozyme and provide an additional layer of regulation.

PKCs from all subfamilies are phosphorylated on tyrosine (Konishi et al., 1997). This phosphorylation is emerging as additional mechanism to fine-tuning PKC activity and may also serve in localization of PKC (Gould and Newton, 2008).

Regulation by Lipid Second Messengers

The characteristic of PKC activation in cells is its translocation to cellular membranes. The mature PKC, after the phosporylations in the kinase domain, is localized to the cytosol where it is in an inactive state with the pseudosubstrate occupying the substrate binding cavity (Figure 1.7) (Dutil and Newton, 2000). When extracellular signals cause the activation of phospholipase C (PLC) it leads to the hydrolysis of PIP2 generating DAG and IP3. IP3 causes the release of Ca^{2+} from the intracellular stores. In case of conventional PKCs, Ca^{2+} binds the C2 domain and pretargets PKC to membrane (Newton, 2001), and this increases the probability of C1 domain finding the membrane-bound DAG (Nalefski and Newton, 2001). The coordinated engagement of both C1 and C2 domains on membranes provides the energy to release the autoinhibitory pseudosubstrate from the substrate binding cavity (Orr et al., 1992). Now in this open conformation (Figure 1.7), PKC can bind its substrates and initiate downstream signaling events. The phorbol esters like TPA cause the translocation and activation of PKCs in the absence of Ca^{2+} as the affinity of the C1 domain for phorbol ester-containing membranes is two orders of magnitude higher than the DAG-containing membranes (Newton, 2001). Moreover, the DAG mediated membrane-recruitment and activation is short-lived as DAG is rapidly metabolized, whereas the more stable phorbol esters result in constitutive activation of PKC.

The activity of all isoforms of PKC is also regulated by phosphatidylserine (PS), a plasmamembrane lipid. In the absence of DAG, PKC displays little selectivity for PS, but the presence of DAG causes PKC to bind PS-containing membranes (Newton and Keranen, 1994; Mosior and Epand, 1993). Thus, the recognition of PS depends on C1 domain ligand.

PKCγ, like other conventional PKCs, is readily activated by DAG in the elevated Ca^{2+} levels, but it can also be translocated to the plasma membrane in Ca^{2+}concentrations which were insufficient to activate PKCα, owing to its two flexible and readily accessible C1 domains (Ananthanarayanan et al., 2003). Novel PKCs, which do not have a Ca^{2+}-binding C2 domain, lack the membrane-pretargeting event and compensate for it by having a C1 domain that binds DAG with an order of magnitude higher affinity than the C1 domain of conventional PKCs. A single residue, present as tryptophan, in the C1B domain of novel PKCs confers this high-affinity binding to DAG, whereas the presence of corresponding tyrosine residue in the conventional PKCs confers low-affinity DAG bindning (Dries et al., 2007). Furthermore, it was found that PKCs with Tyr have a 2-fold selectivity for PS (Dries et al., 2007).

Regulation by Scaffolding Proteins

Because of their ability to interact with partner proteins there is yet another way of PKC regulation is achieved by scaffolding proteins. Once activated or released from their docking partner PKCs can interact with numerous cellular components. PKCs can interact with the plasma membrane, golgi, cytoskeleton, mitochondria and cell nuclei (Gallegos et al., 2006). Scaffolding proteins position PKC near its activators and substrates or at a particular cellular compartment and allow for isozyme-specific signaling (Gould and Newton, 2008). Since PKCs often interact with distinct docking/scaffolding proteins (14-3-3 for PKCγ and RACK5 [receptor for activated C-kinase] for PKCε) peptides derived from the sequences of different PKC isoforms make potent inhibitors and activators (Nguyen et al., 2004).

1.9.4. Signal Termination

The molecular mechanisms that dictate the signal termination and downregulation of PKCs are not as well understood as the activation and signal propagation mechanisms. Just as translocation to the membrane initiates activation, translocation from the membrane initiates the termination process. It has been proposed that PKC must maintain its priming autophosphorylations at the C-terminus in order to disengage from the membrane (Feng et al., 2000). Tyrosine phosphorylation may also play a role in the reverse translocation process (Takahashi et al., 2003). Diacylglycerol kinases (DGKs) phosphorylate DAG, converting it into phosphatidic acid (Luo et al., 2004). Thus, DGKs, by removing the activating cofactor, serve an opposing role to PKCs in signaling pathways. The open conformation of the activated PKC is susceptible to cleavage by both

proteases and dephosphorylation by phosphatases. Phosphorylation of PKC is critical for maintenance of catalytic competence. Dephosphorylation of the three processing sites (activation loop, turn motif, hydrophobic motif) of PKC inactivates the kinase. Studies show that chronic activation of PKC results in a fully dephosphorylated, inactive kinase, which precedes its degradation (Hansra et al., 1999; Lee et al., 1996). This dephosphorylated form accumulates in a cytoskeletal, detergent-insoluble fraction of cells. This mechanism is the classical model of PKC downregulation. The newly discovered protein phosphatase 2C (PP2C) family of phosphatases, the PHLPP family (for PH domain Leucine-rich repeat Protein Phosphatase), has recently been shown to regulate the phosphorylation state, and thus PKC levels (Brognard and Newton, 2008; Gao et al., 2008).

1.9.5. PKC Isoforms in the Lens

In 1993, PKCα and PKCγ were reported for the first time as the major PKC isoforms detected in cultured bovine lens epithelial cells (Gonzalez et al., 1993). PKC isoforms α, γ, ε and ι have been detected in whole chicken lens sections localized to the epithelium and the bow region. PKCγ and PKCε are present in the fiber cells in chick and mouse lenses with some PKCγ localized at the plasma membrane (Berthoud et al., 2000, Barnett et al., 2008). PKCγ has also been detected in the rat lens epithelium and cortex, but PKCα was found only in the epithelial cells and not in fiber cells (Saleh et al., 2001). The rabbit lens epithelial cell line, N/N1003A, expresses PKCα, β, γ, and ε isoforms. As shown in this study PKCγ is detected in the mouse lens fiber cells along with epithelial cells.

Effects of PKC Activation on Lens GJIC

Given the extended lifetime of cells in the lens and the critical role played by the gap junctions in the lens circulation, the proper regulation of GJIC in the lens is critical especially in situations like stress and cell injury. Phosphorylation plays a significant role in the regulation of GJIC. Like other tissues in the body, the connexins expressed in the lens are also PKC substrates, thus under PKC regulation (Solan and Lampe, 2009, Laird, 2005). PKC-dependent phosphorylation of Ser368 in Cx43 leads to decreased intercellular communication owing to a change in single channel behavior (Lampe et al., 2000) and altered permeability (Ek-Vitorin et al., 2006). Phosphorylation at Ser368 has also been implicated in trafficking/assembly of gap

junctions (Solan et al., 2003). Treatment of lens epithelial cells with phorbol esters also revealed similar results leading to a reduction in intercellular communication associated with Cx43 phosphorylation (Reynhout et al., 1992; Tenbroek et al., 1997; Long et al., 2007). TPA-induced phosphorylation of Cx43 targets the protein for proteasomal degradation in cultured bovine epithelial cells (Girão and Pereira, 2003). In cultures of ovine lens epithelial cells, TPA treatment caused a gradual disappearance of Cx43 from gap junction plaques and a transient decrease in Cx43 levels, and a decrease in Cx49 mRNA levels along with the disappearance of the protein from gap junction plaques (Tenbroek et al., 1997). But in N/N1003A cells, PKC activation by TPA leads to a decrease in the gap junction plaques without changes in Cx43 protein levels (Wagner et al., 2002). Similar results were obtained in N/N1003A cells after treatment with DAG, insulin-like growth factor 1 (IGF1), or lens epithelium-derived growth factor (LEDGF), indicating that IGF1 and LEDGF may cause the generation of the second messengers required for PKC activation (Nguyen et al., 2003; Lin et al., 2003).

The effects of phorbol esters and PKC activation on the fiber cell connexins (Cx46 and Cx50) have been studied in lentoid-containing cultures and lens organ cultures. TPA treatment of cultures from chicken lenses decreases dye coupling between lentoid cells (Berthoud et al., 2000). Activation of PKCγ and an increased phosphorylation of Cx56 on Ser118 suggest that phosphorylation probably leads to channel closure (Berthoud et al., 1997). Rat Cx46 hemichannels has also been shown to be modulated by PKC phosphorylation (Ngezahayo et al., 1998). PKCg and Cx46 co-localize in the cortical and equatorial regions of rat lenses with PKCg causing the phosphorylation of Cx46 (Saleh et al., 2001). There may be some species differences in the phorbol ester induced uncoupling of fiber cell communication as Cx49, the ovine Cx50 ortholog, appears not to be a substrate for PKC (Arneson et al., 1995); while Cx45.6, the chicken ortholog, appears to be a good PKC substrate (Jiang and Goodenough, 1998). Treatment of whole rat lenses with TPA leads to an increase in PKCγ activity associated with a decrease in Cx50 in gap junctions, an increase in Cx50 in the nonjunctional plasma membrane (hemichannels), and a decrease in Lucifer yellow transfer in the lens cortex measured in whole lenses. Co-precipitation of PKCγ with caveolin1 after TPA treatment suggests that PKCγ translocates to caveolin1-containing membrane fractions which also contain Cx46 and Cx50. These results indicate that TPA-induced activation of PKC leads to undocking and dispersion of Cx50 hemichannels (Zampighi et al., 2005).

Oxidative Stress Activation of PKC in the Lens

Oxidative stress may be linked to changes in connexins and gap junctions. H_2O_2 leads to differential phosphorylation of Cx56 in chicken lentoid-containing cultures (Berthoud and Beyer, 2009). Treatment of N/N1003A cells with H_2O_2 leads to an increase in PKCγ activity, an effect that appears to result from direct oxidation of the enzyme with formation of disulfide bonds. Activation of PKCγ resulted in increased phosphorylation of Cx43 in Ser368, a decrease in the number of gap junction plaques, and a decrease in dye coupling (Lin and Takemoto, 2005). H_2O_2 induced activation of PKCγ and increased phosphorylation of Cx46 and Cx50 in rat lenses (Lin et al., 2004).

Oxidative stress corresponds to an imbalance between the rate of reactive oxygen species (ROS) production and their rate of degradation, leading to accumulation of oxidized cell components. When this exceeds the cell's ability to repair these components, or the oxidizing stress is too high, apoptosis occurs. Gap junction channels in the lens may propagate apoptosis signals through a bystander-like mechanism as proposed previously for other cell types (Colombo et al., 1995; Lin et al., 1998). However, other studies suggest a role for PKC-dependent closure of gap junction channels as a protective/survival mechanism, because the induced channel closure might prevent the intercellular transmission of apoptotic signals (Lin and Takemoto, 2005). Thus, PKC activation by H_2O_2 can either generate apoptotic signals (that may be propagated through gap junction channels) or lead to closure of those channels (blocking that propagation).

PKCγ in the Lens and the KO Mouse Model

PKCγ is detected in eye tissue, including retina and lens epithelium and cortex as discussed above. It is thought to be involved in the formation of neural plasticity and memory, prevention of brain ischemia and playing a protective role in cell survival.

In 1993, Abeliovich et al. used embryonic stem cell technique to generate the PKCγ knockout (KO) mice by homologous recombination into the germline (Abeliovich et al., 1993). Since then this mouse model has been reported to have slight ataxia, less memory, reduced neuropathic pain, decreased anxiety, impaired long-term potentiation, enhanced opioid responses, increased alcohol consumption and less protection against brain ischemia. Using this KO mouse to determine the role played by PKCγ in the eye, our lab has previously reported that hyperbaric

oxygen treatment causes significant damage to the KO retina (Yevseyenkov et al., 2009). More importantly, KO lenses were demonstrated to be more susceptible to H_2O_2 induced oxidative stress damage leading to lens opacification (Lin et al. 2006). But the effect of the absence of PKCγ on gap junction channel conductance inside the lens and the effect on the connexin phosphorylation had not been completely investigated. These are the questions answered in this dissertation.

1.10. References

Abeliovich, A., Chen, C., Goda, Y., Silva, A. J., Stevens, C. F. and Tonegawa, S. (1993) Modified hippocampal long-term potentiation in PKCgamma-mutant mice. *Cell* 75,1253 -1262.

Albert, D., Jakobiec, F. (1994) Principle and Practice of Ophthalmology. W.B. Saunders Company: Philadelphia.

Alessi, D.R., James, S.R., Downes, C.P., Holmes, A.B., Gaffney, P.R., Reese, C.B., Cohen, P. (1997a) Characterization of a 3-phosphoinositide-dependent protein kinase which phosphorylates and activates protein kinase Balpha. *Curr. Biol*. 7(4):261-9.

Alessi, D. R., Deak, M., Casamayor, A., Caudwell, F. B., Morrice, N., Norman, D. G., Gaffney, P., Reese, C. B., MacDougall, C. N., Harbison, D. et al. (1997b) 3-Phosphoinositide-dependent protein kinase-1 (PDK1) : structural and functional homology with the *Drosophila* DSTPK61 kinase. *Curr. Biol. 7*, 776-789.

Alkon, D.L. (1989). Memory storage and neural systems. Scientific Am., 261, 42-50.

Alexander, D. B., and Goldberg, G. S. (2003). Transfer of biologically important molecules between cells through gap junction channels. *Curr Med Chem* 10, 2045-2058.

Ananthanarayanan, B., Stahelin, R.V., Digman, M.A., Cho, W. (2003) Activation mechanisms of conventional protein kinase C isoforms are determined by the ligand affinity and conformational flexibility of their C1 domains. *J. Biol. Chem.* 278(47):46886-94.

Arneson ML, Cheng HL, Louis CF. (1995) Characterization of the ovine-lens plasma-membrane protein-kinase substrates. *Eur J Biochem.* 234(2):670-9.

Ashendel, C.L. (1985). The phorbol ester receptor: A phospholipid-regulated kinase. Biochim. Biophys. Acta, 822, 219-242.

Baldo, G.J., Mathias, R.T. (1992) Spatial variations in membrane properties in the intact rat lens. *Biophys. J.* 63(2):518-29.

Balendran, A., Hare, G.R., Kieloch, A., Williams, M.R., Alessi, D.R. (2000) Further evidence that 3-phosphoinositide-dependent protein kinase-1 (PDK1) is required for the stability and phosphorylation of protein kinase C (PKC) isoforms. *FEBS Lett.* 484(3):217-23.

Barnett, M., Lin, D., Akoyev, V., Willard, L., Takemoto, D. (2008) Protein kinase C epsilon activates lens mitochondrial cytochrome c oxidase subunit IV during hypoxia. *Exp. Eye Res.* 86(2):226-34.

Baruch A, Greenbaum D, Levy ET, Nielsen PA, Gilula NB, Kumar NM, Bogyo M. (2001) Defining a link between gap junction communication, proteolysis, and cataract formation. *J. Biol. Chem.* 276(31):28999-9006.

Bassnett, S., Beebe, D.C. (1992) Coincident loss of mitochondria and nuclei during lens fiber cell differentiation. *Dev. Dyn.* 194(2):85-93.

Bassnett, S., Kuszak, J.R., Reinisch, L., Brown, H.G., Beebe, D.C. (1994) Intercellular communication between epithelial and fiber cells of the eye lens. *J. Cell Sci.* 107 (Pt 4):799-811.

Bassnett, S. (1995) The fate of the Golgi apparatus and the endoplasmic reticulum during lens fiber cell differentiation. *Invest. Ophthalmol. Vis. Sci.* 36(9):1793-803.

Benedetti, E.L., Emmelot, P. (1968) Hexagonal array of subunits in tight junctions separated from isolated rat liver plasma membranes. *J. Cell Biol.* 38(1):15-24.

Benedetti EL, Dunia I, Bloemendal H. (1974) Development of junctions during differentiation of lens fibers. *Proc. Natl. Acad. Sci. U S A.* 71(12):5073-7.

Benedetti, E.L., Dunia, I., Bentzel, C.J., Vermorken, A.J., Kibbelaar, M., Bloemendal, H. (1976) A portrait of plasma membrane specializations in eye lens epithelium and fibers. *Biochim. Biophys. Acta.* 457(3-4):353-84.

Berthoud, V.M., Beyer, E.C., Kurata, W.E., Lau, A.F., Lampe, P.D. (1997) The gap-junction protein connexin 56 is phosphorylated in the intracellular loop and the carboxy-terminal region. *Eur. J. Biochem.* 244(1):89-97.

Berthoud, V.M., Westphale. E.M., Grigoryeva, A., Beyer, E.C. (2000) PKC isoenzymes in the chicken lens and TPA-induced effects on intercellular communication. *Invest. Ophthalmol. Vis. Sci.* 41(3):850-8.

Berthoud VM, Beyer EC. (2009) Oxidative stress, lens gap junctions, and cataracts. *Antioxid. Redox. Signal*. 11(2):339-53.

Behn-Krappa, A., Newton, A.C. (1999) The hydrophobic phosphorylation motif of conventional protein kinase C is regulated by autophosphorylation. *Curr. Biol.* 9(14):728-37.

Bettelheim, F.A., Siew, E.L. (1983) Effect of change in concentration upon lens turbidity as predicted by the random fluctuation theory. *Biophys. J.* 41(1):29-33.

Bloemendal H, Zweers A, Vermorken F, Dunia I, Benedetti EL. (1972) The plasma membranes of eye lens fibres. Biochemical and structural characterization. *Cell Differ.* 1(2):91-106.

Bloemendal H, Vermorken AJ, Kibbelaar M, Dunia I, Benedetti EL. (1977) Nomenclature for the polypeptide chains of lens plasma membranes. *Exp. Eye Res.* 24(4):413-5.

Bloemendal, H., de Jong, W., Jaenicke, R., Lubsen, N.H., Slingsby, C., Tardieu, A. (2004). Ageing and vision: structure, stability and function of lens crystallins. *Prog Biophys Mol Biol.* 86(3),407-85.

Bornancin, F., Parker, P.J. (1996) Phosphorylation of threonine 638 critically controls the dephosphorylation and inactivation of protein kinase Calpha. *Curr. Biol*. 6(9):1114-23.

Bornancin, F., Parker, P.J. (1997) Phosphorylation of protein kinase C-alpha on serine 657 controls the accumulation of active enzyme and contributes to its phosphatase-resistant state. *J. Biol. Chem.* 272(6):3544-9.

Brightman, M.W., Reese, T.S. (1969) Junctions between intimately apposed cell membranes in the vertebrate brain. *J. Cell Biol.* 40(3):648-77.

Brognard, J., Newton, A.C. (2008) PHLiPPing the switch on Akt and protein kinase C signaling. *Trends Endocrinol. Metab.* 19(6):223-30.

Brown, H.G., Pappas, G.D., Ireland, M.E., Kuszak, J.R. (1990) Ultrastructural, biochemical, and immunologic evidence of receptor-mediated endocytosis in the crystalline lens. *Invest. Ophthalmol. Vis. Sci.* 31(12):2579-92.

Bukauskas, F. F., Jordan, K., Bukauskiene, A., Bennett, M. V., Lampe, P. D., Laird, D. W., and Verselis, V. K. (2000). Clustering of connexin 43-enhanced green fluorescent protein gap junction channels and functional coupling in living cells. *Proc Natl Acad Sci U S A* **97**, 2556-2561.

Candia, O.A., Bentley, P.J., Mills, C.D., Toyofuku, H. (1970). Asymmetrical distribution of the potential differences in the toad lens. *Nature (London)* 227, 852–853.

Candia, O.A., Bentley, P.J., Mills, C.D. (1971). Short-circuit current and active Na transport across isolated lens of the toad. *Am. J. Physiol.* 220, 539–564.

Candia, O.A., Zamudio, A.C., (2002) Regional distribution of the Na(+) and K(+) currents around the crystalline lens of rabbit. Am. J. Physiol., Cell Physiol. 282, C252–C262.

Cenni, V., Doppler, H., Sonnenburg, E. D., Maraldi, N., Newton, A. C. and Toker, A. (2002) Regulation of novel protein kinase C epsilon by phosphorylation. Biochem. J. *363*, 537-545.

Chandy, G., Zampighi, G.A., Kreman, M., Hall, J.E. (1997) Comparison of the water transporting properties of MIP and AQP1. *J. Membr. Biol.* 159, 29–39.

Cho, W. (2001) Membrane targeting by C1 and C2 domains. *J. Biol. Chem.* 276(35):32407-10.

Cho, W., Stahelin, R.V. (2006) Membrane binding and subcellular targeting of C2 domains. *Biochim. Biophys. Acta.* 1761(8):838-49.

Chou, M.M., Hou, W., Johnson, J., Graham, L.K., Lee, M.H., Chen, C.S., Newton, A.C., Schaffhausen, B.S., Toker, A. (1998) Regulation of protein kinase C zeta by PI 3-kinase and PDK-1. *Curr. Biol.* 8(19):1069-77.

Colombo BM, Benedetti S, Ottolenghi S, Mora M, Pollo B, Poli G, Finocchiaro G. (1995) The "bystander effect": association of U-87 cell death with ganciclovir-mediated apoptosis of nearby cells and lack of effect in athymic mice. *Hum. Gene Ther*. 6(6):763-72.

Cooper, K., Mathias, R. T., Rae J.L. (1991) The physiology of lens junctions. In: Biophysics of Gap Junction Channels, edited by C. Peracchia, Boca Raton FL: CRC, 57-74.

Coussens L, Parker PJ, Rhee L, Yang-Feng TL, Chen E, Waterfield MD, Francke U, Ullrich A. (1986) Multiple, distinct forms of bovine and human protein kinase C suggest diversity in cellular signaling pathways. *Science* 233(4766):859-66.

Crow, J.M., Atkinson M.M., Johnson, R.G. (1994) Micromolar levels of intracellular calcium reduce gap junctional permeability in lens cultures. *Invest. Ophthalmol. Vis. Sci.* 35(8):3332-41.

Cutler, JR., R.E., Maizels, E.T., Brooks, E.J., Mizuno, K., Ohno, S., Hunzicker-Dunn, M. (1993). Regulation of δ protein kinase C during rat ovarian di€erentiation. Biochim. Biophys. Acta. 1179, 260-270.

Dahm R., Van Marle J., Prescott A.R., and Quinlan R.A. (1999) Gap junctions containing α8-connexin (MP70) in the adult mammalian lens epithelium suggests a re-evaluation of its role in the lens. *Exp. Eye Res.* 69: 45–56.

Davies, M.J., Truscott, R.J. (2001) Photo-oxidation of proteins and its role in cataractogenesis. *J. Photochem. Photobiol. B.* 63(1-3):114-25.

DeBlack, S.S. (2003) Cigarette smoking as a risk factor for cataract and age-related macular degeneration: a review of the literature. Optometry 74(2):99-110.

Delaye, M., Tardieu, A. (1983) Short-range order of crystallin proteins accounts for eye lens transparency. *Nature* 302(5907):415-7.

Derham, B.K., Harding, J.J. (1999) Alpha-crystallin as a molecular chaperone. *Prog. Retin. Eye Res.* 18(4):463-509.

Donaldson, P., Kistler, J., Mathias, R.T. (2001) Molecular solutions to mammalian lens transparency. *News Physiol. Sci.* 16:118-23.

Dries, D.R., Gallegos, L.L., Newton, A.C. (2007) A single residue in the C1 domain sensitizes novel protein kinase C isoforms to cellular diacylglycerol production. *J. Biol. Chem.* 282(2):826-30.

Duke-Elder, S. and Wybar, K. (1961) The refractive media: *Systems of Ophthalmology* CV Mosby: St Louis.

Duncan, G. (1969). The site of the ion restricting membranes in the toad lens. *Exp. Eye Res.* 8, 406–412.

Dutil, E.M., Toker, A., Newton, A.C. (1998) Regulation of conventional protein kinase C isozymes by phosphoinositide-dependent kinase 1 (PDK-1). *Curr. Biol*. 8(25):1366-75.

Dutil, E.M., Newton, A.C. (2000) Dual role of pseudosubstrate in the coordinated regulation of protein kinase C by phosphorylation and diacylglycerol. *J. Biol. Chem.* 275(14):10697-701.

Eckert, R. (2002) pH gating of lens fibre connexins. *Pflugers Arch.* 443(5-6),843-51.

Edwards, A.S., Newton, A.C. (1997) Regulation of protein kinase C betaII by its C2 domain. *Biochemistry* 36(50):15615-23.

Edwards, A.S., Newton, A.C. (1997b) Phosphorylation at conserved carboxyl-terminal hydrophobic motif regulates the catalytic and regulatory domains of protein kinase C. *J. Biol. Chem.* 272(29):18382-90.

Edwards, A.S., Faux, M.C., Scott, J.D., Newton, A.C. (1999) Carboxyl-terminal phosphorylation regulates the function and subcellular localization of protein kinase C betaII. *J. Biol. Chem.* 274(10):6461-8.

Eisenberg, R.S., Rae, J.L. (1976). Current–voltage relationships in the crystalline lens. *J. Physiol.* 262, 285–300.

Eisenberg, R.S., Barcilon, V., Mathias, R.T. (1979). Electrical properties of spherical syncytia. *Biophys. J.* 25, 151–180.

Ek-Vitorin, J.F., King, T.J., Heyman, N.S., Lampe, P.D., Burt, J.M. (2006) Selectivity of connexin 43 channels is regulated through protein kinase C-dependent phosphorylation. *Circ. Res.* 98(12):1498-505.

Evans, W. H., De Vuyst, E., and Leybaert, L. (2006). The gap junction cellular internet: connexin hemichannels enter the signalling limelight. *Biochem J* 397, 1-14.

Faulkner-Jones, B., Zandy, A.J., Bassnett, S. (2003) RNA stability in terminally differentiating fibre cells of the ocular lens. *Exp. Eye Res.* 77(4):463-76.

Feng, X., Becker, K.P., Stribling, S.D., Peters, K.G., Hannun, Y.A. (2000) Regulation of receptor-mediated protein kinase C membrane trafficking by autophosphorylation. *J. Biol. Chem.* 275(22):17024-34.

Ferrufino-Ponce, Z.K., Henderson, B.A. (2006) Radiotherapy and cataract formation. *Semin. Ophthalmol.* 21(3):171-80.

Fischbarg, J., Diecke, F.P., Kuang, K., Yu, B., Kang, F., Iserovich, P., Li, Y., Rosskothen, H., Koniarek, J.P. (1999) Transport of fluid by lens epithelium. *Am. J. Physiol.* 276(3 Pt 1):C548-57.

Fournier, D.J., Patterson, J.W. (1971) Variations in ATPase activity in the development of experimental cataracts. *Proc. Soc. Exp. Biol. Med.* 137(3):826-32.

Gallegos, L.L., Kunkel, M.T., Newton, A.C. (2006) Targeting protein kinase C activity reporter to discrete intracellular regions reveals spatiotemporal differences in agonist-dependent signaling. *J. Biol. Chem.* 281(41):30947-56.

Gao, J., Sun, X., Yatsula, V., Wymore, R.S., Mathias, R.T., (2000) Isoformspecific function and distribution of Na/K pumps in the frog lens epithelium. *J. Membr. Biol.* 178, 89–101.

Gao J, Sun X, Martinez-Wittinghan FJ, Gong X, White TW, Mathias RT. (2004) Connections between connexins, calcium, and cataracts in the lens. *J. Gen. Physiol.* 124(4):289-300.

Gao, T., Brognard, J., Newton, A.C. (2008) The phosphatase PHLPP controls the cellular levels of protein kinase C. *J. Biol. Chem.* 283(10):6300-11.

Gao, Y. and Spray, D.C. (1998) Structural changes in lenses of mice lacking the gap junction protein connexin43. *Invest. Ophthalmol. Vis. Sci.* 39(7): 1198-1209.

Girão, H., Pereira, P. (2003) Phosphorylation of connexin 43 acts as a stimuli for proteasome-dependent degradation of the protein in lens epithelial cells. *Mol. Vis*. 9:24-30.

Gong X, Li E, Klier G, Huang Q, Wu Y, Lei H, Kumar NM, Horwitz J, Gilula NB. (1997) Disruption of alpha3 connexin gene leads to proteolysis and cataractogenesis in mice. *Cell* 91(6):833-43.

Gonzalez, K., Udovichenko, I., Cunnick, J., Takemoto, D.J. (1993) Protein kinase C in galactosemic and tolrestat-treated lens epithelial cells. *Curr. Eye Res.* 12(4):373-7.

Goldberg, G.S., Valiunas, V., Brink, P.R. (2004) Selective permeability of gap junction channels. *Biochim. Biophys. Acta.* 1662(1-2):96-101.

Goodenough DA, Revel JP. (1970) A fine structural analysis of intercellular junctions in the mouse liver. *J. Cell Biol.* 45(2):272-90.

Goodenough, D.A. (1974) Bulk isolation of mouse hepatocyte gap junctions. Characterization of the principal protein, connexin. *J. Cell Biol.* 1974 May;61(2):557-63.

Goodenough, D.A. (1976) In vitro formation of gap junction vesicles. *J. Cell Biol.* 68(2):220-31.

Goodenough, D.A. (1979) Lens gap junctions: a structural hypothesis for nonregulated low-resistance intercellular pathways. *Invest. Ophthalmol. Vis. Sci.* 18(11):1104-22.

Goodenough, D.A., Dick, J.S. 2nd, Lyons, J.E. (1980) Lens metabolic cooperation: a study of mouse lens transport and permeability visualized with freeze-substitution autoradiography and electron microscopy. *J. Cell Biol.* 86(2):576-89.

Goodenough, D.A. (1992) The crystalline lens. A system networked by gap junctional intercellular communication. *Semin. Cell Biol.* 3(1):49-58.

Goodenough DA, Goliger JA, Paul DL. (1996) Connexins, connexons, and intercellular communication. *Annu. Rev. Biochem.* 65:475-502.

Gould, C.M., Newton, A.C. (2008) The life and death of protein kinase C. *Curr. Drug Targets* 9(8):614-25.

Griner, E.M., Kazanietz, M.G. (2007) Protein kinase C and other diacylglycerol effectors in cancer. *Nat. Rev. Cancer* 7(4):281-94.

Grodsky, N., Li, Y., Bouzida, D., Love, R., Jensen, J., Nodes, B., Nonomiya, J., Grant, S. (2006) Structure of the catalytic domain of human protein kinase C beta II complexed with a bisindolylmaleimide inhibitor. *Biochemistry* 45(47):13970-81.

Gruijters, W.T., Kistler, J., Bullivant, S. (1987) Formation, distribution and dissociation of intercellular junctions in the lens. *J. Cell Sci.* 88 (Pt 3):351-9.

Guleria K, Vanita V, Singh D, Singh JR. (2007) A novel "pearl box" cataract associated with a mutation in the connexin 46 (GJA3) gene. *Mol. Vis.* 13:797-803.

Hanson, S.R., Hasan, A., Smith, D.L., Smith, J.B. (2000) The major in vivo modifications of the human water-insoluble lens crystallins are disulfide bonds, deamidation, methionine oxidation and backbone cleavage. *Exp. Eye Res.* 71(2):195-207.

Hansra. G, Garcia-Paramio, P., Prevostel, C., Whelan, R.D., Bornancin, F., Parker, P.J. (1999) Multisite dephosphorylation and desensitization of conventional protein kinase C isotypes. *Biochem. J.* 342 (Pt 2):337-44.

Harding, J.J. (1997) Lens, in Biochemistry of the Eye. Chapman and Hall, London.

Harris AL. (2001) Emerging issues of connexin channels: biophysics fills the gap. *Q. Rev. Biophys.* 34(3):325-472.

Harris, A. and Locke, D. (2009) Connexins A Guide. Humana Press, New York.

Hejtmancik, J.F., Kantorow, M.. (2004) Molecular genetics of age-related cataract. *Exp. Eye Res.* 79(1):3-9.

Hertzberg, E. L. (2000). *Gap junctions*. Jai Press, Stanford, CT.

Hoehenwarter, W., Klose, J., Jungblut, P.R. (2006) Eye lens proteomics. *Amino Acids.* 30(4):369-89.

Hommel, U., Zurini, M., Luyten, M. (1994) Solution structure of a cysteine rich domain of rat protein kinase C. *Nat. Struct. Biol.* 1(6):383-7.

Horwitz, J. (1992) Alpha-crystallin can function as a molecular chaperone. *Proc. Natl. Acad. Sci. U S A.* 89(21):10449-53.

House, C., Kemp, B.E. (1987) Protein kinase C contains a pseudosubstrate prototope in its regulatory domain. *Science* 238(4834):1726-8.

Hurley, J.H., Misra, S. (2000) Signaling and subcellular targeting by membrane-binding domains. *Annu. Rev. Biophys. Biomol. Struct.* 29:49-79.

Hurley, J.H., Newton, A.C., Parker, P.J., Blumberg, P.M., Nishizuka, Y. (1997) Taxonomy and function of C1 protein kinase C homology domains. *Protein Sci. 6(2):477-80.*

Inoue, M., Kishimoto, A., Takai, Y. & Nishizuka, Y. (1977) Studies on cyclic nucleotide-independent protein kinase and its proenzyme in mammalian tissues. I. Proenzyme and its activationby calcium-dependent protease from rat brain. *J. Biol. Chem*. 252, 7610-7616.

Iovine M.K., Gumpert A.M., Falk M.M., and Mendelson T.C. (2008) Cx23, a connexin with only four extracellular-loop cysteines, forms functional gap junction channels and hemichannels. *FEBS Lett.* 582: 165–170.

Jacob, T.J. (1999) The relationship between cataract, cell swelling and volume regulation. *Prog. Retin. Eye Res.* 18(2):223-33.

Jaffe, N.S. and Horwitz, J. (1992) Lens and cataract. Gower, New York, London.

Jakob, U., Gaestel, M., Engel, K., Buchner, J. (1993) Small heat shock proteins are molecular chaperones. *J. Biol. Chem.* 268(3):1517-20.

Jacobs, M.D., Soeller, C., Cannell, M.B., Donaldson, P.J. (2001) Quantifying changes in gap junction structure as a function of lens fiber cell differentiation. *Cell Commun. Adhes.* 8(4-6):349-53.

Jacobs, M.D., Soeller, C., Sisley, A.M., Cannell, M.B., Donaldson, P.J. (2004) Gap junction processing and redistribution revealed by quantitative optical measurements of connexin46 epitopes in the lens. *Invest. Ophthalmol. Vis Sci.* 45(1):191-9.

Jiang J.X. and Goodenough D.A. (1996) Heteromeric connexons in lens gap junction channels. *Proc. Natl. Acad. Sci. USA* 93:1287–1291.

Jiang J.X. and Goodenough D.A. (1998) Phosphorylation of lens-fiber connexins in lens organ cultures. *Eur. J. Biochem.* 255(1):37-44.

Johnson, J.E., Giorgione, J., Newton, A.C. (2000) The C1 and C2 domains of protein kinase C are independent membrane targeting modules, with specificity for phosphatidylserine conferred by the C1 domain. *Biochemistry* 39(37):11360-9.

Johnson, L.N., Lewis, R.J. (2001) Structural basis for control by phosphorylation. *Chem. Rev.* 101(8):2209-42.

Kannan, R., Stolz, A., Ji, Q., Prasad, P.D., Ganapathy, V. (2001) Vitamin c transport in human lens epithetiai cells: evidence for the presence of SVCT2. *Exp. Eye Res.* 73(2):l 59-65.

Kazanietz, M.G. (2000) Eyes wide shut: protein kinase C isozymes are not the only receptors for the phorbol ester tumor promoters. *Mol. Carcinog.* 28(1):5-11.

Kazanietz, M.G. (2002) Novel "nonkinase" phorbol ester receptors: the C1 domain connection. *Mol. Pharmacol.* 61(4):759-67.

Keranen, L.M., Dutil, E.M., Newton, A.C. (1995) Protein kinase C is regulated in vivo by three functionally distinct phosphorylations. *Curr. Biol.* 5(12):1394-1403.

Kinsey, V.E., Reddy, D.V.N. (1965). Studies of the crystalline lens. XI. The relative role of the epithelium and capsule in transport. *Invest. Ophthalmol.* 4, 104–116.

Knighton, D.R., Zheng, J.H., Ten Eyck, L.F., Xuong, N.H., Taylor, S.S., Sowadski, J.M. (1991) Structure of a peptide inhibitor bound to the catalytic subunit of cyclic adenosine monophosphate-dependent protein kinase. *Science* 253(5018):414-20.

Konishi, H., Tanaka, M., Takemura, Y., Matsuzaki, H., Ono, Y., Kikkawa, U., Nishizuka, Y. (1997) Activation of protein kinase C by tyrosine phosphorylation in response to H2O2. *Proc. Natl. Acad. Sci. U S A.* 94(21):11233-7.

Kumar, N. M., and Gilula, N. B. (1992). Molecular biology and genetics of gap junction channels. *Semin Cell Biol* 3, 3-16.

Kumar, N.M., Gilula, N.B. (1996) The gap junction communication channel. *Cell* 84(3):381-8.

Kuszak, J.R., Ennesser, C.A., Umlas, J., Macsai-Kaplan, M.S., Weinstein, R.S. (1988) The ultrastructure of fiber cells in primate lenses: a model for studying membrane senescence. *J. Ultrastruct. Mol. Struct. Res.* 100(1):60-74.

Kuszak, J.R. and Brown H.G. (1994) Embryology and Anatomy of the Lens: in Princi Principle and Practice of Ophthalmology. W.B. Saunders Company: Philadelphia.

Kuszak, J.R. (1995) The ultrastructure of epithelial and fiber cells in the crystalline lens. *Int. Rev. Cytol.* 163:305-50.

Kuszak, J.R., Novak, L.A., Brown, H.G. (1995) An ultrastructural analysis of the epithelial-fiber interface (EFI) in primate lenses. *Exp. Eye Res.* 61(5):579-97.

Kuszak, J.R., Zoltoski, R.K., Sivertson, C. (2004) Fibre cell organization in crystalline lenses. *Exp. Eye Res.* 78(3):673-87.

Kruse, A., Hertel, M., Hindsholm, M., Viskum, S. (2005) Trinitrotoluene (TNT)-induced cataract in Danish arms factory workers. *Acta. Ophthalmol. Scand.* 83(1):26-30.

Kyselova Z, Stefek M, Bauer V. (2004) Pharmacological prevention of diabetic cataract. *J. Diabetes Complications* 18(2):129-40.

Laird, D.W. (2005) Connexin phosphorylation as a regulatory event linked to gap junction internalization and degradation. *Biochim. Biophys. Acta.* 1711(2):172-82.

Laird, D.W. (2006) Life cycle of connexins in health and disease. *Biochem. J.* 394(Pt 3):527-43.

Lampe PD, Lau AF. (2000) Regulation of gap junctions by phosphorylation of connexins. *Arch. Biochem. Biophys.* 384(2):205-15.

Lampe, P.D., TenBroek, E.M., Burt, J.M., Kurata, W.E., Johnson, R.G., Lau, A.F. (2000) Phosphorylation of connexin43 on serine368 by protein kinase C regulates gap junctional communication. *J. Cell Biol.* 149(7):1503-12.

Le, A.C., Musil, L.S. (1998) Normal differentiation of cultured lens cells after inhibition of gap junction-mediated intercellular communication. *Dev. Biol.* 204(1):80-96.

Le Good, J.A., Ziegler, W.H., Parekh, D.B., Alessi, D.R., Cohen, P., Parker, P.J. (1998) Protein kinase C isotypes controlled by phosphoinositide 3-kinase through the protein kinase PDK1. *Science* 281(5385):2042-5.

Lee, H.W., Smith, L., Pettit, G.R., Bingham Smith, J. (1996) Dephosphorylation of activated protein kinase C contributes to downregulation by bryostatin. *Am. J. Physiol.* 271(1 Pt 1):C304-11.

Lim, J., Lam, Y.C., Kistler, J., Donaldson, P.J. (2005) Molecular characterization of the cystine/glutamate exchanger and the excitatory amino acid transporters in the rat lens. *Invest Ophthalmol Vis Sci.* 46(8):2869-77.

Lim, J., Lorentzen, K.A., Kistler, J., Donaldson, P.J. (2006) Molecular identification and characterisation of the glycine transporter (GLYT1) and the glutamine/glutamate transporter (ASCT2) in the rat lens. *Exp. Eye Res. b*83(2):447-55.

Lin, D., Boyle, D.L., Takemoto, D.J. (2003) IGF-I-induced phosphorylation of connexin 43 by PKCgamma: regulation of gap junctions in rabbit lens epithelial cells. *Invest. Ophthalmol. Vis. Sci.* 44(3):1160-8.

Lin D, Lobell S, Jewell A, Takemoto DJ. (2004) Differential phosphorylation of connexin46 and connexin50 by H2O2 activation of protein kinase Cgamma. *Mol. Vis*. 10:688-95.

Lin, D., Takemoto, D.J. (2005) Oxidative activation of protein kinase Cgamma through the C1 domain. Effects on gap junctions. *J. Biol. Chem.* 280(14):13682-93.

Lin D, Barnett M, Lobell S, Madgwick D, Shanks D, Willard L, Zampighi GA, Takemoto DJ. (2006) PKCgamma knockout mouse lenses are more susceptible to oxidative stress damage. *J Exp Biol.*209(Pt 21):4371-8.

Lin JH, Weigel H, Cotrina ML, Liu S, Bueno E, Hansen AJ, Hansen TW, Goldman S, Nedergaard M. (1998) Gap-junction-mediated propagation and amplification of cell injury. *Nat. Neurosci.* 1(6):494-500.

Lin J.S., Eckert R., Kistler J., and Donaldson P. (1998) Spatial differences in gap junction gating in the lens are a consequence of connexin cleavage. *Eur. J. Cell Biol.* 76:246-250.

Liu, T. F., and Johnson, R. G. (1999) Effects of TPA on dye transfer and dye leakage in fibroblasts transfected with a connexin 43 mutation at ser368. *Methods Find Exp. Clin. Pharmacol.* 21, 387-390.

Lo, W.K., Harding, C.V. (1986) Structure and distribution of gap junctions in lens epithelium and fiber cells. *Cell Tissue Res.* 244(2):253-63.

Lo, W.K. (1987) In vivo and in vitro observations on permeability and diffusion pathways of tracers in rat and frog lenses. *Exp. Eye Res.* 45(3):393-406.

Long, A.C., Colitz, C.M., Bomser, J.A. (2007) Regulation of gap junction intercellular communication in primary canine lens epithelial cells: role of protein kinase C. *Curr. Eye Res.* 32(3):223-31.

Luo, B., Regier, D.S., Prescott, S.M., Topham, M.K. (2004) Diacylglycerol kinases. *Cell Signal.* 16(9):983-9.

Mackay D., Ionides A., Kibar Z., Rouleau G., Berry V., Moore A., Shiels A., and Bhattacharya S. (1999) Connexin46 mutations in autosomal dominant congenital cataract. *American Journal of Human Genetics.* 64: 1357-1364.

Mackay, K., Mochly-Rosen, D. (2001) Localization, anchoring, and functions of protein kinase C isozymes in the heart. *J. Mol. Cell Cardiol.* 33(7):1301-7.

Marshall, B.S., Price, G., Powell, C.T. (2000) Rat protein kinase c zeta gene contains alternative promoters for generation of dual transcripts with 5'-end heterogeneity. *DNA Cell Biol.* 19(12):707-19.

Martinez-Wittinghan FJ, Sellitto C, Li L, Gong X, Brink PR, Mathias RT, White TW. (2003) Dominant cataracts result from incongruous mixing of wild-type lens connexins. *J. Cell Biol.* 161(5):969-78.

Mathias, R.T., Rae, J.L., Eisenberg, R.S. (1979) Electrical properties of structural components of the crystalline lens. *Biophys. J.* 25(1):181-201.

Mathias RT, Rae JL, Eisenberg RS. (1981) The lens as a nonuniform spherical syncytium. *Biophys. J.* 34(1):61-83.

Mathias, R.T., Rae, J.L., Ebihara, L., McCarthy, R.T. (1985) The localization of transport properties in the frog lens. *Biophys. J.* 48(3):423-34.

Mathias, R.T., Riquelme, G., Rae, J.L. (1991) Cell to cell communication and pH in the frog lens. *J. Gen. Physiol.* 98(6):1085-1103.

Mathias, R.T., Rae, J.L., Baldo, G.J. (1997) Physiological properties of the normal lens. *Physiol. Rev*. 77(1):21-50.

Mathias, R.T., Rae, J.L. (2004) The lens: local transport and global transparency. *Exp. Eye Res.* 78(3):689-98.

Medkova, M., Cho, W. (1998) Mutagenesis of the C2 domain of protein kinase C-alpha. Differential roles of Ca2+ ligands and membrane binding residues. *J. Biol. Chem.* 273(28):17544-52.

Mellor, H., Parker, P.J. (1998) The extended protein kinase C superfamily. *Biochem. J.* 332 (Pt 2):281-92.

Menko AS, Klukas KA, Liu TF, Quade B, Sas DF, Preus DM, Johnson RG. (1987) Junctions between lens cells in differentiating cultures: structure, formation, intercellular permeability, and junctional protein expression. *Dev. Biol.* 123(2):307-20.

Merriman-Smith, R., Donaldson, P., Kistler, J. (1999) Differential expression of facilitative glucose transporters GLUT1 and GLUT3 in the lens. *Invest. Ophthalmol. Vis. Sci.* 40(13):3224-30.

Merriman-Smith BR, Krushinsky A, Kistler J, Donaldson PJ. (2003) Expression patterns for glucose transporters GLUT1 and GLUT3 in the normal rat lens and in models of diabetic cataract. *Invest. Ophthalmol. Vis. Sci.* 44(8):3458-66.

Messerschmidt, A., Macieira, S., Velarde, M., Bädeker, M., Benda, C., Jestel, A., Brandstetter, H., Neuefeind, T., Blaesse, M. (2005) Crystal structure of the catalytic domain of human atypical protein kinase C-iota reveals interaction mode of phosphorylation site in turn motif. *J. Mol. Biol.* 352(4):918-31.

Morris, M.S., Jacques, P.F., Hankinson, S.E., Chylack, L.T. Jr., Willett, W.C., Taylor, A. (2004) Moderate alcoholic beverage intake and early nuclear and cortical lens opacities. *Ophthalmic Epidemiol.* 11(1):53-65.

Mosior, M., Epand, R.M. (1993) Mechanism of activation of protein kinase C: roles of diolein and phosphatidylserine. *Biochemistry* 32(1):66-75.

Murray, N.R., Baumgardner, G.P., Burns, D.J., Fields, A.P. (1993). Protein kinase C isotypes in human erythroleukaemia (K562) cell proliferation and differentiation. *J. Biol. Chem.* 268, 15847-15853.

Musil L.S., Beyer E.C., and Goodenough D.A. (1990). Expression of the gap junction protein connexin43 in embryonic chick lens: molecular cloning, ultrastructural localization, and post-translational phosphorylation. *J. Membr. Biol.* 116: 163–175.

Nalefski, E.A., Falke, J.J. (1996) The C2 domain calcium-binding motif: structural and functional diversity. *Protein Sci.* 5(12):2375-90.

Nalefski, E.A., Newton, A.C. (2001) Membrane binding kinetics of protein kinase C betaII mediated by the C2 domain. *Biochemistry* 40(44):13216-29.

Newton, A.C., Keranen, L.M. (1994) Phosphatidyl-L-serine is necessary for protein kinase C's high-affinity interaction with diacylglycerol-containing membranes. *Biochemistry* 33(21):6651-8.

Newton, A.C. (1995) Protein kinase C: structure, function, and regulation. *J. Biol. Chem.* 270(48):28495-8.

Newton, A.C. (1997) Regulation of protein kinase C. *Curr. Opin. Cell Biol.* 9(2):161-7.

Newton, A.C., Johnson, J.E. (1998) Protein kinase C: a paradigm for regulation of protein function by two membrane-targeting modules. *Biochim. Biophys. Acta.* 1376(2):155-72.

Newton, A.C. (2001) Protein kinase C: structural and spatial regulation by phosphorylation, cofactors, and macromolecular interactions. *Chem. Rev.* 101(8):2353-64.

Newton, A.C. (2003) Regulation of the ABC kinases by phosphorylation: protein kinase C as a paradigm. *Biochem. J.* 370(Pt 2):361-71.

Newton, A.C. (2003b) The ins and outs of protein kinase C. *Methods Mol. Biol.* 233:3-7.

Ngezahayo A, Zeilinger C, Todt I I, Marten I I, Kolb H. (1998) Inactivation of expressed and conducting rCx46 hemichannels by phosphorylation. *Pflugers Arch.* 436(4):627-9.

Nguyen, T.A., Boyle, D.L., Wagner, L.M., Shinohara, T., Takemoto, D.J. (2003) LEDGF activation of PKC gamma and gap junction disassembly in lens epithelial cells. *Exp. Eye Res*. 2003 May;76(5):565-72.

Nguyen, T.A., Takemoto, L.J., Takemoto, D.J. (2004) Inhibition of gap junction activity through the release of the C1B domain of protein kinase Cgamma (PKCgamma) from 14-3-3: identification of PKCgamma-binding sites. *J. Biol. Chem.* 279(50):52714-25.

Nolen, B., Taylor, S., Ghosh, G. (2004) Regulation of protein kinases; controlling activity through activation segment conformation. *Mol. Cell* 15(5):661-75.

Nonaka T, Nishiura M, Ohkuma M. (1976) Gap junctions of lens fiber cells in freeze-fracture replicas. *J. Electron Microsc (Tokyo)* 25(1):35-6.

Otte, A.P., Kramer, I.M., Durston, A.J. (1991). Protein kinase C and the regulation of the local competence of xenopus ectoderm. *Science* 251: 570-573.

Orr, J.W., Keranen, L.M., Newton, A.C. (1992) Reversible exposure of the pseudosubstrate domain of protein kinase C by phosphatidylserine and diacylglycerol. *J. Biol. Chem.* 267(22):15263-6.

Orr, J.W., Newton, A.C. (1994) Intrapeptide regulation of protein kinase C. *J. Biol. Chem.* 269(11):8383-7.

Orr, J.W., Newton, A.C. (1994b) Requirement for negative charge on "activation loop" of protein kinase C. *J. Biol. Chem*. 269(44):27715-8.

Oyamada, M., Oyamada, Y., Takamatsu, T. (1998). Gap junctions in health and disease. *Medical Electron Microscopy* 31, 115-120.

Oyster C.W. (1999) The Human Eye: Structure and Function. *Sinauer Associates: Sunderland, Massachusetts.*

Pahujaa, M., Anikin M., Goldberg, G.S. (2007) Phosphorylation of connexin43 induced by Src: regulation of gap junctional communication between transformed cells. *Exp. Cell Res.* 313(20):4083-90.

Paul D.L., Ebihara L., Takemoto L.J., Swenson K.I., and Goodenough D.A. (1991) Connexin46, a novel lens gap junction protein, induces voltage-gated currents in nonjunctional plasma membrane of *Xenopus* oocytes. *J Cell Biol.* 115: 1077–1089.

Parekh, D.B., Ziegler, W., Parker, P.J. (2000) Multiple pathways control protein kinase C phosphorylation. *EMBO J.* 19(4):496-503.

Puk, O., Loster, J., Dalke, C., Soewarto, D., Fuchs, H., Budde, B., Nurnberg, P., Wolf, E., De Angelis, M.H., and Graw, J. (2008) Mutation in a novel connexin-like gene (*Gjf1*) in the mouse affects early lens development and causes a variable smalleye phenotype. *Invest. Ophthalmol. Vis. Sci.* 49: 1525–1532.

Rae, J.L., Hoffert, J.R., Fromm, P.O. (1970). Studies on the normal lens potential of the rainbow trout (Salmo gairdneri). *Exp. Eye Res.* 10, 93–101.

Rae, J.L. (1973). The potential difference of the frog lens. *Exp. Eye Res.* 15, 485–494.

Rae, J.L., Truitt, K.D., Kuszak, J.R. (1982) A simple fluorescence technique for light microscopy of the crystalline lens. *Curr. Eye Res.* 2, 1-5.

Rae, J.L., Kuszak, J.R. (1983) The electrical coupling of epithelium and fibers in the frog lens. *Exp. Eye Res.* 36(3):317-26.

Rae, J.L., Bartling, C., Rae, J., Mathias, R.T. (1996) Dye transfer between cells of the lens. *J. Membr. Biol.* 150(1):89-103.

Revel, J.P., Karnovsky, M.J. (1967) Hexagonal array of subunits in intercellular junctions of the mouse heart and liver. *J. Cell Biol.* 33(3):C7-C12.

Reynhout, J.K., Lampe, P.D., Johnson, R.G. (1992) An activator of protein kinase C inhibits gap junction communication between cultured bovine lens cells. *Exp. Cell Res.* 1992 Feb;198(2):337-42.

Robinson, K.R., Patterson, J.W. (1982-1983). Localization of steady currents in the lens. *Curr. Eye Res.* 2, 843–847.

Rong P, Wang X, Niesman I, Wu Y, Benedetti LE, Dunia I, Levy E, Gong X. (2002) Disruption of Gja8 (alpha8 connexin) in mice leads to microphthalmia associated with retardation of lens growth and lens fiber maturation. *Development* 129(1):167-74.

Saez, J. C., Berthoud, V. M., Branes, M. C., Martinez, A. D., and Beyer, E. C. (2003). Plasma membrane channels formed by connexins: their regulation and functions. *Physiol Rev* 83, 1359-1400.

Saleh, S.M., Takemoto, L.J., Zoukhri, D., Takemoto, D.J. (2001) PKC-gamma phosphorylation of connexin 46 in the lens cortex. *Mol. Vis*. 7:240-6.

Schechtman, D., Mochly-Rosen, D. (2001) Adaptor proteins in protein kinase C-mediated signal transduction. *Oncogene.* 20(44):6339-47.

Sellitto C, Li L, White TW. (2004) Connexin50 is essential for normal postnatal lens cell proliferation. *Invest. Ophthalmol. Vis. Sci.* 45(9):3196-202.

Sisley AMG. (2007) Gap Junctions in the lens: Is location everything? PhD Dissertation, The University of Auckland.

Simon, A.M., Goodenough, D.A. (1998) Diverse functions of vertebrate gap junctions. *Trends Cell Biol.* 8(12):477-83.

Solan, J.L., Fry, M.D., TenBroek, E.M., Lampe, P.D. (2003) Connexin43 phosphorylation at S368 is acute during S and G2/M and in response to protein kinase C activation. *J. Cell Sci.* 116(Pt 11):2203-11.

Solan, J.L., Lampe, P.D. (2005) Connexin phosphorylation as a regulatory event linked to gap junction channel assembly. *Biochim. Biophys. Acta*. 1711(2):154-63.

Solan, J.L., Lampe, P.D. (2009) Connexin43 phosphorylation: structural changes and biological effects. *Biochem. J.* 419(2):261-72.

Sosinsky, G. E. (1996). Molecular organization of gap junction membrane channels. *J Bioenerg Biomembr* **28**, 297-309.

Sosinsky GE, Nicholson BJ. (2005) Structural organization of gap junction channels. *Biochim. Biophys. Acta*. 1711(2):99-125.

Spitaler, M., Cantrell, D.A. (2004) Protein kinase C and beyond. *Nat Immunol.* 5(8):785-90.

Stahelin, R.V., Digman, M.A., Medkova, M., Ananthanarayanan, B., Melowic, H.R., Rafter, J.D., Cho, W. (2005a) Diacylglycerol-induced membrane targeting and activation of protein kinase Cepsilon: mechanistic differences between protein kinases Cdelta and Cepsilon. *J. Biol. Chem.* 280(20):19784-93.

Stahelin, R.V., Wang, J., Blatner, N.R., Rafter, J.D., Murray, D., Cho, W. (2005b) The origin of C1A-C2 interdomain interactions in protein kinase Calpha. *J. Biol. Chem.* 280(43):36452-63.

Steinberg, T. H., Civitelli, R., Geist, S. T., Robertson, A. J., Hick, E., Veenstra, R. D., Wang, H. Z., Warlow, P. M., Westphale, E. M., Laing, J. G., and et al. (1994). Connexin43 and connexin45 form gap junctions with different molecular permeabilities in osteoblastic cells. *EMBO J* 13, 744-750.

Steinberg, S.F. (2008) Structural basis of protein kinase C isoform function. *Physiol Rev.* 88(4):1341-78.

Stephens, L., Anderson, K., Stokoe, D., Erdjument-Bromage, H., Painter, G. F., Holmes, A. B., Gaffney, P. R. J., Reese, C. B., McCormick, F., Tempst, P., Coadwell, J. and Hawkins, P. T. (1998) Protein kinase B kinases that mediate phosphatidylinositol 3,4,5-trisphosphate-dependent activation of protein kinase B. *Science 279*, 710-714.

Stokoe, D., Stephens, L. R., Copeland, T., Gaffney, P. R., Reese, C. B., Painter, G. F., Holmes, A. B., McCormick, F. and Hawkins, P. T. (1997) Dual role of phosphatidylinositol-3,4,5-trisphosphate in the activation of protein kinase B. *Science 277*, 567-570.

Su, L., Parissenti, A.M., Riedel, H. (1993) Functional carboxyl terminal deletion map of protein kinase C alpha. *Receptors Channels* 1(1):1-9.

Sutton, R.B., Davletov, B.A., Berghuis, A.M., Südhof, T.C., Sprang, S.R. (1995) Structure of the first C2 domain of synaptotagmin I: a novel Ca2+/phospholipid-binding fold. *Cell* 80(6):929-38.

Sutton, R.B., Sprang, S.R. (1998) Structure of the protein kinase Cbeta phospholipid-binding C2 domain complexed with Ca2+. *Structure* 6(11):1395-405.

Takahashi, H., Suzuki, K., Namiki, H. (2003) Phenylarsine oxide and H2O2 plus vanadate induce reverse translocation of phorbol-ester-activated PKCbetaII. *Cell Struct. Funct.* 28(2):123-30.

Takai, Y., Kishimoto, A., Inoue, M. & Nishizuka, Y. (1977) Studies on a cyclic nucleotide-independent protein kinase and its proenzyme in mammalian tissues. I. Purification and characterization of an active enzyme from bovine cerebellum. *J. Biol. Chem.* 252, 7603-7609.

Tamiya, S., Dean, W.L., Paterson, C.A., Delamere, N.A. (2003) Regional distribution of Na,K-ATPase activity in porcine lens epithelium. *Invest. Ophthalmol. Vis. Sci.* 44(10):4395-9.

Tan, S.L., Parker, P.J. (2003). Emerging and diverse roles of protein kinase C in immune cell signalling. Biochem. J. 376, 545-52.

Tardieu, A. (1998) alpha-Crystallin quaternary structure and interactive properties control eye lens transparency. *Int. J. Biol. Macromol.* 22(3-4):211-7.

Taylor A, Hobbs M. (2001) 2001 assessment of nutritional influences on risk for cataract. *Nutrition* 17(10):845-57.

Tenbroek, E.M., Louis, C.F., Johnson, R. (1997) The differential effects of 12-O-tetradecanoylphorbol-13-acetate on the gap junctions and connexins of the developing mammalian lens. *Dev. Biol.* 191(1):88-102.

Trosko, J. E., and Ruch, R. J. (1998). Cell-cell communication in carcinogenesis. *Front Biosci* **3**, d208-236.

Truscott, R.J. (2005) Age-related nuclear cataract-oxidation is the key. *Exp. Eye Res.* 80(5):709-25.

Valiunas V, Beyer EC, Brink PR. (2002) Cardiac gap junction channels show quantitative differences in selectivity. *Circ. Res.* 91(2):104-11.

Varadaraj, K., Kushmerick, C., Baldo, G.J., Bassnett, S., Shiels, A., Mathias, R.T. (1999) The role of MIP in lens fiber cell membrane transport. *J. Membr. Biol.* 170, 191–203.

Verdaguer, N., Corbalan-Garcia, S., Ochoa, W.F., Fita, I., Gómez-Fernández, J.C. (1999) Ca(2+) bridges the C2 membrane-binding domain of protein kinase Calpha directly to phosphatidylserine. *EMBO J.* 18(22):6329-38.

Violin, J.D., Newton, A.C. (2003) Pathway illuminated: visualizing protein kinase C signaling. *IUBMB Life* 55(12):653-60.

Wagner, L.M., Saleh, S.M., Boyle, D.J., Takemoto, D.J. (2002) Effect of protein kinase Cgamma on gap junction disassembly in lens epithelial cells and retinal cells in culture. *Mol. Vis.* 8:59-66.

Weber PA, Chang HC, Spaeth KE, Nitsche JM, Nicholson BJ. (2004) The permeability of gap junction channels to probes of different size is dependent on connexin composition and permeant-pore affinities. *Biophys. J.* 87(2):958-73.

Werner, R. (1998). In *Gap Junctions* (G. A. Perkins, Goodenough, D.A., Sosinsky, G.E., Ed.), pp. 13. IOS Press, Amsterdam, Netherlands.

White, T.W., Bruzzone, R., Goodenough, D.A., and Paul, D.L. (1992) Mouse Cx50, a functional member of the connexin family of gap junction proteins, is the lens fiber protein MP70. *Mol. Biol. Cell* 3: 711–720.

White TW, Bruzzone R, Wolfram S, Paul DL, Goodenough DA. (1994) Selective interactions among the multiple connexin proteins expressed in the vertebrate lens: the second extracellular domain is a determinant of compatibility between connexins. *J. Cell Biol.* 125(4):879-92.

White, T.W., Goodenough, D.A., Paul, D.L. (1998) Targeted ablation of connexin50 in mice results in microphthalmia and zonular pulverulent cataracts. *J. Cell Biol.* 143(3):815-25.

White, T.W., Paul, D.L. (1999) Genetic diseases and gene knockouts reveal diverse connexin functions. *Annu. Rev. Physiol.* 61:283-310.

White, T.W., Sellitto, C., Paul, D.L., Goodenough, D.A. (2001) Prenatal lens development in connexin43 and connexin50 double knockout mice. *Invest. Ophthalmol. Vis. Sci*. 42(12):2916-23.

White, T.W. (2002) Unique and redundant connexin contributions to lens development. *Science* 295(5553):319-20.

World Health Organisation (2005) State of the World's Sight: Vision 2020: the Right to Sight: 1999-2005. WHO Press.

Xia, C.H., Cheng, C., Huang, Q., Cheung, D., Li, L., Dunia, I., Benedetti, L.E., Horwitz, J., Gong, X. (2006) Absence of alpha3 (Cx46) and alpha8 (Cx50) connexins leads to cataracts by affecting lens inner fiber cells. *Exp. Eye Res.* 83(3):688-96. Epub 2006 May 11.

Xu, R.X., Pawelczyk, T., Xia, T.H., Brown, S.C. (1997) NMR structure of a protein kinase C-gamma phorbol-binding domain and study of protein-lipid micelle interactions. *Biochemistry* 36(35):10709-17.

Xu, Z.B., Chaudhary, D., Olland, S., Wolfrom, S., Czerwinski, R., Malakian, K., Lin, L., Stahl, M.L., Joseph-McCarthy, D., Benander, C., Fitz, L., Greco, R., Somers, W.S., Mosyak, L. (2004) Catalytic domain crystal structure of protein kinase C-theta (PKCtheta). *J. Biol. Chem.* 279(48):50401-9.

Yaffe, M.B., Rittinger, K., Volinia, S., Caron, P.R., Aitken, A., Leffers, H., Gamblin, S.J., Smerdon, S.J., Cantley, L.C. (1997) The structural basis for 14-3-3:phosphopeptide binding specificity. *Cell* 91(7):961-71.

Yevseyenkov, V.V., Das, S., Lin, D., Willard, L., Davidson, H., Sitaramayya, A., Giblin, F.J., Dang, L., Takemoto, D.J. (2009) Loss of protein kinase Cgamma in knockout mice and increased retinal sensitivity to hyperbaric oxygen. *Arch. Ophthalmol.*127(4):500-6.

Zampighi, G.A., Eskandari, S., Kreman, M. (2000) Epithelial organization of the mammalian lens. *Exp. Eye Res.* 71(4):415-35.

Zampighi, G.A., Planells, A.M., Lin, D., Takemoto, D. (2005) Regulation of lens cell-to-cell communication by activation of PKCgamma and disassembly of Cx50 channels. *Invest. Ophthalmol. Vis. Sci.* 46(9):3247-55.

Zhang, G., Kazanietz, M.G., Blumberg, P.M., Hurley, J.H. (1995) Crystal structure of the cys2 activator-binding domain of protein kinase C delta in complex with phorbol ester. *Cell* 81(6):917-24.

Chapter 2 - PKCγ, a key player in lens epithelial cell differentiation and lens gap junction coupling

2.1. *Introduction*

The lens focuses light onto the retina at the back of the eye. The fully developed lens has an anterior layer of epithelial cells, peripheral differentiating fibers (DF) in the cortex, and nuclear mature fibers (MF) (Figure 2.1A). The avascular lens circulatory system is dependent upon ion channels, Na/K pumps, gap junctions and water channels (Mathias and Rae, 2004; Mathias et al., 1997; Mathias et al., 2007; Bassnett, et al. 1994). Vertebrate gap junctions are groups of intermembrane protein channels formed by the docking of two hemichannels in adjacent cells, with each hemi channel formed from six Connexin (Cx) proteins. The resulting channels allow the passage of ions and small metabolites up to the size of ~1000 Daltons between adjacent cells (White and Paul, 1999; Sohl and Willecke, 2004; Saez et al., 2003; Harris, 2007). The lens epithelial cells express Cx43 and Cx50, but the expression of Cx43 is turned off as the epithelial cells differentiate into fiber cells in the equatorial region and the expression of Cx46 begins (See Fig. 2.1A)(Mathias and Rae, 2004; Mathias et al., 1997; Saleh et al., 2001; Berthoud and Beyer, 2009). Both Cx46 and Cx50 are expressed in the DF and MF, but have different structural and functional roles (Goodenough et al., 1996; Kumar and Gilula, 1996; Gong et al., 1997; White et al., 1998; White et al., 2002). While Cx46 and Cx50 appear to contribute equally for the gap junctional communication in the DF, only Cx46 channels seem to be functional in the MF (Gong et al,. 1998; Baldo et al., 2001; Martinez-Wittinghan et al., 2004; Gao et al., 2004; Wang et al., 2009).

Cxs have a high turn over rate with reports of their half-lives between 2-6 hrs (Li et al., 2008; Solan and Lampe, 2009). Therefore regulation of this dynamic process is critical for the control of intercellular gap junctional communication (Laird, 2006). All three Cxs expressed in the lens are phosphoproteins and phosphorylation plays an important role throughout the Cx life cycle including gap junction channel gating and Cx degradation (Solan and Lampe, 2009). Several studies from our lab have previously implicated protein kinase Cγ (PKCγ) in the phosphorylation of the lens gap junction proteins (Saleh et al., 2001; Lin et al., 2004; Lin et al., 2006; Zampighi et al., 2005).

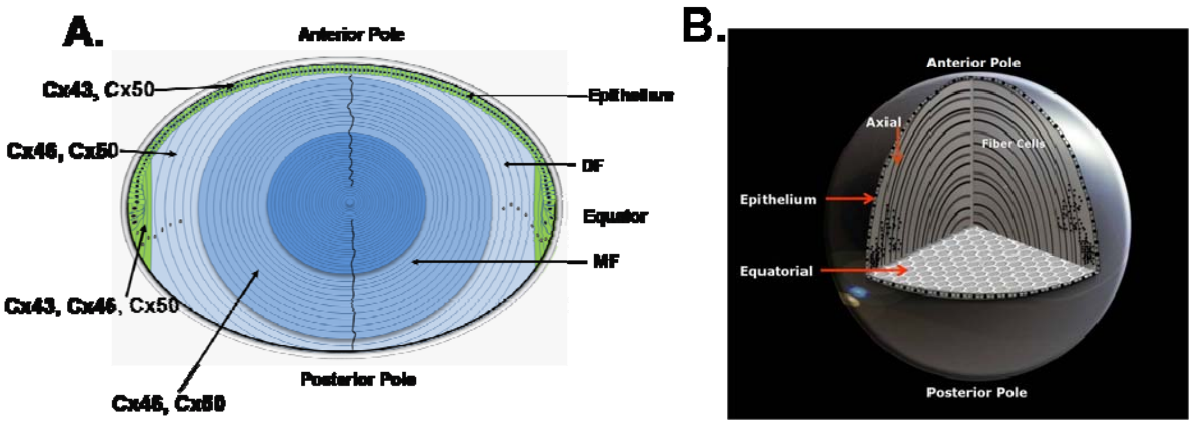

Figure 2.1 The Structure of the Lens. (A) Diagram of the lens showing the single layer of epithelial cells at the anterior surface. At the equator the epithelial cells differentiate into fiber cells, which occurs in the outer layer of differentiating fibers (DF). The mature fibers (MF) occupy the core of the lens; have no organelles and very low level of metabolic activity. Gap junctions connect all these cells and the expression of gap junction proteins, Cxs, in the different regions of the lens is shown. (B) Schematic diagram of lens morphology showing axial and equatorial sectioning planes, the fiber cell morphology on the two sectioning planes and the dispersion of fiber cell nuclei. Axial sections were used in our studies.

PKCγ, a phospholipid-dependent classic serine/threonine kinase, is primarily expressed in the central and peripheral nervous systems (Shutoh et al., 2003). This PKC isoform is detected in eye tissue, including retina and lens epithelium and cortex (Saleh et al., 2001; Yevseyenkov et al., 2009). Like other conventional PKCs, PKCγ also gets activated by calcium, diacylglycerol, phorbol ester (TPA) and oxidative stress signals like H_2O_2. PKCγ moves to the plasma membrane following activation and phosphorylates targets such as receptors, structural proteins and gap junction proteins (Zampighi et al., 2005; Lin and Takemoto, 2005). PKCγ prevents brain ischemia and plays a protective role in cell survival (Schrenk et al., 2002; Aronowski et al., 2000). We have previously shown that activation of PKCγ by TPA, insulin-like growth factor-1 (IGF-1), or H_2O_2 results in an increase in the PKCγ enzyme activity which, in turn, phosphorylates Cx43 leading to loss of functional gap junctional communication and a decrease in gap junction plaques in lens epithelial cells in culture (Nguyen et al., 2003; Lin et al., 2003;

Akoyev et al., 2009). We have also demonstrated phosphorylation of Cx46 and Cx50 by PKCγ in rat lens studies (Saleh et al., 2001; Lin et al., 2004; Lin et al., 2006).

The PKCγ knock out (γ-KO) mice have slight ataxia, less memory, reduced neuropathic pain, decreased anxiety, impaired long-term potentiation, enhanced opioid responses, increased alcohol consumption and less protection against brain ischemia (Aronowski et al., 2000; Abeliovich et al., 1993; Bowers and Wehner, 2001; Malmberg et al., 1997; Narita et al., 2001; Ohsawa et al., 2001; Verbeek et al., 2005). Since PKCγ has been implicated in the phosphorylation of all three Cxs expressed in the lens, the γ-KO mouse is a very useful model to study the role of PKCγ in regulating the lens gap junctions. In our observation of up to 8 months of age in KO animals, no lenses develop cataracts. However, we have previously reported that hyperbaric oxygen treatment causes significant damage to the γ-KO retina (Yevseyenkov et al., 2009). γ-KO lenses were demonstrated to be more susceptible to H_2O_2 induced oxidative stress damage leading to lens opacification (Lin et al., 2006). We had implicated phosphorylation of Cx50 by PKCγ as one of the reasons for this.

The purpose of this study was to investigate the regulations of Cx43 and Cx46 by PKCγ in the lens, and the effect of KO of PKCγ on the gap junction channel coupling and gating. In the KO lenses, we observed a large increase in the amount of total Cx43, persistence of Cx43 expression into differentiating fibers, significant increase in gap junction coupling both in the DF and MF and considerable reduction in the phosphorylation of Cx43 and Cx46.

2.2. Materials and Methods

Fetal bovine serum was purchased from Atlanta Biologicals (Norcross, GA). phenylmethylsulfonyl fluoride (PMSF), and protease inhibitor cocktail (# P8340) were from Sigma-Aldrich (St. Louis, MO). Phosphatase inhibitors cocktail set II (# 524625) was purchased from Calbiochem (La Jolla, CA). Protein A/G plus agarose beads (# sc-2003), 2X electrophoresis sample buffer (#sc-24945), were purchased from Santa Cruz Biotechnology (Santa Cruz, CA). All electrophoresis reagents and protein molecular weight markers for electrophoresis and protein assay dye were purchased from Bio-Rad Laboratories (Hercules, CA). Chemiluminescence substrate (SuperSignal West Femto Substrate Kit) with secondary anti-mouse or anti-rabbit IgG conjugated with horseradish peroxidase (# 34095) was purchased from

Pierce (Rockford, IL). Optimal cutting temperature (OCT) compound and superfrost plus gold microscope slides were purchased from Electron Microscopy Sciences (Hatfield, PA). Unless otherwise noted chemicals and supplies were obtained from Fisher Scientific (Hampton, NH).

2.2.1. Animals

All animal procedures were approved by the Kansas State University (KSU) Institutional Animal Care and Use Committee. Mice, including wild-type control (WT) and PKCγ knockout (KO) mice, were obtained from Jackson Laboratories (Bar Harbor, ME) and maintained as colonies in the Animal Research Facility at the College of Veterinary Medicine, KSU. PKCγ KO mice were obtained by breeding homozygous individuals and the genotyping of the offspring was performed by PCR of tail snips. The control mice were B6129PF2/J and the PKCγ homozygous KO mice were B6;129P2-*Prkcc*^{tm1Stl}/J. Only homozygous KO-PKCγ mice were used from breeding of homozygous pairs. All mice were used at 8-12 weeks of age. The failure of the PKCγ mice to produce PKCγ protein was further verified by Western blot analysis. The mice were sacrificed by CO_2 asphyxiation followed by cervical dislocation. All experiments conformed to the ARVO Statement for Use of Animals in Ophthalmic and Vision Research.

2.2.2. Lens Lysate Preparations

Lenses were dissected out of mice eye balls within 15 minutes of sacrificing the animal and homogenized on ice in sample buffer containing 62.5 mM Tris–HCl (pH 6.8), 2% SDS, 5% β-mercaptoethanol, protease inhibitor cocktail (1:100), 2mM PMSF and phosphatase inhibitor cocktail (1:100). After homogenization, lysates were sonicated on ice and centrifuged at 12,000 rpm for 15 minutes at 4°C. Protein concentration was equalized in all supernatants and used immediately for western blotting.

For localization purposes, lenses were dissected into outer (consisting of the epithelial cells), cortical (containing the differentiating fibers), and nuclear (consisting of the mature fibers) sections under a dissection microscope. Lysates of the different sections were prepared in the sample buffer and used for western blotting.

2.2.3. Immunoprecipitation

Lenses were homogenized in RIPA buffer (#9806, Cell Signaling Technology; Danvers, MA) supplemented with protease- and phosphatase-inhibitors (1:100 each) followed by sonication and centrifugation at 12,000 rpm for 15 minutes at 4°C. The supernatants were used as whole-lens extracts and protein concentration was equalized in all samples. For pre-clearing, the whole-lens extracts were incubated with 0.25 μg of the normal rabbit IgG together with 20 μl of Protein A/G-Agarose beads for 30 minutes at 4°C. Beads were pelleted by centrifugation at 3,000 rpm for 30 seconds at 4° C. 5 μg of C-terminus rabbit Cx46 antibody was added to the resulting supernatants, and incubated at 4°C overnight with constant mixing. After that, 20 μl of Protein A/G-Agarose beads were added to the mixture and were further incubated for another 2 hrs at 4°C. The beads were collected by centrifugation at 3,000 rpm for 30 seconds at 4° C, and then washed with RIPA buffer three times. The pulled down proteins were extracted with 40 μL 2x electrophoresis sample buffer, boiled for 5 minutes, and analyzed by western blotting.

2.2.4. Western Blot and Antisera

Western blot analyses were performed as previously described (Das et al., 2008). Mouse anti-N-terminal-Cx43 (# Cx43NT1) was purchased from Fred Hutchinson Cancer Center (Seattle, WA); rabbit anti-phospho-Cx43 (Ser-368) (# 3511S) from Cell Signaling Technologies (Danvers, MA); mouse anti-PKCγ (# P20420) from Transduction Laboratories (Lexington, KY); rabbit anti-C-terminal-Cx43 (# C6219), mouse anti-β-actin (# A5441) from Sigma-Aldrich (St. Louis, MO); rabbit anti-Cx46 (# C7858-07A) from US Biological (Swampscott, MA); goat anti-Cx46 (M-19) (# sc-20861) from Santa Cruz Biotechnology (Santa Cruz, CA); mouse anti-Cx50 (# 33-4300) from Zymed-Invitrogen (San Franscisco, CA); mouse anti-phosphoserine (# 525280), and mouse anti-phosphothreonine (# 525287) from Calbiochem (La Jolla, CA). Rabbit polyclonal Cx46 antibodies directed against the cytoplasmic loop (residues 115-128) of rat Cx46 was a kind gift from Dr. Xiaohua Gong (University of California, Berkeley).

2.2.5. RNA Isolation and Real-Time RT-PCR

Total RNA was extracted from WT and KO mouse lenses using Trizol reagent (Invitrogen). RNA was quantified using a spectrophotometer and equal amounts of total RNA were reverse-transcribed using SuperScript III First-Strand Synthesis System for RT-PCR (Invitrogen) and following the manufacturer's protocol. Then RT reaction mixture (1 μl) from

each treatment was subjected to PCR using specific primers for Cx43, Cx46, Cx50 and β-actin. The specificity of primers (refer Table 2.1) was confirmed by NCBI-BLAST analysis. The PCR products were then analyzed in 1.5% agarose-gel.

Table 2.1 Primers used for RT- and Real-Time PCR. The primers are identified as forward (F), and reverse (R).

Target gene	Primer	Nucleotide sequence	GenBank accession no.
β-actin	F	5'-GGCTCCTAGCACCATGAAGA-3'	NM_007393.3
	R	5'- CCACCGATCCACACAGAGTA-3'	
Cx43	F	5'- TCCAAGGAGTTCCACCACTT-3'	NM_010288.3
	R	5'- AAATGAAGAGCACCGACAGC-3'	
Cx46	F	5'-GGTTAGCTGTTGGGAGCAAT-3'	NM_016975.2
	R	5'-CAGAATGCGGAAGATGAACA-3'	
Cx50	F	5'-CGGAGCAGCAAGAGAGAAAG-3'	NM_008123.2
	R	5'-TGCTCATTCACCTCTTCCAA-3'	

Real-time PCR was performed using a BioRad iQ iCycler Detection System (BioRad Laboratories, Ltd) with SYBR green SuperMix (BioRad). Reactions were performed in a total volume of 25 µL—including 12.5 µL 2x SYBR buffer SuperMix, 1 µL of each primer at 10 µM concentration, and 10.5 µL of the previously dilution-optimized reverse-transcribed cDNA template.

Protocols for each primer set were optimized using four serial 5x dilutions of template cDNA obtained from Lenses. The protocols used are as follows: denaturation (95°C for 5 mins), amplification repeated 40 times (95°C for 15 s, 60°C for 45 s). A melt curve analysis was performed following every run to ensure a single amplified product for every reaction. All reactions were carried out in at least triplicate for every sample. The same reference standard dilution series was repeated on every experimental plate.

2.2.6. Lens Sectioning and Confocal Scanning Fluorescent Microscopy

Lenses were dissected in PBS (137 mM NaCl, 2.7 mM KCl, 10 mM Na_2HPO_4, 2 mM KH_2PO_4) and fixed in 1.5% wt/vol paraformaldehyde in PBS for 24 hours at room temperature. Cryoprotection and sectioning of the lenses were done as described previously (Jacobs et al., 2004). Ten-µm-thick axially sectioned lens sections (See Fig. 1B) were placed onto superfrost gold microscope slides. Slides were then washed three times in PBS-T (PBS with 0.1% Tween-20) for 5 minutes each, blocked for 2 hrs at room temperature in 5% wt/vol BSA in PBS-T (blocking solution), and treated overnight at 4°C with anti-Cx43 antibody (# Cx43IF1; Fred Hutchinson Cancer Center, Seattle, WA) diluted 1:100 in blocking solution. Slides were washed three times for 10 min each in PBS-T and treated for 2 hrs in the dark at room temperature with anti-mouse Alexa Fluor 488 antibody (#A-11029; Invitrogen-Molecular Probes, Eugene, OR) diluted 1:200 in blocking solution. After washing three times for 5 minutes each in PBS-T, slides were labeled for 10 minutes in the dark at room temperature with 500nM DAPI in PBS to stain nuclei. Finally, after three more washes for 5 min each in PBS, slides were mounted in antifade reagent (# P36934; Invitrogen-Molecular Probes, Eugene, OR). Cryosections were viewed by confocal microscopy (LSM 510 Meta, Carl Zeiss, Göttingen, Germany) and laser-scanning images were obtained at 2.5X and 40X (oil immersion) objectives. Images were obtained using filters BP 505-530 and BP 420-480.

2.2.7. Lens Light Microscopy

All lenses were removed immediately and fixed in a solution of 2% paraformaldehyde, 2.5% glutaraldehyde, and 0.1 mol l^{-1} cacodylate. Lenses were post-fixed with osmium tetroxide, dehydrated, and embedded in Epon (LX112). Sections (1 µm thick) were stained with Toluidine Blue, and viewed and photographed under a Nikon microscope.

2.2.8. Impedance Studies and Model of Gap Junctional Coupling

Impedance studies were perfomed at Dr. Mathias's lab at SUNY, New York as described earlier (Gong et al., 1998; Baldo et al., 2001; Wang et al., 2009; Mathias et al., 1991). Briefly, WT and γ-KO mice were sacrificed by injection with sodium pentobarbitone solution (100 mg/kg of weight). The dissected lenses were placed in Tyrode solution (137.7 mM NaCl; 5.4 mM KCl; 2.3 mM NaOH; 1 mM $MgCl_2$; 10 mM glucose; 5 mM Hepes; pH 7.4). To perform impedance studies, a current passing microelectrode was placed in a central fiber cell. A second

voltage recording microelectrode was placed into the lens at different depths. Impedance was calculated by a fast Fourier analyzer (model 5420A; Hewlett-Packard, Palo Alto, CA). The high frequency impedance series resistance (R_s) is proportional to the gap junction coupling resistance between the point of voltage recording and the surface of the lens. To test pH gating properties, the lens was supefused with Tyrode solution that had been bubbled with 100% CO_2 for about 10 min (Martinez-Wittinghan et al., 2004). The R_s data were used to calculate the effective intracellular coupling resistivity (R_i Ω-cm) of gap junctions in the DF ($R_i = R_{DF}$ Ω-cm) and MF ($R_i = R_{MF}$ Ω-cm) in intact lenses. Fiber cells are approximately 3 μm in width, so the coupling conductance per area of cell to cell contact (G_i S/cm^2) was calculated from $G_i = 1/(3x10^{-4}R_i)$. For detailed method refer to Appendix.

2.2.9. Statistical Analyses

All experiments were performed at least in triplicates. Commercial software (Origin; Microcal Software Inc., Northampton, MA) was used for statistical analyses. Results were expressed as the mean ± SD. Differences at $P < 0.05$ were considered to be statistically significant.

2.3. Results

2.3.1. PKCγ in the KO mouse lens

Only homozygous PKCγ KO mice, genotyped by PCR of tail snips, were used for the experiments. To confirm the lack of expression of PKCγ protein in the lens of KO mice, western blotting was performed on whole lens lysates. Fig. 2.2A demonstrates a clear absence of PKCγ protein in the KO mouse lens, whereas it's expression is well detected in the WT lens. To check the localization of PKCγ protein in the WT lens, western blotting was done on lysates prepared from different sections of the lens. PKCγ is well expressed in the outer layer of epithelial cells, cortical layer of differentiating fiber cells, and with minimal levels in the nuclear section of mature fiber cells (Fig. 2.2B). This is consistent with our previous observations in rat lenses (Saleh et al., 2001).

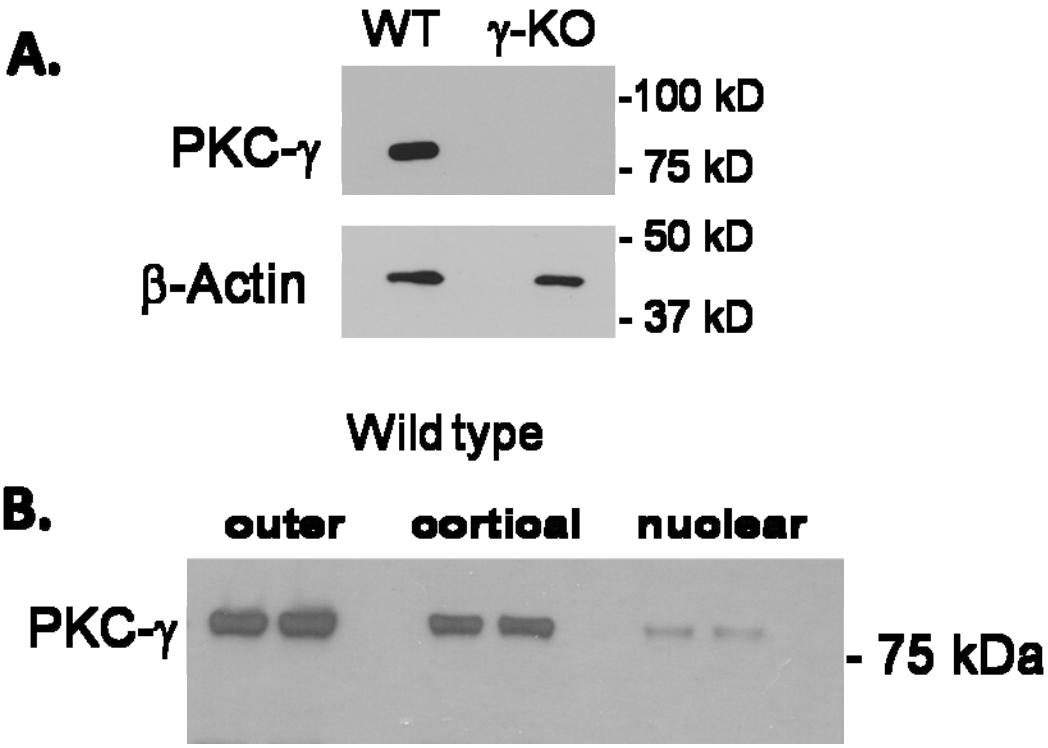

Figure 2.2 Expression and Distribution of PKCγ in the Mouse Lens. (A) Whole lens lysates from 8 -12 week old wild type (WT) and PKCγKO (γ-KO) mice were loaded in sample loading buffer at 10 μg protein per lane and immunoblotted with anti-PKCγ and anti-β-actin. The γ-KO lane shows no detectable expression of PKCγ. β-actin was used as loading control. Molecular weights on the right side are expressed in kDa. **(B)** Lysates from different sections of the wild type lenses were prepared as described in "Materials and Methods", loaded in sample loading buffer, and immunoblotted with anti PKCγ. Outer sections containing epithelial cells and cortical section containing differentiating fiber cells show very good expression of PKCγ, whereas there is minimal detection of PKCγ in the nuclear section containing only mature fibers. Each western blot was repeated at least three times.

2.3.2. Effect of the Loss of PKCγ on Connexin Protein Levels

Gap junctions play a critical role in maintaining the transparency and homeostasis of the avascular lens tissue (Mathias and Rae, 2004; Mathias et al., 1997; Berthoud and Beyer, 2009). All the three Cxs expressed in the lens can be phosphorylated by PKCγ (Saleh et al., 2001; Lin et al., 2004) and several studies have previously demonstrated that phosphorylation plays a significant role in the degradation of Cxs (Solan and Lampe 2009; Lin et al., 2003; Yin et al.,

2000; Laird, 2005). To test the effect of loss of PKCγ on Cxs, we performed western blotting to compare the amount of Cxs present in the KO lenses with WT lenses. Figures 2.3A and B show that, there is a significant increase (~150% more) in the total amount of Cx43 present in the KO lenses over WT lenses as detected by both a C-terminal and an N-terminal anti-Cx43 antibody. We did not find any significant change in the Cx46 and Cx50 protein levels detected by antibodies directed against the C-terminal region of the Cxs in the KO mice lenses in comparison to WT lenses (Fig. 2.3C, E, F, and G). However, when an antibody directed against the cytoplasmic loop of Cx46 was used for the western blotting multiple bands ranging from 60-kDa to 16-kDa were detected (Fig. 2.3D). This antibody detects Cx46 proteins which retain the cytoplasmic loop epitope (Gong et al., 1998; Wang et al., 2009). While we observed similar amount of detection for the full length Cx46 (bands at 60- and 46- kDa, Fig. 3D); the amount of higher mobility bands (36, 32, 29 kDa), which may represent the cleaved forms of Cx46, was much more in the KO lenses over WT lenses. Higher amount of the cleaved versions of Cx46 was detected in the nuclear MF in the KO lenses (Fig. 2.3H).

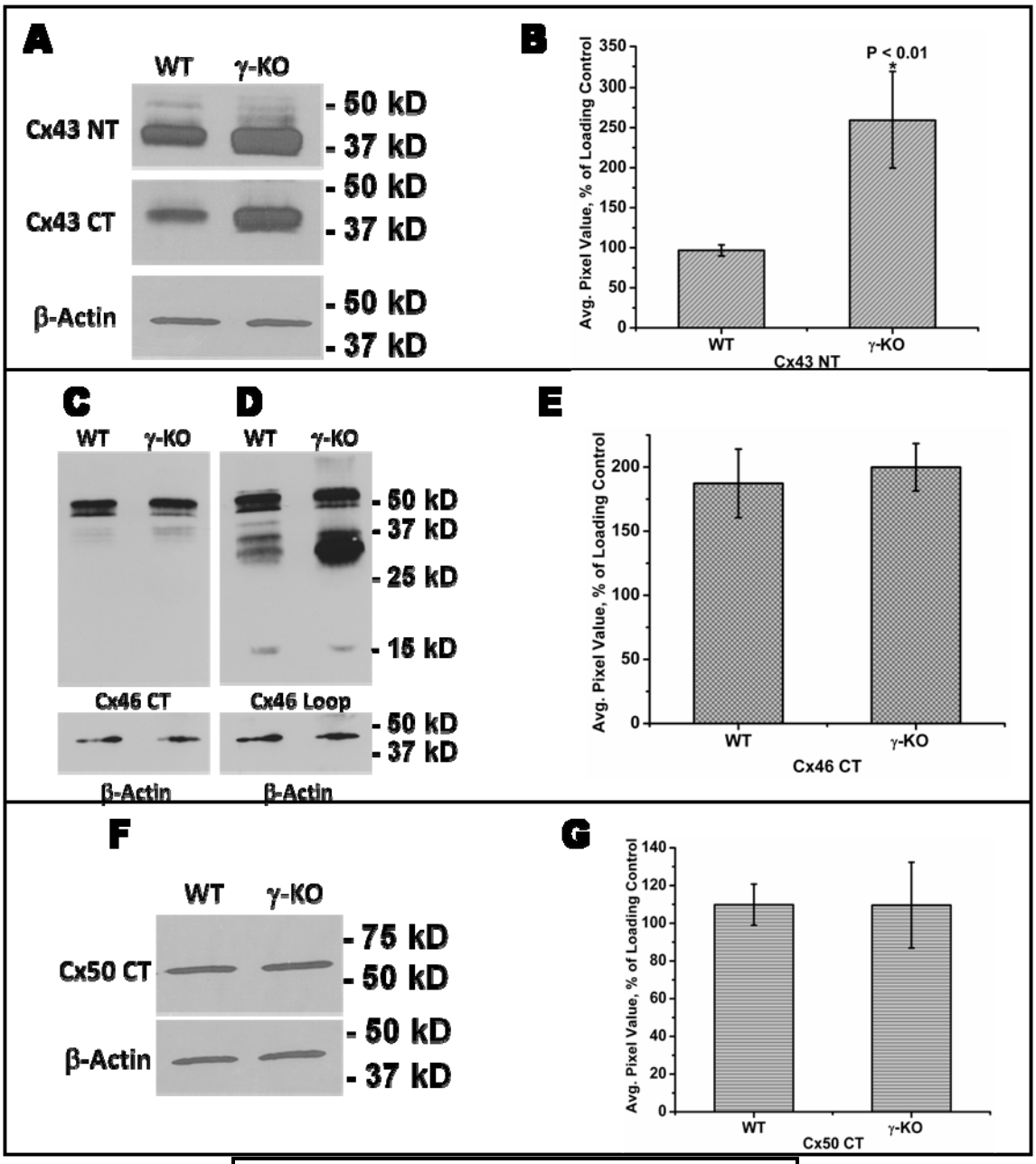
A
WT
γ-KO
Cx43 NT
- 50 kD
- 37 kD
Cx43 CT
- 50 kD
- 37 kD
β-Actin
- 50 kD
- 37 kD
B
Avg. Pixel Value, % of Loading Control
350
300
250
200
150
100
50
0
P < 0.01
*
WT
γ-KO
Cx43 NT
C
D
WT
γ-KO
WT
γ-KO
- 50 kD
- 37 kD
- 25 kD
- 15 kD
Cx46 CT
Cx46 Loop
- 50 kD
- 37 kD
β-Actin
β-Actin
E
Avg. Pixel Value, % of Loading Control
200
150
100
50
0
WT
γ-KO
Cx46 CT
F
WT
γ-KO
Cx50 CT
- 75 kD
- 50 kD
β-Actin
- 50 kD
- 37 kD
G
Avg. Pixel Value, % of Loading Control
140
120
100
80
60
40
20
0
WT
γ-KO
Cx50 CT
H
WT
γ-KO
C
N
C
N
Cx46 loop
-75kDa
-50 kDa
-37 kDa
-25 kDa
-20 kDa
-15kDa
β-Actin
-50 kDa
-37 kDa

Figure 2.3 Effect of Loss of PKCγ on Cx Protein Levels in the γ-KO Mouse. Whole lens lysates of WT and γ-KO mice were prepared and loaded in sample loading buffer at 10 μg of protein per lane. (A) Western blot of Cx43 using antibodies to both C-terminus (CT) and N-terminus (NT) region of Cx43. (C) Western blot of Cx46 using an antibody to the C-terminus, which is cleaved at the DF-MF transition; hence these data represent DF mostly. (D) Western blot of Cx46 using an antibody to the cytoplasmic loop, which is not cleaved; hence, these data represent Cx46 in both the DF and MF. (F) Western blot of Cx50 using an antibody to its C-terminus. β-actin is used as loading control in all the blots. (B, E, G) Quantitative comparison of the antibody staining of intact Cx43 NT, Cx46 CT and Cx50 CT respectively in γ-KO and WT lenses relative to the loading control β-actin. All bands were digitized by UN-SCAN-It gel software. The average pixel values for each Cx band was calculated, then normalized and plotted in % of loading control. Both Cx43 antibodies demonstrate significantly high (~150% more) amount of Cx43 in the γ-KO lenses. Digitized average pixel values of the N-terminal Cx43 band is plotted here. There is no significant change in the amount of detectable Cx46 and Cx50 by the C-terminal antibody. (H) Lysates from cortical (C) and nuclear (N) sections of the WT and PKCγ KO lenses were prepared as described in "Materials and Methods", loaded in sample loading buffer, and immunoblotted with anti-Cx46 (cytoplasmic loop antibody). Whereas the full-length forms of the Cx46 remained comparable in the WT and PKCγ KO cortical sections, higher amount of the clipped versions of Cx46 was detected in the nuclear MF of the KO lenses in comparison to nuclear sections of the WT lenses.

To test if the high amount of Cx43 present in the KO lens is message driven, we isolated total RNA from the lenses and performed both RT-PCR and quantitative real-time PCR to compare the message level of all three Cxs in WT and KO lenses. We did not observe any considerable change in mRNA level for any of the three Cxs (Fig. 2.4A & B). These data suggest that PKCγ regulates the amount of Cx43 expressed in the mouse lenses and that regulation is at the protein level.

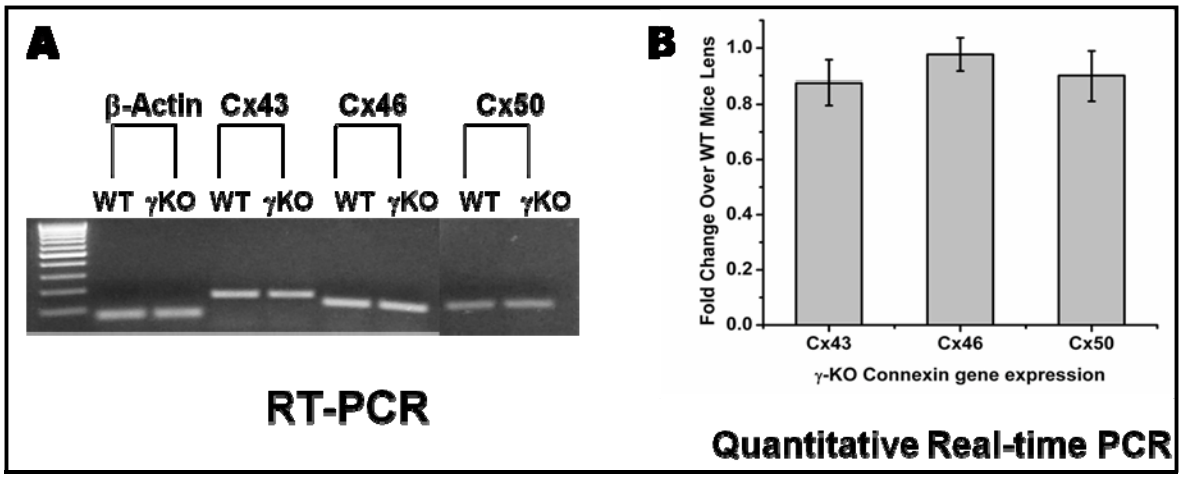

Figure 2.4 Effect of Loss of PKCγ on Cx Message Levels. (A) RT-PCR of Cx genes from WT and γ-KO lenses. Equal amount of total RNA was loaded for the reverse transcription and equal amount of cDNA was loaded for the PCR. The DNA ladder is a 100-bp ladder showing bands starting from 100 bp at the bottom to 1 kb at the top. β-actin used as the house keeping gene has a product size of 69 bp, and the Cx43, Cx46 and Cx50 genes' product sizes are at 161 bp, 123 bp, and 112 bp respectively. No observable change in any of the Cx gene expression was detectable. (B) The RT-PCR result was confirmed by quantitative real-time PCR. Fold change of Cx gene expression in the γ-KO lenses over the WT lenses is plotted in the bar graph. There is no significant change in any of the Cx gene expression. β-actin was used as the house-keeping gene.

2.3.3. Localization of Cx43 in the WT and γ-KO Lenses

A large body of work has shown that Cx43 is expressed only in the epithelial cell layer and its expression is lost as the epithelial cells differentiate into fiber cells in the equatorial region in the lens (Berthoud and Beyer, 2009; Gruijters et al., 1987; Musil et al., 1990; Beyer et al., 1989). We examined the localization of the excess Cx43 in different regions of the PKCγ KO mice lenses in comparison to WT lenses both by western blotting and immunocytochemistry. Cx43 was detected only in the outer epithelial cells in WT lenses by western blotting, but the expression persisted into the differentiating fibers in the cortical sections of γKO lenses (Fig. 2.5A). Immunocytochemistry was used to further confirm the western blotting results of presence of Cx43 in the DF in the KO lenses. WT lens sections showed binding of the Cx43 antibody only to the epithelial cell layer (Fig. 2.5B & 2.5D) and in the equatorial region of differentiation zone (Fig. 2.5C). γ-KO lens sections (Fig. 2.5E) clearly showed a higher amount

of Cx43 fluorescence than the WT sections supporting our whole lens lysate western blotting result (Fig. 2.3A). The 40X magnification images of the equatorial (Fig. 2.5F) and anterior (Fig. 2.5G) regions illustrated intense binding of anti-Cx43 antibody into the cortical fiber cells along with the epithelial cell layer. These results demonstrate the requirement of PKCγ for the regulation and loss of Cx43 expression during the differentiation of lens epithelial cells to fiber cells.

We also observed the presence of nuclei in the typical nuclei free region in the MF in KO lenses (Fig. 2.5I), whereas the WT lenses showed typical nuclei distribution with the nuclei being degraded in the DF to MF transition zone (Fig. 2.5H). This difference in nuclei degradation was also confirmed by light microscopy images (Fig. 2.5J to 2.5M).

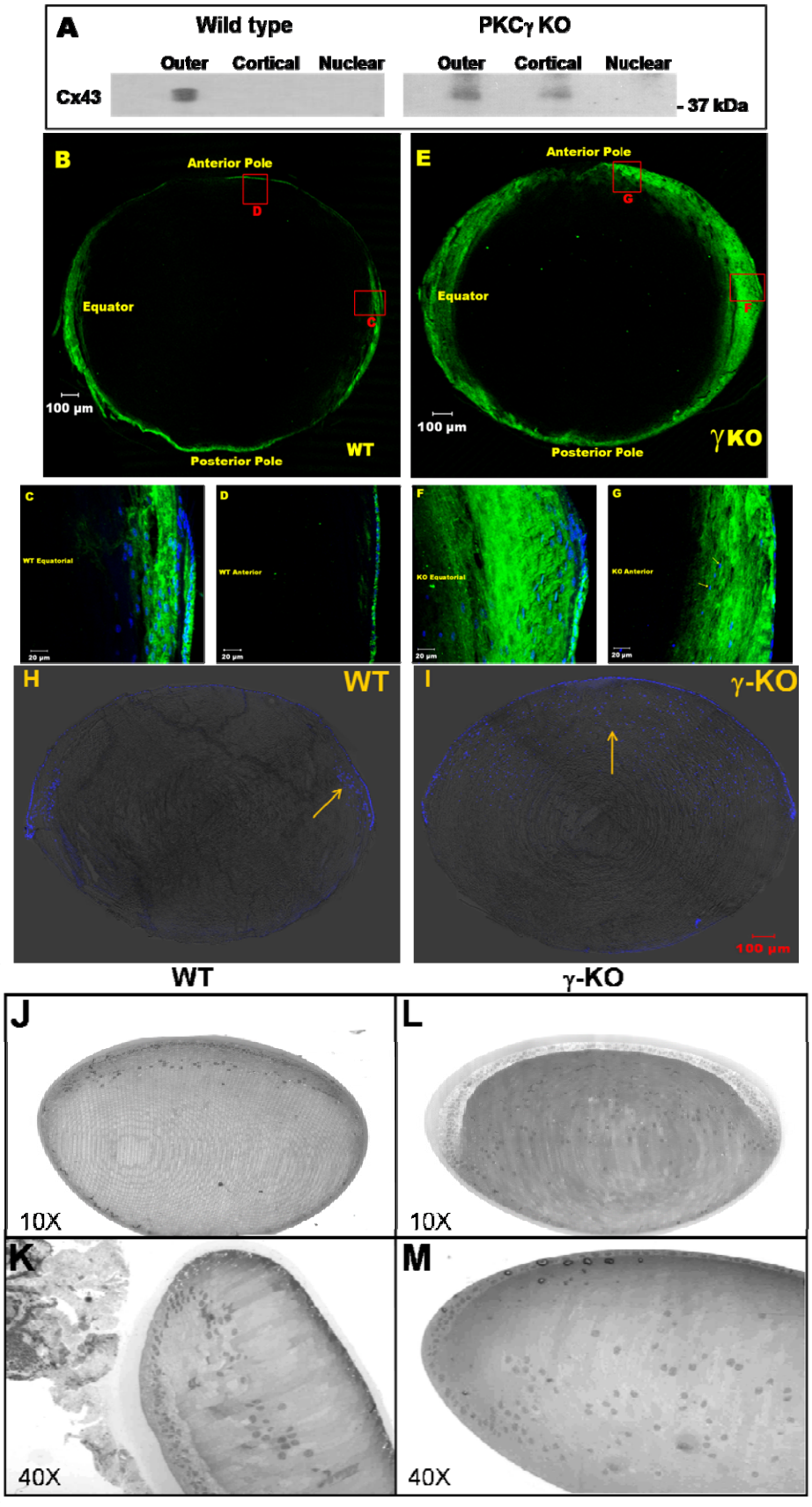
A
Wild type
PKCγ KO
Outer
Cortical
Nuclear
Outer
Cortical
Nuclear
Cx43
37 kDa
B
Anterior Pole
D
Equator
C
100 µm
Posterior Pole
WT
E
Anterior Pole
G
Equator
F
100 µm
Posterior Pole
γKO
C
WT Equatorial
D
WT Anterior
F
KO Equatorial
G
KO Anterior
H
WT
I
γ-KO
100 µm
WT
γ-KO
J
10X
L
10X
K
40X
M
40X

Figure 2.5 Localization of Cx43 in the Lens. (A) Lysates from different sections of the WT and PKCγ KO lenses were prepared as described in "Materials and Methods", loaded in sample loading buffer, and immunoblotted with anti-Cx43 (N-terminal antibody).Cx43 is detected only in the outer epithelial cells in the WT lens whereas the expression is detected in the differentiating fibers in the cortical section in the KO lenses. (B-I) Confocal microscopy of WT and PKCγ KO lens cryosections. Lenses have been dissected axially. Green represents Cx43 and Blue is DAPI staining of nuclei. B & E are whole lens images captured at 2.5X magnification. The KO lens sections clearly show higher staining for Cx43 compared to the WT lens. Insets in B and E are magnified portions of the lens sections acquired at 40X magnification in C, D, F and G. (C) Equatorial regions of the WT lens showing expression of Cx43 in the epithelium and the epithelial cell differentiation zone. (D) Anterior regions of WT lens show the expression of Cx43 only in the epithelial layer of cells. (F) Equatorial regions of KO lens show detection of Cx43 in the cortex (compared with C). (G) Anterior regions of KO lens show clear expression of Cx43 in the cortex along with the epithelial layer. Arrows point to existence of nuclei in the typical nucleus free region of normal lens (compare with D). (H) & (I) are whole lens sections at 10X magnification of WT and γ-KO mouse showing DAPI staining of nuclei. WT lens shows typical nucleus free zone in the MF whereas there is an abundance of nuclei in the DF in γ-KO lens. (J) and (L) are light microscopy pictures of stained WT and γ-KO mice lenses taken at 10X. (K) and (M) also light microscopy pictures of stained WT and γ-KO mice lenses taken at 40X magnification showing the equatorial region. The typical V-shaped distribution and eventual degradation of nuclei is visible in WT lenses (J and K), whereas the nuclei continues to be present in the typical organ-free zone of γ-KO lenses (L and M) as observed in the confocal microscopy images. (Tissue processing, sectioning and staining for light microscopy was done by Llyod Willard at the College of Veterinary Medicine, Kansas State University)

2.3.4. Gap Junction Coupling

Lenses from 2-month-old PKCγ-KO mice are not significantly different in size from WT (Lin et al., 2006). There were no significant differences in radii, resting voltages and input resistances (the impedance at 0 Hz) (Table-2.2). The transparency of γ-KO lenses was comparable to the WT lenses (Lin et al., 2006). The WT data were from 8 lenses taken from 5 mice and the γ-KO data were from 10 lenses taken from 7 mice. The resting voltage measured

near the lens surface was not significantly different in WT (-68±4 mV) vs. γ-KO (-67±2 mV). The average input resistance measured near the lens surface was also not significantly different in WT lenses (3.5±0.3 KΩ) vs. γ-KO lenses (3.6±0.2 KΩ). These data imply that KO of PKCγ has no significant effect on membrane conductance at this early age.

In differentiating fibers (DF), the coupling conductance varies from equator to poles, with the lowest values at the poles; whereas in mature fibers (MF), cell-to-cell coupling is relatively uniform (Baldo and Mathias 1992). All of our data were recorded at 45° from the posterior pole, where the current density and coupling conductance are close to their angular averages. This section compares the average gap junction coupling conductance in γ-KO lenses with that in WT lenses of mice at the same age.

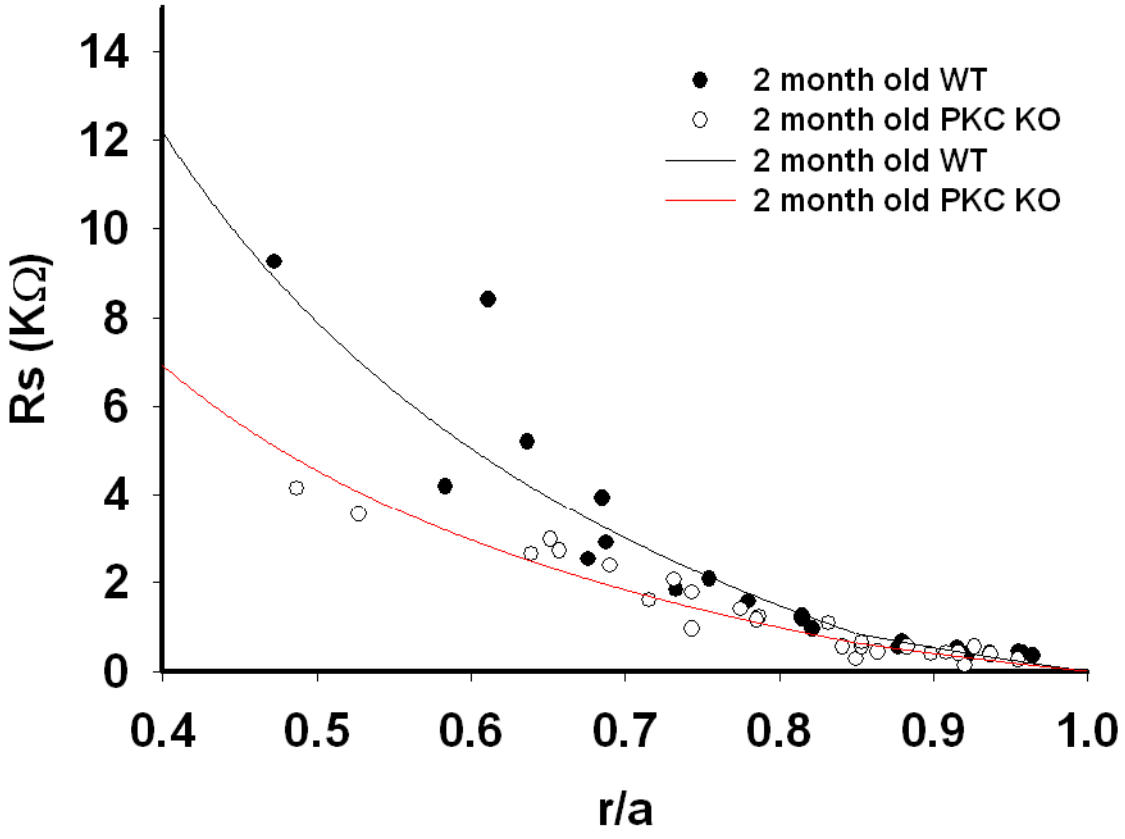

Figure 2.6 Impedance Studies from WT and PKCγ KO Lenses. The series resistance (R_S, KΩ) due to gap junction coupling between the point of recording r cm from the lens center and the surface of the lens at $r = a$ cm. The data are graphed as a function of the fractional distance from the lens center, r/a. The WT data were from 8 lenses taken from 5 mice. The KO data were

from 10 lenses taken from 7 mice. In each lens, one or two measurements of R_S in the DF were made, then the voltage microelectrode was advanced into the MF where R_S was determined at one or more locations. The values of R_S in the WT lenses are higher than those in PKCγ KO lenses, suggesting PKCγ down regulated gap junction coupling. (Experiments performed in Dr. Mathias' lab by Dr. Huan Wang at the State University of New York (SUNY), NY)

Figure 2.6 shows R_S data from γ-KO and WT lenses and the curve fit of the R_s model to these data. R_s (Ω) represents the cumulative series resistance due to gap junctions between the surface of the lens and the point of recording. The lesser R_S at all radial locations in the γ-KO relative to WT lenses suggests that there is more coupling in the KO lenses. At the DF-to-MF transition, the effective intracellular resistivity in either type of lens increases. This can be seen as a change in the slope of the smooth curves. Without this increase in resistivity at the DF-to-MF transition, the data in MF would fall above the model curve, with the fit becoming increasingly poor with depth. The graph is scaled to the relatively large resistance in MF, so the fit to the DF data look trivial. This is not the case however. The DF data are more accurate and therefore have a lower standard deviation than the MF data since errors in locating the voltage recording microelectrode increase with depth into the lens (as distance from the center to the point of voltage recording gets smaller). The value of R_{DF} is not affected by these uncertainties as it is determined before the value of R_{MF} can be estimated and is therefore very well determined.

Table 2.2 A comparison of transport properties of lenses from PKCγ KO and WT mice. There were no significant differences in radii, resting voltages and input resistances (the impedance at 0 Hz). All lenses were transparent. In PKCγ KO lenses, however, the average coupling conductance was significantly higher than in WT lenses (*P < 0.05). This was particularly evident in the inner core of MF where the coupling conductance of PKCγ KO lenses was elevated significantly when compared with that of WT lenses. (Data obtained from experiments performed in Dr. Mathias' lab by Dr. Huan Wang at the SUNY, NY)

			WT	PKCγ KO
radius		cm	0.112±0.004	0.110±0.002
Input resistance		KΩ	3.5±0.3	3.6±0.2
Resting voltage		mV	-68±4	-67±2
Coupling Conductance	DF	S/cm²	0.50±0.08	0.67±0.05
	MF	S/cm²	0.28±0.03	0.51±0.02
Normalized Coupling Conductance	DF	-	1	1.34±0.24*
	MF	-	1	1.82±0.21*

The coupling conductance per unit area of cell-to-cell contact was calculated for DF ($G_{DF} = 1/wR_{DF}$) and MF ($G_{MF} = 1/wR_{MF}$), where R_{DF} and R_{MF} are determined by curve fitting and $w \approx 3 \times 10^{-4}$ (cm) is the width of a fiber cell. At 2 months of age, in the absence of any cataract formation, statistically significant increases in G_{DF} and G_{MF} were found when the PKCγ gene was knocked out. Table 2.2 summarizes gap junction coupling in these lenses. The conductances in Table 2.2 were determined by curve fitting data from each lens studied.

2.3.5. Gap Junction Channel Gating

Gap junction channels made from most connexins show a decrease in conductance with a reduction in intracellular pH (Spray et al., 1981). However in the lens, MF coupling conductance, which depends on Cx46 channels, is pH-insensitive whereas DF coupling conductance, which depends on both Cx46 and Cx50 channels, is pH-sensitive (Mathias et al., 2007). Loss or blockage of Cx50 channels leads to the loss of pH sensitivity of DF channels (Baldo et al., 2001; Martinez-Wittinghan et al., 2006). The stoichiometry of Cx46/Cx50 channels appears to be important for pH gating in the lens, such that selective damage to Cx50, but not Cx46, would alter pH-mediated gating.

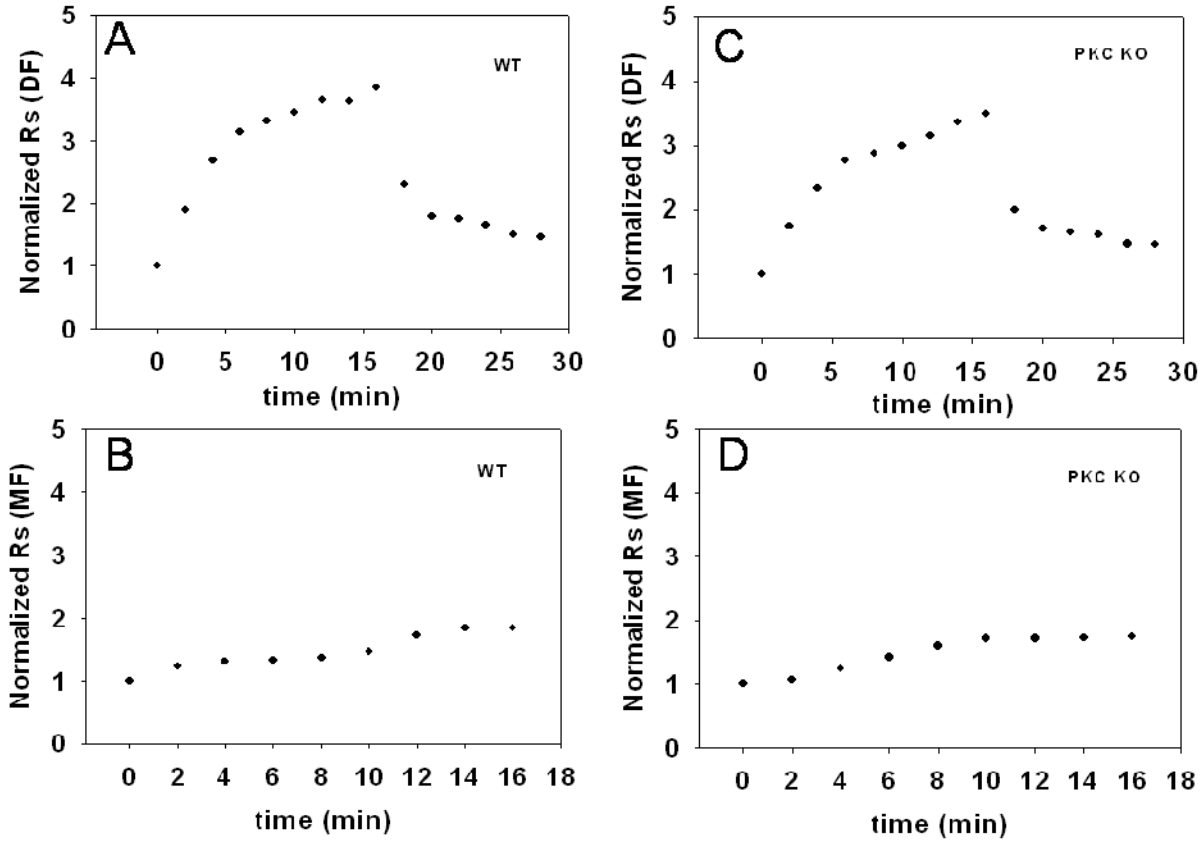

Figure 2.7 Gating properties of gap junction channels in 2-month-old WT and PKCγ KO lenses. To test pH gating properties, the lens was superfused with Tyrode solution that had been bubbled with 100% CO_2 for about 10 min. (A) and (B) show the gating properties in 2-month-old WT lenses. The increase is about 4 fold in Rs (series resistance) when the pH drops to ~ 5.8. This means DF gap junction channels are pH sensitive. When the point of voltage recording is in the MF, the increase in Rs is relatively small when pH decreases, and the small increase is due to

the increase of Rs in DF. (C) and (D) show similar pattern of changes in Rs in 2-month-old PKCγ KO lenses. Therefore, the DF gap junction channels are pH sensitive, whereas the MF gap junction channels are pH insensitive. The data in this figure are from one experiment representative of n=3. (Experiments performed in Dr. Mathias lab by Dr. Huan Wang at SUNY, NY).

To test gap junction channel gating properties in response to a drop in pH, the lens was superfused with normal Tyrode solution that had been bubbled with 100% CO_2 (see "Materials and Methods"). When the voltage electrode was placed in the DF of γ-KO lenses, there was a large increase in R_s (series resistance) when pH dropped (Fig. 2.7). This implies that DF gap junction channels are pH-sensitive. Since the DF channels retain normal pH sensitivity, these data suggest there is no significant change to the Cx50 channel gating. When the point of voltage recording was in the MF, the percent increase in R_s was relatively small. R_s depends on the cumulative resistance of DF in series with MF (Wang et al., 2009) and since coupling of MF is not pH-sensitive, the fractional increase in R_s measured in the MF will be small and dependent on uncoupling of DF (Mathias et al., 1991). Thus, pH gating properties of γ-KO lenses were the same as those of control lenses, in which the DF gap junction channels are pH-sensitive and the MF gap junction channels are pH-insensitive.

2.3.6. Phosphorylation of Cx43 and Cx46

Phosphorylation by PKCγ leads to uncoupling of gap junction channels. After observing the difference in the gap junction coupling in the impedance studies between WT and γ-KO lenses, we compared the phosphorylation status of Cx43 at the PKC site, serine 368 (Ser368), and general phosphorylation of serine and threonine residues in Cx46 protein by immunoprecipitating the Cx46 protein and then probing with phospho-serine and phospho-threonine antibodies. Although the phosphorylation levels at Ser368 of Cx43 looked similar in both WT and KO lenses, when they were normalized to total Cx43 protein, significantly less amount (~150% less) of phosphorylation was found in the KO lenses (Fig. 2.8A & B). The detection of phosphor-Ser368Cx43 bands in the KO lenses could be because of the phosphorylation caused by other PKC isoforms, PKCα or PKCε, detected in the lens. Both phospho-serine-Cx46 and phospho-threonine-Cx46 detection levels were less in the KO lenses,

but a statistically significant difference was observed only in the phospho-serine-Cx46 levels (Fig. 2.8C, D & E). The apparent non-detection of phospho-serine-Cx46 in the KO lenses could be attributed to minimal loading of immunoprecipitated Cx46. Another possibility is that PKCγ phosphorylation of Cx46 serine residues could be more prominent in the lens cortex than by other kinases. These results indicate that PKCγ regulates these gap junctions by phosphorylation and this could explain the higher gap junction coupling observed in the DF of KO lenses in our impedance studies. Cx50 had shown similar phosphorylation results in our previous study in PKCγ KO lenses (Lin et al., 2006). However, the significant increase in MF coupling conductance in the KO relative to WT lenses is not explained by the presence of Cx43 since its expression disappears in the MF.

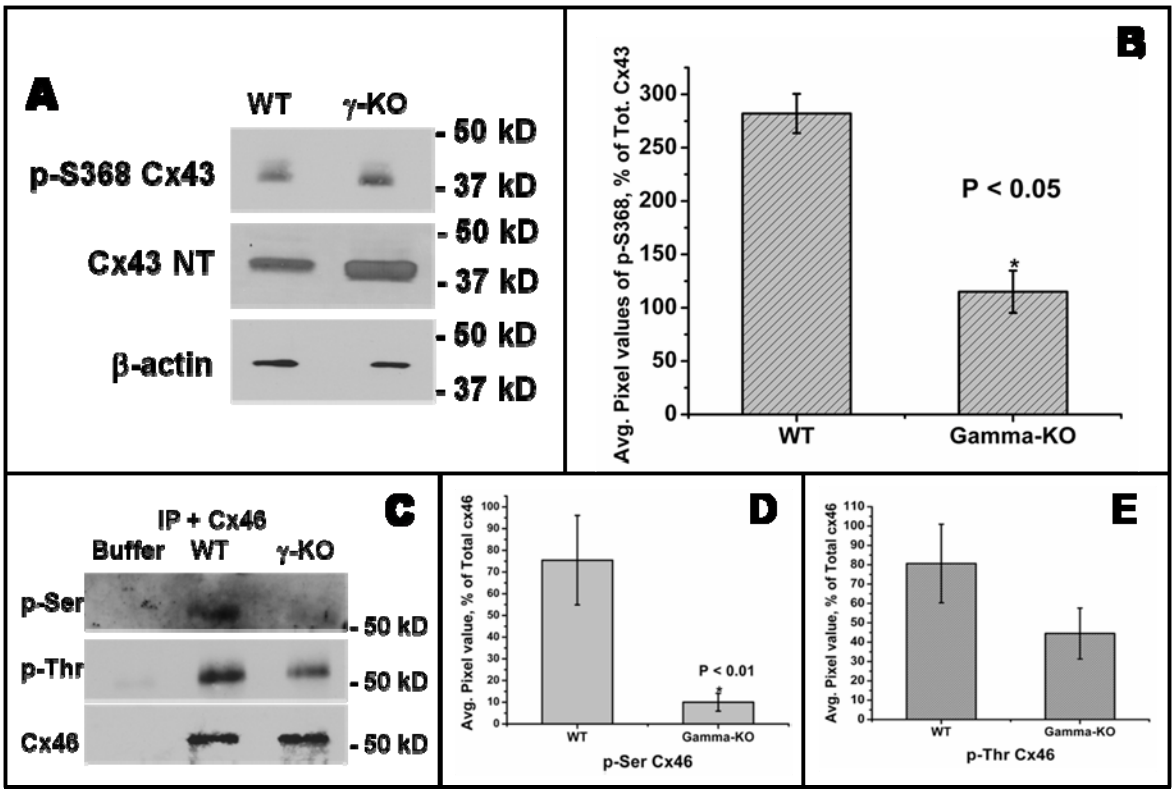

Figure 2.8 **Phosphorylation of Cx43 and Cx46. (A)** Whole lens lysates of WT and γ-KO mice were loaded in sample loading buffer at 10 μg of protein per lane and probed by anti-Cx43 (N-terminal) and anti phospho-ser368 (the PKC phosphorylation site in Cx43 in western blotting. β-actin was used as loading control. **(B)** Quantitative comparison of the phospho-ser368 antibody staining in γ-KO and WT lenses relative to the total Cx43. Phosphorylation at serine

368 is >150% less in the KO lenses compared to wild type. **(C)** Cx46 was immunoprecipitated from 500 μg of protein in the whole lens extract (refer to "Material and Methods") from WT and γ-KO lenses and probed with anti-phosho-serine and anti-phospho-threonine antibody to detect phosphorylation of Cx46. Cx46 was probed to show equal loading. Buffer alone was used as a negative control in the immunoprecipitation. Signifiantly less amount of phospho-serine-Cx46 was detected in the PKCγ KO lenses. **(D)** Quantitative comparison of the phospho-serine antibody staining in γ-KO and WT lenses normalized to the total Cx46. **(E)** Quantitative comparison of phospho-threonine antibody staining in WT and γ-KO mice lenses normalized to the total Cx46 protein.

2.4. Discussion

To achieve the main function of focusing a clear image on the retina, the avascular lens tissue must maintain its transparency. Gap junctions are a major player in the lens circulatory system coordinating lens growth and maintaining its transparency throughout life. Given the dynamic nature of the Cx life cycle, appropriate regulation of gap junction channels is critical for maintaining the lens transparency. PKCs have been extensively implicated in the regulation of gap junctions through phosphorylation in a variety of tissues (Solan and Lampe, 2009; Laird 2006). We have previously reported the role played by PKCγ as an oxidative stress sensor in regulating the gap junctions both in lens epithelial cells and whole lens in culture (Lin et al., 2004; Zampighi et al., 2005; Lin and Takemoto 2005). Our earlier study in the γ-KO mice had demonstrated the regulation of Cx50 by PKCγ in response to oxidative stress. This study reveals that PKCγ is involved in the regulation of all three Cxs in the lens, controls the expression and distribution of Cx43, and plays a major role in gap junction coupling.

Although it is well established that both Cx43 and Cx50 are expressed in the anterior layer of epithelial cells of the lens and the expression of Cx43 is turned off in the equatorial differentiation zone as the epithelial cells differentiate into fiber cells, how this is achieved is not clear. Our data offer clear evidence that PKCγ plays a major role in this process as, in the absence of PKCγ, Cx43 expression continues into the differentiating fiber cells. Phosphorylation of Cx43 by PKC leads to gap junction plaque internalization and subsequent degradation (Solan and Lampe, 2009). Not only PKC activators, like TPA and oxidative stress caused by H_2O_2, but

growth factors like insulin-like growth factor I (IGF-I) and lens epithelial derived growth factor (LEDGF) have also been reported to activate PKCγ in lens epithelial cells, resulting in the phosphorylation of Cx43 (Nguyen et al., 2003; Lin et al., 2003; Saleh and Takemoto 2000).

We believe growth factors drive PKCγ in its role in turning off the expression of Cx43 in the differentiation zone. We have previously reported the presence of PKCα and PKCγ as the predominant conventional PKC isoforms in the lens epithelium, but only PKCγ is present in the rat lens cortex. Our current data also detects the presence of PKCγ in the mouse lens cortex. The other stress sensing PKC in the lens cortex, PKCε, has been studied for its role in protecting the lens from opacity and did not appear to be involved in gap junction regulation. This isoform is activated in response to hypoxia (Akoyev et al., 2009) and is localized to mitochondria in lens epithelial cells (Barnett et al., 2008). These findings suggest that the presence of PKCγ is essential for the regulation of gap junctions in the lens.

Gap junctions have been called both "good samaritans" and "executioners," terms that refer to their ability to pass both necessary metabolites and apoptotic signals from cell to cell (Farahani et al., 2005). While passage of necessary metabolites through the gap junctions helps maintain the lens homeostasis, the uncontrolled passage of oxidative stress signals can lead to cataract formation (Berthoud and Beyer, 2009). Oxidative stress triggers the activation of PKCγ and leads to the uncoupling of gap junctions in the lens epithelial cells and lens in culture, which helps in preventing the spread of the stress signal (Solan and Lampe, 2009; Zampighi et al., 2005; Lin and Takemoto, 2005). Our data demonstrated that in the absence of PKCγ there is significantly higher gap junctional channel conductance both in the DF and MF cells of γKO lenses relative to WT. The highly reduced Cx46 phosphorylation and presence of Cx43 in the DF of the PKCγ KO lenses contribute to this. Our previous finding of non-phosphorylation of Cx50 in the γKO mice may also contribute to the higher DF coupling conductance (Lin et al., 2006).

A prolonged accumulation of sublethal oxidative stress damage through open gap junctions would be harmful and may lead to cataract formation. Thus, PKCγ plays a very prominent role in the regulation of all three gap junction channels in the lens and in the differentiation of the lens. Possibly the loss of Cx43 in the DF is necessary to maintain the structural integrity of the lens and the persistence of Cx43 into the fiber cells could be reason for

the vacuoles observed in the KO lenses. The stoichiometry of gap junctions in the differentiating fiber cells of PKCγ KO mice needs further investigation.

Whereas the presence of Cx43 in the DF and the reduced phosphorylation of Cx46 on serine residues explains the higher gap junction coupling observed in the DF in KO lenses, the much larger increase in gap junction coupling observed in MF of KO lenses could be because of the higher amount of the cleaved versions of the Cx46 detected by the cytoplasmic loop Cx46 antibody. Cx46 cleavage occurs at two distinct stages, initially in the outer DF coinciding with the dispersal of fiber cell nuclei followed by a second cleavage in the zone associated with the loss of fiber cell nuclei during fiber cell differentiation (Jacobs et al., 2004). It is possible that phosphorylation of Cx46 by PKCγ plays a role in regulating the amout of clipped Cx46 versions present in the MF. Moreover, the persistence of nuclei into the inner DFs could also have an implication on the amount of different proteins observed in the KO lenses over WT lenses.

Wang et al (Wang and Schey, 2009) recently reported the truncation sites of bovine lens Cx46. Although they found the truncation of Cx46 in the N-terminal, cytoplasmic loop, and C-terminal tail regions, the major truncation region of Cx46 in the nuclear MF was suggested to be in the C-terminus tail region corresponding to amino acid residues 251-285 in the bovine lens. If the mouse lens Cx46 follows a similar clipping pattern, then the cytoplasmic loop antibody we have used (targeted for residues 115-128) might not detect the Cx46 truncated in the cytoplasmic loop region. But the major truncation site in the MF of the lens (residues 251-285) would result in the fragment sizes (36 to 29 kDa) we have detected in our western blot. Hence, the accumulation of these fragments observed in the KO mice lens MF could explain the much larger gap junction coupling observed in the KO mice lens MF over WT lens MF. The truncation and PKC phosphorylation sites in the mouse lens Cx46 needs to be identified to understand how the loss of PKCγ causes accumulation of the cleaved versions of Cx46 in the lens MF.

Our confocal and light microscopy data shows the abnormal persistence of nuclei in the typical nucleus-free zone of the lens in the KO lenses. This suggests that differentiation is delayed in the KO lenses and PKCγ has an important role in this process. Although a few different mechanisms have been proposed for organelle elimination in the lens, the whole process involves a complex series of independent steps (Bassnett, 2009; Dahm, 2004; Bassnett, 2002). PKCs including the conventional PKCs (e.g. PKCβII) (Chiarini et al., 2002), and novel PKCs (e.g. PKCδ)(Cross et al., 2000) have been implicated in nuclear lamina disassembly in

apoptosis. Degradation of nuclear lamina and concomitant change in nuclear shape being an early step in the nuclei degradation process (Bassnett, 2009), our data indicate that PKCγ is an important cog in the wheel of the entire nuclei degradation process and needs further study to explain the mechanism.

2.5. References

Abeliovich, A., Chen, C., Goda, Y., Silva, A. J., Stevens, C. F. and Tonegawa, S. (1993) Modified hippocampal long-term potentiation in PKCgamma-mutant mice. *Cell* 75,1253 -1262.

Akoyev, V., Das, S., Jena, S., Grauer, L., Takemoto, D.J. (2009) Hypoxia-regulated activity of PKCepsilon in the lens. *Invest Ophthalmol Vis Sci.* 50(3):1271-82.

Aronowski, J., Grotta, J., Strong, R. and Waxman, M. (2000) Interplay between the gamma isoform of PKC and calcineurin in regulation of vulnerability to focal cerebral ischemia. *J Cereb Blood Flow Metab.* 20:343-349.

Baldo, G.J., Gong, X., Martinez-Wittinghan, F.J., Kumar, N.M., Gilula, N.B., Mathias, R.T. (2001) Gap junctional coupling in lenses from alpha(8) connexin knockout mice. J Gen Physiol 118(5):447–456

Baldo, G.J., Mathias, R.T. (1992) Spatial variations in membrane properties in the intact rat lens. *Biophys J.* 63(2):518–529

Barnett, M., Lin, D., Akoyev, V., Willard, L., Takemoto, D. (2008) Protein kinase C epsilon activates lens mitochondrial cytochrome c oxidase subunit IV during hypoxia. *Exp Eye Res.* 86(2):226-34.

Bassnett, S. (2002) Lens organelle degradation. *Exp. Eye Res.* 74:1–6.

Bassnett, S. (2009) On the mechanism of organelle degradation in the vertebrate lens. *Exp Eye Res.* 88(2):133-9.

Bassnett, S., Kuszak, J.R., Reinisch, L., Brown, H.G., Beebe, D.C. (1994) Intercellular communication between epithelial and fiber cells of the eye lens. *J Cell Sci.* 107:799-811.

Berthoud, V.M., Beyer, E.C. (2009) Oxidative stress, lens gap junctions, and cataracts. *Antioxid Redox Signal.* 11(2):339-53.

Beyer, E.C., Kistler, J., Paul, D.L., Goodenough, D.A. (1989) Antisera directed against connexin43 peptides react with a 43-kD protein localized to gap junctions in myocardium and other tissues. *J Cell Biol*. 108:595–605

Bowers, B. and Wehner, J. (2001) Ethanol consumption and behavioral impulsivity are increased in protein kinase C gamma null mutant mice. *J. Neurosci.* 21, RC180:1 -5.

Chiarini, A., Whitfield, J.F, Armato, U., Dal Pra, I. (2002) Protein kinase C-beta II Is an apoptotic lamin kinase in polyomavirus-transformed, etoposide-treated pyF111 rat fibroblasts. *J Biol Chem.* 277(21):18827-39.

Cross, T., Griffiths, G., Deacon, E., Sallis, R., Gough, M., Watters, D., Lord, J.M. (2000) PKC-delta is an apoptotic lamin kinase. *Oncogene.* 19(19):2331-7.

Dahm, R. (2004) Dying to see. *Sci. Am.* 291:82–89.

Das, S., Lin, D., Jena, S., Shi, A., Battina, S., Hua, D.H., Allbaugh, R., Takemoto,

D.J. (2008) Protection of retinal cells from ischemia by a novel gap junction inhibitor. *Biochem Biophys Res Commun.* 373(4):504-8.

Eisenberg, R.S., Barcilon, V., Mathias, R.T. (1979) Electrical properties of spherical syncytia. *Biophys J.* 25(1):151–180

Farahani, R., Pina-Benabou, M. H., Kyrozis, A., Siddiq, A., Barradas, P. C., Chiu, F. C., Cavalcante, L. A., Lai, J. C., Stanton, P. K. and Rozental, R. (2005) Alterations in metabolism and gap junction expression may determine the role of astrocytes as `good samaritans' or executioners. *Glia* 50:351 -361.

Gao, J., Sun, X., Martinez-Wittinghan, F.J., Gong, X., White, T.W., Mathias, R.T. (2004) Connections between connexins, calcium, and cataracts in the lens. J Gen Physiol 124(4):289–300

Gong, X., Baldo, G.J., Kumar, N.M., Gilula, N.B., Mathias, R.T. (1998) Gap junctional coupling in lenses lacking alpha3 connexin. Proc Natl Acad Sci USA 95(26):15303–15308

Gong, X., Li, E., Klier, G., Huang, Q., Wu, Y., Lei, H., Kumar, N.M., Horwitz, J., Gilula, N.B. (1997) Disruption of alpha3 connexin gene leads to proteolysis and cataractogenesis in mice. Cell 91:833-43.

Goodenough, D.A., Goliger, J.A., Paul, D.L. (1996) Connexins, connexons, and intercellular communication. Annu Rev Biochem 65:475–502.

Gruijters, W.T., Kistler, J., Bullivant, S. (1987) Formation, distribution and dissociation of intercellular junctions in the lens. *J Cell Sci.* 88:351-9

Harris, A. L. (2007) Connexin channel permeability to cytoplasmic molecules. *Prog. Biophys. Mol. Biol.* 94, 120–143.

Jacobs, M.D., Soeller, C., Sisley, A.M., Cannell, M.B., Donaldson, P.J. (2004) Gap junction processing and redistribution revealed by quantitative optical measurements of connexin46 epitopes in the lens. *Invest Ophthalmol Vis Sci.* 45(1):191-9.

Kumar, N.M., Gilula, N.B. (1996) The gap junction communication channel. Cell 84(3):381–388

Laird, D. W. (2006) Life cycle of connexins in health and disease. Biochem. J. 394, 527–543

Laird, D.W. (2005) Connexin phosphorylation as a regulatory event linked to gap junction internalization and degradation. *Biochimica et Biophysica Acta* 1711:172– 182.

Li, X., Su, V., Kurata, W.E., Jin, C., Lau, A.F. (2008) A novel connexin43-interacting protein, CIP75, which belongs to the UbL-UBA protein family, regulates the turnover of connexin43. *J Biol Chem.* 283(9):5748-59.

Lin, D., Barnett, M., Lobell, S., Madgwick, D., Shanks, D., Willard, L., Zampighi, G.A., Takemoto, D.J. (2006) PKCgamma knockout mouse lenses are more susceptible to oxidative stress damage. *J Exp Biol.* 209(Pt 21):4371-8.

Lin, D., Boyle, D.L., Takemoto, D.J. (2003) IGF-I-induced phosphorylation of connexin 43 by PKCgamma: regulation of gap junctions in rabbit lens epithelial cells. *Invest Ophthalmol Vis Sci.* 44:1160-8.

Lin, D., Lobell, S., Jewell, A., Takemoto, D.J. (2004) Differential phosphorylation of connexin46 and connexin50 by H2O2 activation of protein kinase Cgamma. *Mol Vis.* 10:688-95.

Lin, D., Takemoto, D.J. (2005) Oxidative activation of protein kinase Cgamma through the C1 domain. Effects on gap junctions. *J Biol Chem.* 280(14):13682-93.

Malmberg, A. B., Chen, C., Tonegawa, S. and Basbaum, A. I. (1997) Preserved acute pain and reduced neuropathic pain in mice lacking PKCgamma. *Science* 278,279 -283.

Martinez-Wittinghan, F.J., Sellitto, C., White, T.W., Mathias, R.T., Paul, D., Goodenough, D.A. (2004) Lens gap junctional coupling is modulated by connexin identity and the locus of gene expression. Invest Ophthalmol Vis Sci 45(10):3629–3637

Martinez-Wittinghan, F.J., Srinivas, M., Sellitto, C., White, T.W., Mathias, R.T. (2006) Mefloquine effects on the lens suggest cooperative gating of gap junction channels. *J Membr Biol.* 211(3):163–171

Mathias, R.T., Kistler, J., Donaldson, P. (2007) The lens circulation. *J Membr Biol.* 216(1):1-16.

Mathias, R.T., Rae, J.L. (2004) The lens: local transport and global transparency. *Exp. Eye Res.* 78(3):689-98.

Mathias, R.T., Rae, J.L., Baldo, G.J. (1997) Physiological properties of the Normal Lens. *Physiological Reviews* 77(1):21-50.

Mathias, R.T., Riquelme, G., Rae, J.L. (1991) Cell to cell communication and pH in the frog lens. *J Gen Physiol.* 98(6):1085–1103

Musil, L.S., Beyer, E.C., and Goodenough, D.A. (1990) Expression of the gap junction protein connexin43 in embryonic chick lens: molecular cloning, ultrastructural localization, and post-translational phosphorylation. *J Membr Biol* 116: 163–175.

Narita, M., Mizoguchi, H., Suzuki, T., Narita, M., Dun, N., Imai, S., Yajima, Y., Nagase, H., Suzuki, T. and Tseng, L. (2001) Enhanced opioid responses in the spinal cord of mice lacking protein kinase C gamma isoform. *J. Biol. Chem.* 276,15409 -15414.

Nguyen, T.A., Boyle, D.L., Wagner, L.M., Shinohara, T., Takemoto, D.J. (2003) LEDGF activation of PKC gamma and gap junction disassembly in lens epithelial cells. *Exp Eye Res.* 76:565-72.

Ohsawa, M., Narita, M., Mizoguchi, H., Cheng, F. and Tseng, L. (2001) Reduced hyperalgesia induced by nerve injury, but not by inflammation in mice lacking protein kinase gamma isoform. *Eur. J. Pharmacol.* 429,157 -160.

Saez, J. C., Berthoud, V. M., Branes, M. C., Martinez, A. D. and Beyer, E. C. (2003) Plasma membrane channels formed by connexins: their regulation and functions. Physiol. Rev. 83, 1359–1400

Saleh, S.M., Takemoto, D.J. (2000) Overexpression of protein kinase Cgamma inhibits gap junctional intercellular communication in the lens epithelial cells. *Exp Eye Res.* 71(1):99-102.

Saleh, S.M., Takemoto, L.J., Zoukhri, D., Takemoto, D.J. (2001) PKC-gamma phosphorylation of connexin 46 in the lens cortex. *Mol Vis.* 7:240-6.

Schrenk, K., Kapfhammer, J. and Metzer, F. (2002) Altered dendritic development of cerebellar Purkinje cells in slice cultures from protein kinase Cγ -deficient mice. *Neuroscience.* 110:675-689.

Shutoh, F., Katoh, A., Ohki, M., Itohara, S., Tonegawa, S. and Nagao, S. (2003) Role of protein kinase C family in the cerebellum-dependent adaptive learning of horizontal optokinetic response eye movements in mice. *J. Neurosci.* 18,134 -142.

Sohl, G. and Willecke, K. (2004) Gap junctions and the connexin protein family. *Cardiovasc. Res.* 62, 228–232.

Solan, J.L., Lampe, P.D. (2009) Connexin43 phosphorylation: structural changes and biological effects. *Biochem J.* 419(2):261-72.

Spray, D.C., Harris, A.L., Bennett, M.V. (1981) Gap junctional conductance is a simple and sensitive function of intracellular pH. *Science* 211(4483):712–715

Verbeek, D. S., Knight, M. A., Harmison, G. G., Fischbeck, K. H. and Howell, B. W. (2005) Protein kinase C gamma mutations in spinocerebellar ataxia increase kinase activity and alter membrane targeting. *Brain* 128,436 -442.

Wang, H., Gao, J., Sun, X., Martinez-Wittinghan, F.J., Li, L., Varadaraj, K., Farrell, M., Reddy, V.N., White, T.W., Mathias, R.T. (2009) The effects of GPX-1 knockout on membrane transport and intracellular homeostasis in the lens. *J Membr Biol.* 227(1):25-37.

Wang, Z., Schey, K.L. (2009) Phosphorylation and truncation sites of bovine lens connexin 46 and connexin 50. *Exp Eye Res.* Jul 29.

White, T. and Paul, D. (1999) Genetic diseases and gene knockouts reveal diverse connexin functions. *Annu. Rev. Physiol.* 61, 283–310.

White, T.W. (2002) Unique and redundant connexin contributions to lens development. Science 295:319-20.

White, T.W., Goodenough, D.A., Paul, D.L. (1998) Targeted ablation of connexin50 in mice results in microphthalmia and zonular pulverulent cataracts. J Cell Biol 143:815-25.

Yevseyenkov, V.V., Das, S., Lin, D., Willard, L., Davidson, H., Sitaramayya, A., Giblin, F.J., Dang, L., Takemoto, D.J. (2009) Loss of protein kinase Cgamma in knockout mice and increased retinal sensitivity to hyperbaric oxygen. *Arch Ophthalmol.* 127(4):500-6.

Yin, X., Jedrzejewski, P.T., Jiang, J.X. (2000) Casein kinase II phosphorylates lens connexin 45.6 and is involved in its degradation. J Biol Chem 275:6850-6.

Zampighi, G.A., Planells, A.M., Lin, D., Takemoto, D. (2005) Regulation of lens cell-to-cell communication by activation of PKCgamma and disassembly of Cx50 channels. *Invest Ophthalmol Vis Sci.* 46(9):3247-55.

Chapter 3 - Contrasting Regulation of Gap Junction Proteins Connexin43 and Connexin46 in response to 12-*O*-Tetradecanoylphorbol-13-Acetate Treatment

3.1. Introduction

Gap junctions are intercellular aqueous channels composed of transmembrane proteins called connexins. These channels adjoin neighboring cell plasma membranes allowing direct contact between the cytoplasms and play an important role in intercellular communication (Goodenough et al., 1996). Gap junction channels allow the passage of small molecules of < 1 kDa including ions (K^+ and Ca^{2+}), second messengers (cAMP, cGMP, and inositol 1,4,5-triphosphate (IP3)), and small metabolites (glucose), allowing electrical and biochemical coupling between cells (Meşe et al., 2007). Gap junctional intercellular communication (GJIC) is involved in a variety of cellular processes including growth, proliferation, differentiation, and cell death. Interruption of GJIC has been associated with a variety of pathological conditions (Laird, 2006; Lai-Cheong et al., 2007).

Gap junction assembly and disassembly is a very dynamic process with connexin proteins having half-lives ranging from 1.5 -5h depending on the tissue or cell type studied (Lampe, 1994; Gaietta et al., 2002, Thomas et al., 2003). To maintain optimum GJIC, connexin proteins need to be critically regulated. Several factors including transjunctional voltage, pH and phosphorylation of the connexin proteins regulate GJIC (Mathias et al., 1997). There are 21 connexin isoforms expressed in humans (Laird, 2006) and most of the connexin proteins are phosphoproteins (Solan and Lampe, 2005; Laird, 2005). Cx43 is the most widely studied connexin isoform and at least 13 phosphorylation sites have already been identified in the C-terminal cytoplasmic tail of Cx43 (Laird, 2005; Solan and Lampe, 2009). Phosphorylation in the C-terminal tail of Cx43 leads to both increase and decrease in gap junction permeability, assembly and disassembly (Solan and Lampe, 2009).

Several growth factors and carcinogenic chemicals influence gap junction channels (Lampe and Lau, 2000). The tumor-promoting protein kinase C (PKC)-activator phorbol ester 12-O-tetradecanoylphorbol-13-acetate (TPA) has been shown to cause rapid phosphorylation of

Cx43 and inhibition of GJIC in a variety of cells. Prolonged exposure to TPA has been shown to cause ubiquitination of Cx43 in a PKC dependent manner leading to eventual proteasomal degradation (Leithe and Rivedal, 2004). Our lab has previously reported TPA induced PKCγ-mediated phosphorylation of Cx43, Cx46 and Cx50 in cultured lens epithelial cells and in the whole lens (Akoyev and Takemoto, 2007; Zampighi et al., 2003; Lin et al., 2006). However, not much is known about the TPA-mediated regulation of connexins other than Cx43.

Here, we have studied the effect of prolonged TPA exposure on multiple connexins (Cx43, Cx46, Cx50) expressed endogenously in an immortalized cultured lens epithelial cell line. We show evidence that Cx43 is phosphorylated by a PKC-mediated way in response to TPA treatment which leads to gap junction internalization and eventual degradation by the proteasomal pathway. Phosphorylation on the serine 368 residue (ser368) in the C-terminal tail is a degradation signal for Cx43. Moreover prolonged TPA exposure causes up regulation of Cx46 message and protein levels, which does not form functional gap junctions in the cultured epithelial cells. Thus, TPA causes contrasting regulation of different connexin isoforms in the lens epithelial cells.

3.2. Materials and Methods

3.2.1. Materials

Dulbecco's modified Eagle's medium (DMEM; low glucose), trypsin-EDTA, gentamicin, and penicillin/streptomycin were purchased from Invitrogen Corp. (Carlsbad, CA). Dithiothreitol (DTT) and bovine serum albumin (BSA) were purchased from Fisher Scientific (Hampton, NH). Fetal bovine serum was purchased from Atlanta Biologicals (Norcross, GA). Phenylmethylsulfonyl fluoride (PMSF), protease inhibitor cocktail (# P8340) and N-(benzyloxycarbonyl)leucinylleucinylleucinal [Z-Leu-Leu-Leu-al (MG132)] (# C2211) were purchased from Sigma-Aldrich (St. Louis, MO). Phosphatase inhibitors cocktail set II (# 524625), Phorbol-12-myristate-13-acetate (TPA, # 524400) and 4α-phorbol-12, 13-didecanoate (PDD, # 524394) were purchased from Calbiochem (La Jolla, CA). 2X electrophoresis sample buffer (#sc-24945) was purchased from Santa Cruz Biotechnology (Santa Cruz, CA). All electrophoresis reagents and protein molecular weight markers for electrophoresis and protein assay dye were purchased from Bio-Rad Laboratories (Hercules, CA). Chemiluminescence

substrate (SuperSignal West Femto Substrate Kit) with secondary anti-mouse or anti-rabbit IgG conjugated with horseradish peroxidase (# 34095) was purchased from Pierce (Rockford, IL). RNeasy Mini Kit (#74104) was purchased from Qiagen (Valencia, CA). Unless otherwise noted, chemicals and supplies were obtained from Fisher Scientific (Hampton, NH).

3.2.2. Cell Culture

Immortalized human lens epithelial cells (HLEC) were grown in 75-cm^2 flasks or in 6-well plates in DMEM supplemented with 10% fetal bovine serum (FBS), 50 μg/mL gentamicin, 0.05 U/mL penicillin, and 50 μg/mL streptomycin (pH 7.4) at 37 °C in an atmosphere of 95% air and 5% CO_2 until 90% confluent (100% for dye transfer studies). When the cells reached 90% confluency, they were treated with TPA or PDD (used as a negative control for TPA treatment). For proteasomal degradation inhibition experiments, cells were treated with 10μM MG132 for half an hour followed by TPA treatment.

3.2.3. Whole cell homogenate preparations (WCH)

Cells were washed three times with cold phosphate-buffered saline (PBS) and collected by scraping from plates, sedimented, and washed two more times in cold PBS. The cell pellets were lysed on ice with cell lysis buffer containing 20 mM Tris–HCl, pH 7.5, 0.5 mM EDTA, 0.5 mM EGTA, 1% Triton X-100, 0.1% protease inhibitor mixture cocktail, 0.1% phosphatase inhibitor cocktail and 2 mM PMSF. Lysates were sonicated for 20 s on ice and centrifuged at 13,000 rpm for 30 min at 4ºC. Supernatants were collected and protein concentration of each sample was measured using Bio-Rad Protein Assay and samples were diluted to make concentrations equal in all samples for future analyses.

3.2.4. Western Blot and Antisera

Western blot analyses were performed as previously described (Das et al., 2008). Briefly, 25μg of WCH was resolved by 8% or 12.5% SDS-polyacrylamide gel electrophoresis (PAGE) and transferred to nitrocellulose membrane (Midwest Scientific, Saint Louis, MO). Nitrocellulose membrane was blocked in 5% milk for an hr at room temperature and then incubated with primary antibodies followed by species-specific secondary antibodies. Mouse anti-β-actin was used as loading control primary antibodies for all samples. Mouse anti-N-terminal-Cx43 (# Cx43NT1) and anti-C-terminal-Cx43 (# Cx43 CT1) were purchased from Fred

Hutchinson Cancer Center (Seattle, WA); rabbit anti-phospho-Cx43 (Ser-368) (# 3511S) from Cell Signaling Technologies (Danvers, MA); rabbit anti-C-terminal-Cx43 (# C6219), mouse anti-β-actin (# A5441) from Sigma-Aldrich (St. Louis, MO); rabbit anti-Cx46 (# C7858-07A) from US Biological (Swampscott, MA); mouse anti-Cx50 (# 33-4300) from Zymed-Invitrogen (San Franscisco, CA); and the mouse mitochondrial antibody cocktail (# MSA12) containing antibodies against cytochrome c, glyceraldehyde-3-phosphodehydrogenase (GAPDH), pyruvate dehydrogenase subunit E1-alpha (PDHE1α) and ATP synthase subunit alpha (ATP5A1) was purchased from MitoSciences (Eugene, OR).

3.2.5. Dye transfer-gap junction activity assay

To measure gap junction activity, scrape load/dye transfer (SL/DT) assay was performed as described earlier (Lin and Takemoto, 2005; Nguyen et al., 2003). Briefly, cells were grown to 100% confluency on cover slips, treated with 300 nM TPA for different time periods. After that cells were washed three times with PBS. The 2.5 μl of 1% (w/v) Lucifer yellow (# L-453, Invitrogen-Molecular Probes, Eugene, OR) and .75% (w/v) of Rhodamine Dextran (# D1817, Invitrogen-Molecular Probes, Eugene, OR) was mixed and added in the center of the coverslip. A single cut, using a razor blade, was made in the center of the coverslip. After three minutes, cells were washed three times with PBS and incubated at 37°C in tissue culture media for 20 min. The cells were then washed with PBS three times and fixed in 2.5% paraformaldehyde for 10 min. Cells were mounted on a slide, sealed and visualized under a fluorescence microscope. Gap junction activity was expressed as the number of cells transferring lucifer yellow minus cells with rhodamine dextran per total number of DAPI-stained cells in the microscopic field of view at 20X magnification. Three different areas along each scrape were analyzed with at least 100 cells counted.

3.2.6. RNA Isolation and Real-Time RT-PCR

Total RNA was extracted from control or TPA-treated HLECs using the RNeasy minikit. RNA was quantified using a spectrophotometer and equal amounts of total RNA were reverse-transcribed using SuperScript III First-Strand Synthesis System for RT-PCR (Invitrogen) and following the manufacturer's protocol. The RT reaction mixture (1 μl) from each treatment was subjected to PCR using specific primers for Cx43, Cx46 and β-actin. The specificity of primers

(refer Table-3.1) was confirmed by NCBI-BLAST analysis. The PCR products were then analyzed in 1.5% agarose-gel.

Real-time PCR was performed using a BioRad iQ iCycler Detection System (BioRad Laboratories, Ltd) with SYBR green SuperMix (BioRad). Reactions were performed in a total volume of 25 µL—including 12.5 µL 2x SYBR buffer SuperMix, 1 µL of each primer at 10 µM concentration, and 10.5 µL of the previously dilution-optimized reverse-transcribed cDNA template.

Protocols for each primer set were optimized using four serial 5x dilutions of template cDNA obtained from Lenses. The protocols used are as follows: denaturation (95°C for 5 mins), amplification repeated 40 times (95°C for 15 s, 60°C for 45 s). A melt curve analysis was performed following every run to ensure a single amplified product for every reaction. All reactions were carried out in at least triplicate for every sample. The same reference standard dilution series was repeated on every experimental plate.

Table 3.1 Primers used for RT- and Real time-PCR. The primers are identified as forward (F), and reverse (R). β-actin primers have been designed previously by (Spann et al., 2004)

Target gene	Primer	Nucleotide Sequence	GenBank Accession Number
β-actin	F	5'-GGCATCCACGAAACTACCTT-3'	NM_001101
	R	5'-AGCACTGTGTTGGCGTACAG-3'	
Cx43	F	5'-GTGCCTGAACTTGCCTTTTC-3'	NM_000165
	R	5'-CCCTCCAGCAGTTGAGTAGG-3'	
Cx46	F	5'-ACCGCACGTGTGAAAGGAAT-3'	NM_021954.3
	R	5'-GGAGTGCTCCTGTGCATTTT-3'	

3.2.7. Immunofluorescent labeling and confocal microscopy

In order to reveal the location of Cx43 and Cx46 in whole cells confocal microscopy of immunolabeled Cx43 and Cx46 was done. HLECs were grown on glass coverslips in six-well plates until 80% confluency and treated with 300 nM TPA for different time periods at 37 °C. The cells were fixed with 4% paraformaldehyde, quenched with 50 mM Glycine, washed with PBS, permeabilized with 0.05% Triton-X100 in PBS for 30 min, washed, and blocked with 5%

BSA (blocking solution) in PBS-T (PBS with 0.1% Tween-20) for at least 1 h at room temperature. Cells were then treated overnight at 4°C with rabbit anti-C-terminal-Cx43 antibody or rabbit anti-Cx46 antibody diluted 1:250 in blocking solution with constant gentle shaking. For staining golgi-apparatus, the golgi marker mouse anti-golgi 58K protein/Formiminotransferase Cyclodeaminase (FTCD) (# G2404; Sigma-Aldrich, St. Louis, MO) was used. After incubation with primary antibodies coverslips with cells were washed with blocking solution and stained with secondary Alexa Fluor-488 (green color) anti-rabbit and/or Alexa Fluor-594 (red color) anti-mouse antibodies (Invitrogen-Molecular Probes, Eugene, OR) for 2 h at room temperature. After washing three times for 5 minutes each in PBS-T, slides were labeled for 10 minutes in the dark at room temperature with 500nM DAPI in PBS to stain nuclei. Finally, after three more washes for 5 min each in PBS, slides were mounted in antifade reagent (# P36934; Invitrogen-Molecular Probes, Eugene, OR). At least three separate experiments were done in each case. For staining mitochondria, cells on coverslips were incubated with 300nM MitoTracker Red (in Invitrogen-Molecular Probes, Eugene, OR) serum-free media for 20 minutes before fixation with 4% paraformaldehyde. Finally, slides were viewed by confocal microscopy (LSM 510 Meta, Carl Zeiss, Göttingen, Germany) and laser-scanning images were obtained at 40X (oil immersion) objectives. Images were obtained using filters BP 505-530, LP 585 and BP 420-480.

3.2.8. Cell Fractionation

HLECs with or without 300nM TPA treatment were fractionated into cytosolic, mitochondrial and nuclear fractions using the standard cell fractionation kit (# MS861) from MitoSciences (Eugene, OR) following the manufacturer's protocol. Different fractions of the cells were then analyzed by western blotting to determine the localization of Cx46.

3.2.9. Statistical Analyses

All experiments were performed at least in triplicates. Commercial software (Origin; Microcal Software Inc., Northampton, MA) was used for statistical analyses. Results were expressed as the mean ± SD. Differences at $P < 0.05$ (one-way analysis of variance with the Bonferroni multiple comparisons test) were considered to be statistically significant.

3.3. Results

3.3.1. Effect of TPA on the connexin isoforms in HLECs

The HLECs express all the three connexin isoforms (Cx43, Cx46 and Cx50) found in the lens. These three connexins are phosphoproteins and are phosphorylated in response to TPA stimulated PKC activation (Solan and Lampe, 2009, Zampighi et al., 2003). Among these connexin isoforms, phosphorylation of Cx43 has been studied extensively. In gap junctional communication-competent cells, Cx43 usually forms three major bands in SDS-PAGE based on its phosphorylation status on different residues. The fastest migrating Cx43 band is termed Cx43-P0 and the other two slower migrating forms are termed Cx43-P1 and Cx43-P2 respectively (Fig. 3.2A) (Musil et al., 1990; Musi and Goodenough, 1991). One of the serine residues, serine 368, in the C-terminal tail of Cx43 has been shown to be phosphorylated by PKC (Lampe et al., 2000) and several reports from our lab have shown the interaction between PKCγ and Cx43 in response to TPA, growth factors and oxidative stress (H_2O_2) (Akoyev and Takemoto, 2007 and Akoyev et al., 2009).

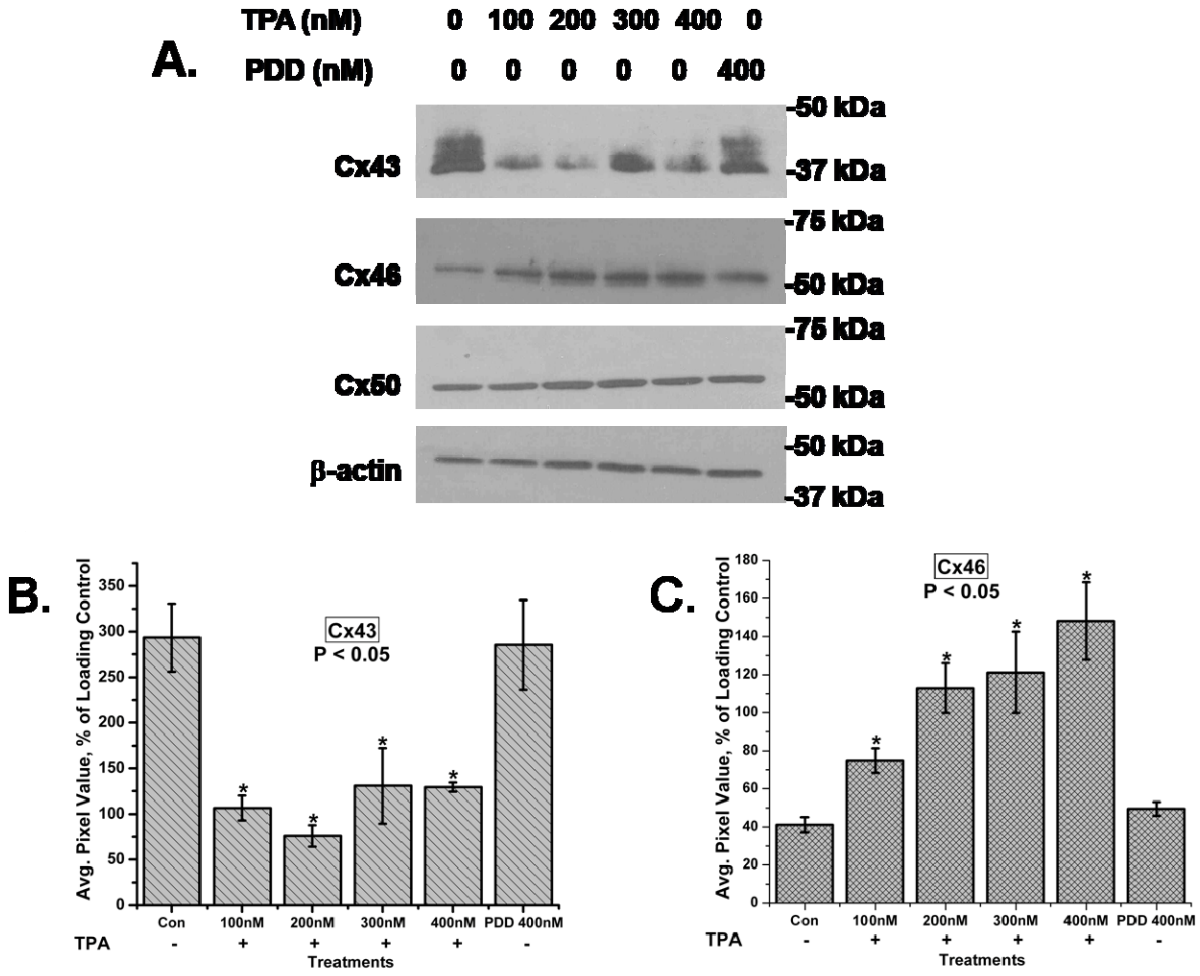

Figure 3.1 TPA causes depletion of Cx43 and increase of Cx46 protein levels. (A) Whole cell homogenates of HLECs treated with the indicated doses of TPA for 6 hrs were analyzed by western blotting with anti-Cx43, Cx46 and Cx50 antibodies. β-actin is used as loading control. PDD, the inactive structural analog of TPA, was used as a negative control. **(B)** and **(C)** Quantitative comparison of the detected protein levels of Cx43 (pixel intensity of multiple Cx43 bands detected were calculated together), Cx46 respectively in different treatments were normalized to the levels of loading control β-actin. The 0 hr treatment is regarded as a control. All bands were digitized by UN-SCAN-It gel software. The average pixel values for each Cx band was calculated, then normalized and plotted in % of loading control. While Cx43 protein levels decreased significantly in response to TPA treatment, Cx46 protein levels increased significantly at the same time. The asterisks indicate significantly different amount of protein levels in comparison to the control ($p < 0.05$). No significant change in the Cx50 protein levels were detected (histogram not shown). Data is representative of three independent experiments.

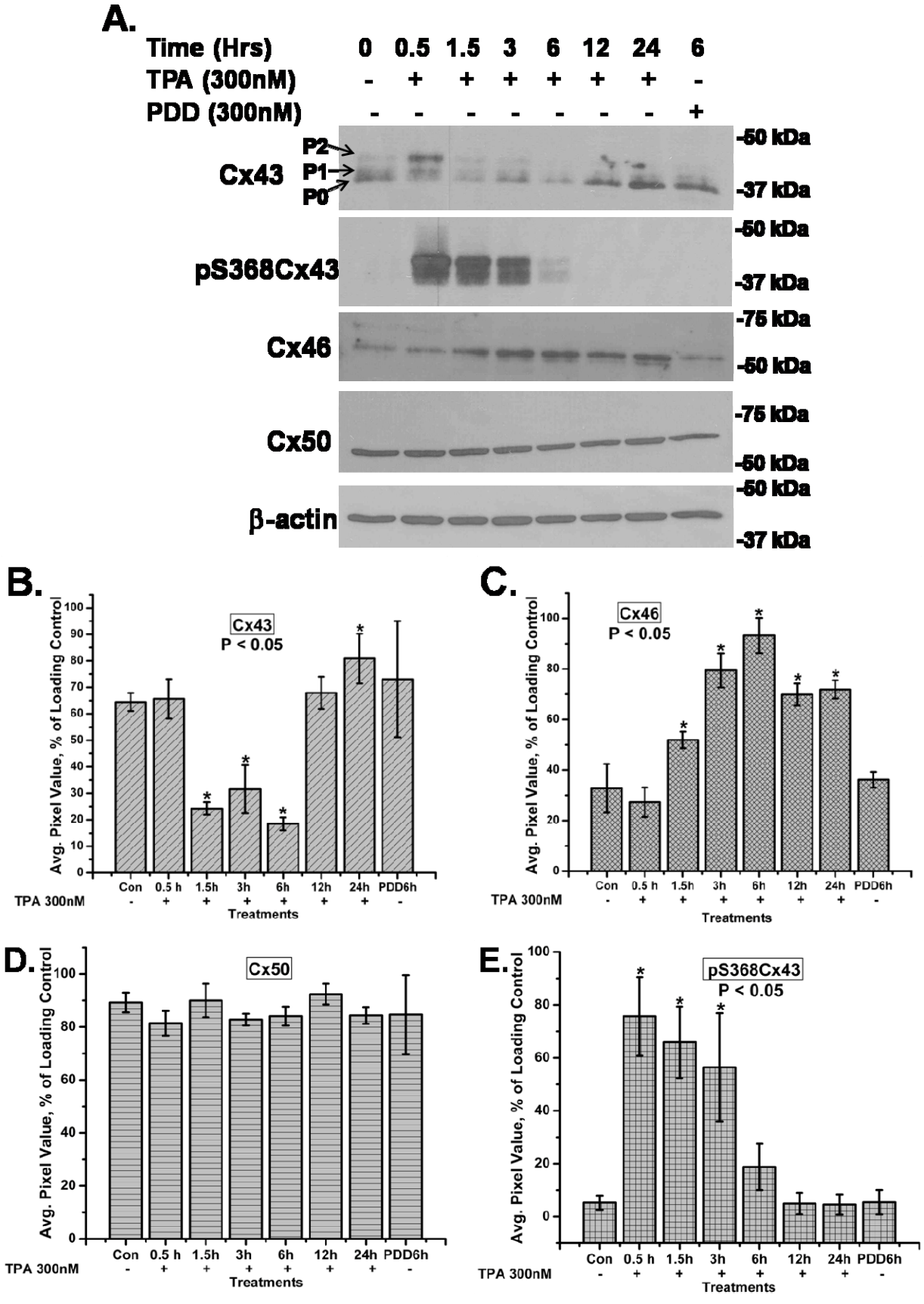
A.
Time (Hrs) 0 0.5 1.5 3 6 12 24 6
TPA (300nM) - + + + + + + -
PDD (300nM) - - - - - - - +
P2
P1
P0
Cx43
pS368Cx43
Cx46
Cx50
β-actin
-50 kDa
-37 kDa
-75 kDa
B.
Cx43
P < 0.05
C.
Cx46
P < 0.05
D.
Cx50
E.
pS368Cx43
P < 0.05
Avg. Pixel Value, % of Loading Control
TPA 300nM
Con 0.5 h 1.5h 3h 6h 12h 24h PDD6h
Treatments

Figure 3.2 Time-course analysis of connexin protein and phosphorylation levels in response to treatment with 300nM TPA treatment. (A) Whole cell homogenates of HLECs treated with 300nM TPA for the indicated time periods were analyzed by western blotting with anti-Cx43, phospho-ser368Cx43, Cx46 and Cx50 antibodies. β-actin was used as loading control. PDD was used as a negative control. **(B), (C), (D)** and **(E)** Quantitative comparison of the detected protein levels of Cx43 (pixel intensity of multiple Cx43 bands detected were calculated together), Cx46, Cx50 and phosphor-ser368Cx43 respectively in different treatments normalized to the levels of loading control β-actin. The asterisks indicate significantly different amount of protein levels in comparison to the control ($p < 0.05$). Data is representative of three independent experiments.

However, prolonged exposure to TPA has been shown to cause hyperphosphorylation of Cx43 leading to ubiquitination and reduction in Cx43 protein levels in cultured WB and IAR20 liver cell lines (Oh et al., 1991, Leithe and Rivedal, 2004). In order to investigate whether Cx43 is regulated in a similar way in lens epithelial cells and the effect of prolonged TPA exposure on Cx46 and Cx50, we first examined the effect of prolonged TPA treatment on these three connexin protein levels. As revealed by western blotting, Cx43 protein levels got depleted in a dose-dependent manner (Fig. 3.1A and B) after six hours of TPA treatment. Surprisingly, the protein levels of Cx46 increased in response to TPA treatment, whereas the Cx50 protein levels did not alter much in response to the TPA treatment (Fig. 3.1A and C). TPA treatment at 300nM caused significant depletion of Cx43 protein level and major increase in Cx46 protein levels. So, further studies were done at the same dose.

In the time course study, 300nM TPA treatment induced hyperphosphorylation of Cx43 in HLECs within 30 minutes, seen as an increase in the Cx43-P1 and Cx43-P2 bands and a loss of the Cx43-P0 band (Fig. 3.2A). The TPA-induced hyperphosphorylation led to depletion of Cx43 protein levels until 6 hrs and after 12 hrs the level of Cx43-P2 band was reduced and the level of Cx43-P0 and Cx43-P1 recovered with the overall Cx43 protein levels becoming comparable with the control levels (Fig. 3.2A and B). The transient nature of the phosphorylation and the involvement of PKC in the phosphorylation of Cx43 were confirmed by western blotting with the pS368Cx43 antibody which recognizes only the Cx43 forms phosphorylated at the Serine 368 (Ser368) residue. The transient depletion of total Cx43 protein levels was concomitant with the phosphorylation at the Ser368 residue, suggesting that the phosphorylation

of Cx43 at this residue by PKC leads to the degradation of Cx43 protein as reported previously (Solan and Lampe, 2009). The phosphor-serine368-Cx43 forms were not detected after 12 hrs when the Cx43-P0 form started recovering.

Significantly higher levels of Cx46 were detected after 1.5 hrs of 300nM TPA treatment (Fig. 3.2A and C) with the highest levels of Cx46 detected after 6 hrs, which coincides with the maximum reduced levels of Cx43. There was no visible change in the Cx50 protein levels throughout the 24 hrs of 300nM TPA treatment (Fig. 3.2A). These data indicate that TPA causes activation of PKC leading to PKC-mediated phosphorylation and subsequent depletion of Cx43 levels. The increase in Cx46 protein levels in response to TPA treatment is a novel finding and was studied further.

3.3.2. Effect of TPA treatment on GJIC (Gap Junctional Intercellular Communication)

Scrape load/dye transfer (SL/DT) assay is routinely used to measure GJIC. TPA induced phosphorylation of Cx43 has been reported to cause inhibition of GJIC in a number of cell types (Lampe, 1994; Rivedal et al., 1994; Lampe et al., 2000). HLECs express multiple connexins and considering the apparent reciprocal regulation of the Cx43 and Cx46 protein levels by TPA treatment, we checked the functional gap junctional communication in the HLECs following treatment with 300nM TPA at different time intervals (Fig. 3.3). In agreement with the previous findings in other cultured cell lines and the observed phosphorylation of Cx43 in our western blotting experiments, GJIC was rapidly inhibited between HLECs after 30 minutes of TPA time period.

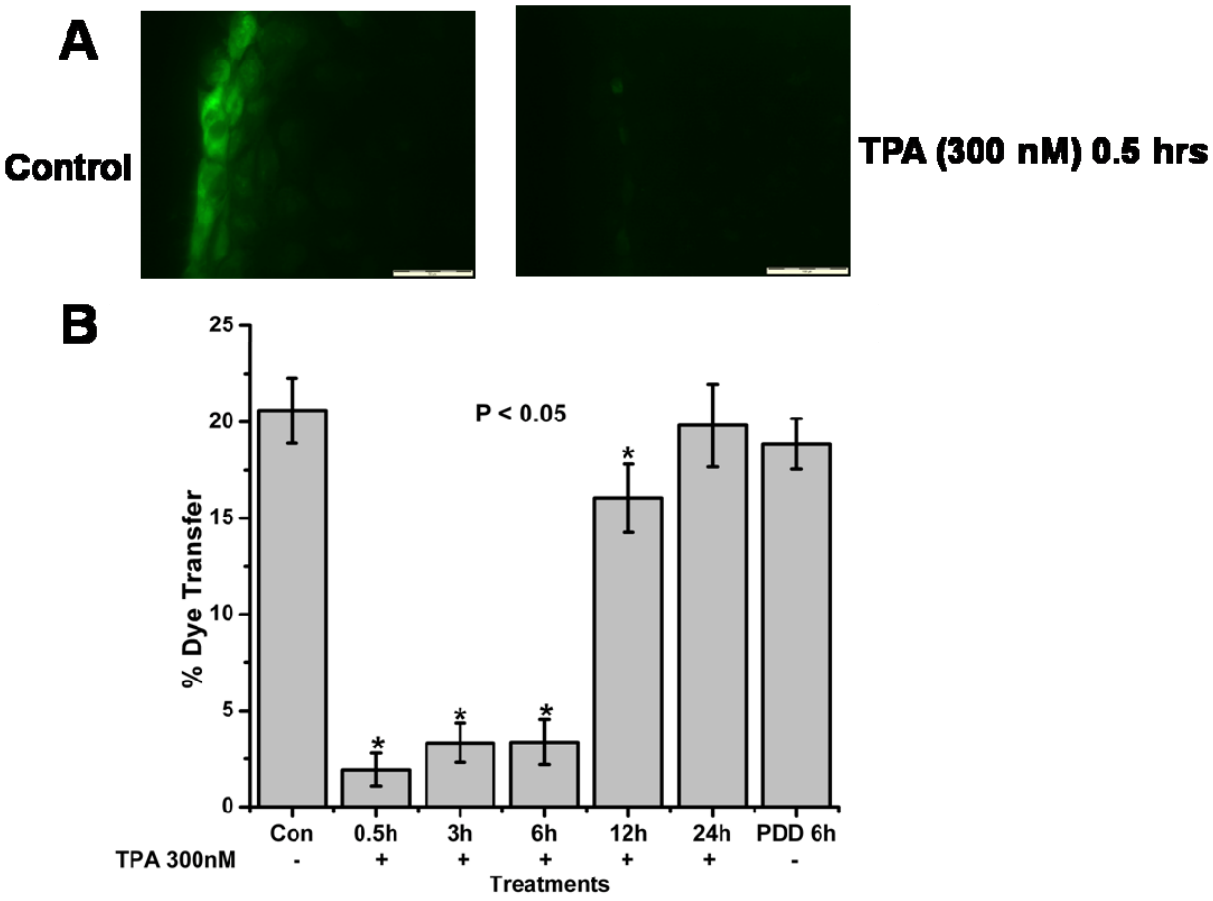

Figure 3.3 Dye transfer-functional gap junctional activity assay. Dye transfer was expressed in percentages as the number of cells transferring lucifer yellow minus cells with rhodamine dextran per total number of DAPI-stained cells counted (at least 100 cells per scrape). **(A)** Representative pictures showing the passage of LY (green color) in control untreated cell and cells treated with TPA 300nM for 30 mins. **(B)** Histogram showing % LY dye transfer between cells after different treatments. The asterisks indicate significantly reduced GJIC between HLECs compared to control cells. Data is representative of three independent experiments.

However, like the Cx43 protein levels, the GJIC inhibition was also transient and GJIC became comparable to the control cells after 12 hrs of treatment, attaining normal levels at the 24 hrs time point. The increased levels of Cx46 did not have any effect on the GJIC, when Cx43 was phosphorylated or depleted. We then wished to determine cellular localization of Cx43 and Cx46 following TPA treatments.

3.3.3. Localization of Cx43 in response to TPA treatment in HLECs

Previously, we have localized Cx43 mostly to the apposed membranes of neighboring cells in HLECs (Akoyev et al., 2009). Here we examined the fate of Cx43 after its TPA-induced phosphorylation and depletion using confocal microscopy. In agreement with our previous findings, Cx43 was found mostly in the apposed cell membranes forming punctuate gap junction plaques and some cytoplasmic occurrence surrounding the nuclei (Fig. 3.4). The faint cytoplasmic staining of Cx43 co-localized with a golgi-marker (see Appendix B Fig. S1). Within 30 minutes of 300nM TPA treatment most of the Cx43 was internalized from the plasma membrane with increase in the intracellular localization. TPA treatment for 6 hrs caused a nearly complete loss of Cx43 immunofluorescence staining except for a faint signal in the perinuclear area (Fig. 3.4). After 12 hrs of TPA treatment Cx43 gap junction plaques reappeared on the apposed plasma membranes and after 24 hrs the Cx43 staining was comparable to the control cells. These data are in accordance with the amounts of Cx43 proteins detected at different time points in the western blot experiments.

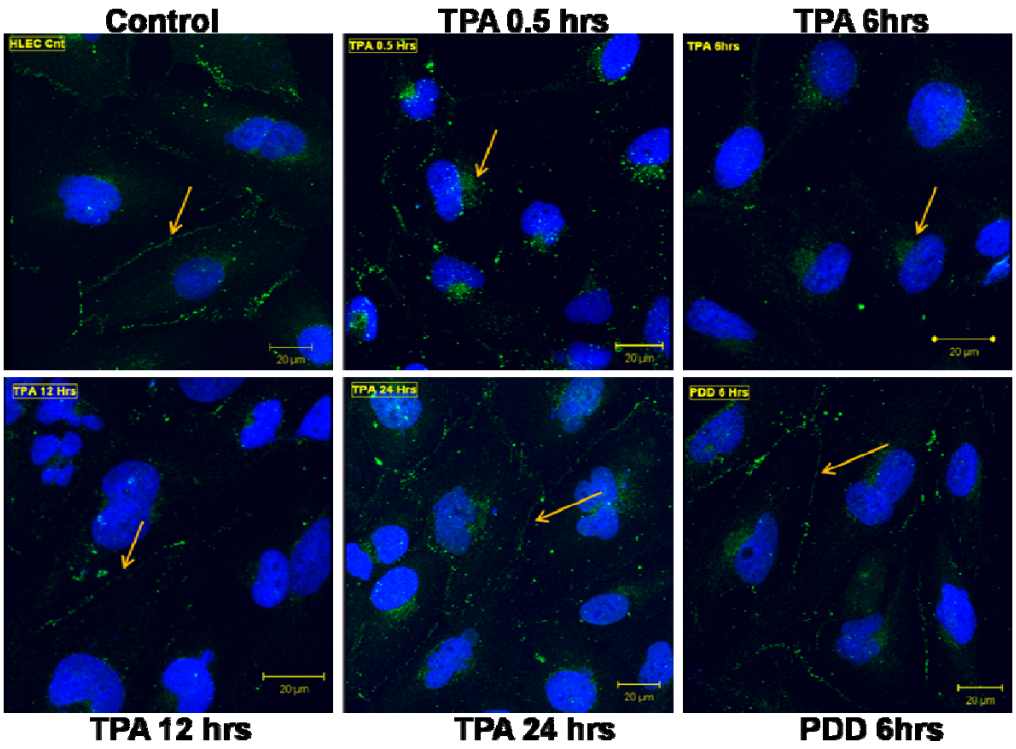

Figure 3.4 TPA induces PKC-dependent internalization of Cx43 in HLECs. HLECs were treated with or without 300nM TPA for different time periods as indicated in the figure and immunostained with anti-Cx43 antibody (green). DAPI (blue) was used to stain nuclei. Arrows

point to the gap junction plaques in all panels except the 0.5 and 6 hr time points where arrows indicate the cytosolic internalization of Cx43.

3.3.4. Localization of Cx46 in the HLECs

Although Cx46 is a known gap junction protein in the lens, a few studies have reported the localization of Cx46 to the perinuclear region of osteoblastic cells and bone tissue (Koval et al., 1997; Das Sarma et al., 2001, Sanches et al., 2009). Immunocytochemistry using anti-Cx46 antibody detected Cx46 in the perinuclear regions of the HLECs (Fig. 3.5A and B). To identify the subcellular compartment Cx46 is localized to, a golgi-complex marker antibody (anti-golgi 58K antibody), an endoplasmic reticulum (ER) marker antibody (anti-calnexin antibody) and the Mito-Tracker red dye were used to stain golgi-complex, ER and mitochondria respectively (See Appendix B Fig. S2). The Cx46 antibody staining nicely co-localized with the mitochondria marker (Fig. 3.5A) staining. Even after 6hrs of 300nM TPA treatment when the highest amount of CX46 was detected by western blotting, Cx46 continued to localize to the perinuclear region with more punctuate staining and co-localized with the mitochondria marker dye (Fig. 3.5A).

To further confirm the mitochondrial presence of Cx46, cultured HLECs were fractionated into cytosolic, mitochondrial and nuclear fractions following treatment with or without 300nM TPA using a cell fractionation kit and western blotting was performed using anti-Cx46 antibody, and mitochondrial and cytosolic markers cocktail antibody. The majority of Cx46 protein was detected in the mitochondrial fraction with very minimal detection in the cytosolic fraction (Fig. 3.5B). These data explain why the increased presence of gap junction protein Cx46 in response to TPA treatment, when the Cx43 protein levels were low, did not contribute to GJIC and suggests that Cx46 probably does not form functional gap junctions in the cultured HLECs grown in normoxic conditions. However, Cx46 is a functional gap junction channel in the whole lens (Jacobs et al., 2004).

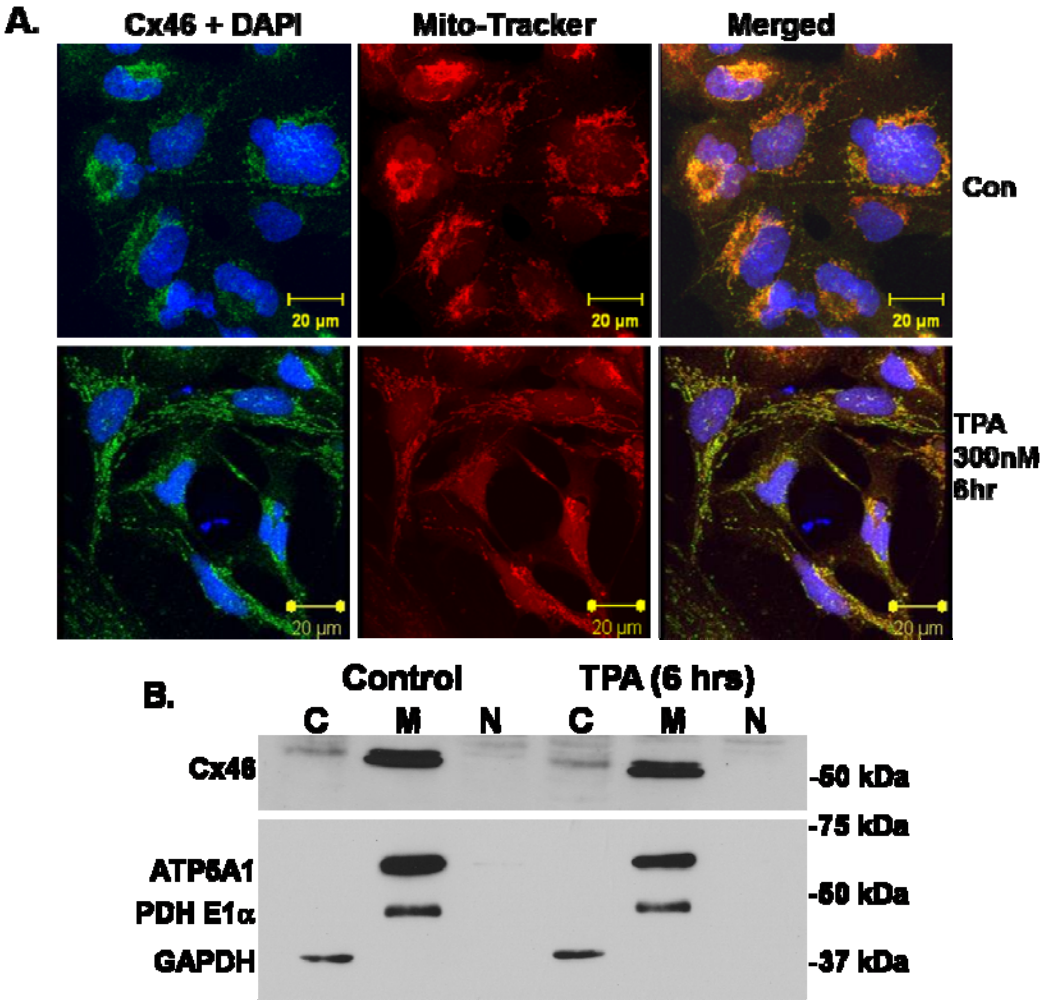

Figure 3.5 Localization of Cx46 in the HLECs. A. Control HLECs were treated with Mito-Tracker red to stain mitochondria followed by immunostaining with anti-Cx46 antibody (green) (Upper row). DAPI (blue) was used to stain the nuclei. Cx46 antibody nicely co-localized with the Mito-Tracker dye. After 6 hrs of 300nM TPA treatment more punctuate localization of Cx46 and co-localization with Mito-Tracker was observed (Lower row). DAPI (blue) was used to stain nuclei. **B.** To confirm the localization of Cx46 HLECs were fractionated into cytosolic (C), mitochondrial (M) and nuclear (N) fractions. The majority of the Cx46 band was observed in the mitochondrial fraction with minimal detection in the cytosolic fraction. A cocktail of antibodies containing a mitochondria matrix marker protein antibody against pyruvate dehydrogenase subunit E1-alpha (PDHE1α), a mitochondrial inner membrane marker antibody against ATP synthase subunit alpha (ATP5A1) and a cytosolic marker protein antibody against glyceraldehyde-3-phosphodehydrogenase (GAPDH) was used to show the accurate fractionation of the cells.

3.3.5. Effect of TPA treatment on connexin message level

To investigate whether the opposing regulation of Cx43 and Cx46 is at the protein level or message level, reverse transcription was performed to check the message levels of Cx43 and Cx46 in response to 300nM TPA treatment at different time intervals. As shown in Fig. 3.6, both RT-PCR and quantitative real-time PCR revealed that while there was no significant change in Cx43 message levels, there was a ~3 fold increase in Cx46 message levels in response to three hours of 300nM TPA treatment. The observed increase in Cx46 message was time-dependent, after reaching a maximum of 3 fold increase over the control cells, it continued to decrease until 12 hrs (although still significantly higher than control cells). This increase in Cx46 message corresponds with the similar amount of increase in Cx46 protein levels in response to TPA treatment and suggests that TPA causes the up regulation of Cx46 at the message level. Also, these data suggest that the decrease in Cx43 protein levels is a result of the PKC-mediated Cx43 protein phosphorylation and subsequent Cx43 degradation as the Cx43 message remains unchanged throughout the TPA treatment time period. This was further verified using proteasomal inhibitors.

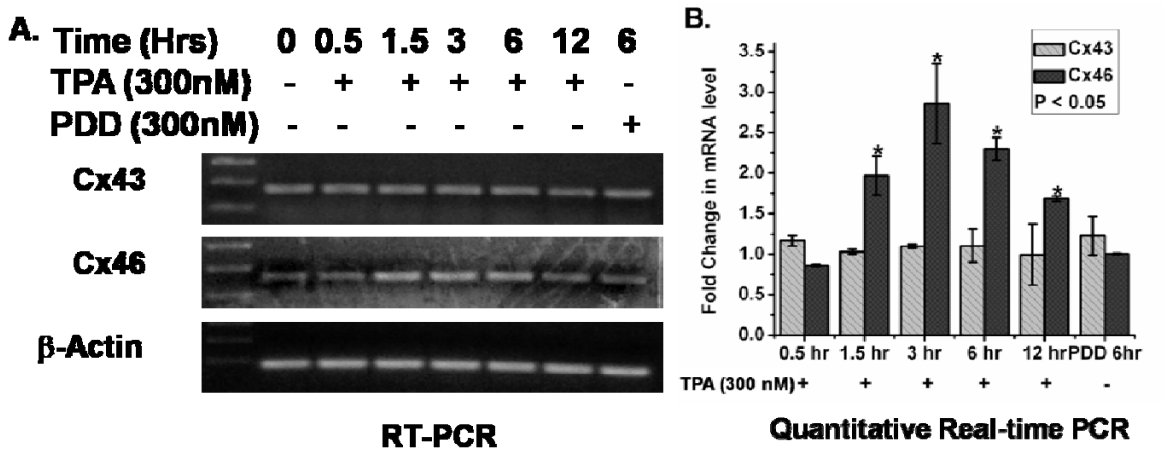

Figure 3.6 Effect of TPA treatment on Cx43 and Cx46 message levels. (A) RT-PCR and **(B)** quantitative real-time PCR was done as described in the methods. Both A and B show that while the Cx43 message level remains constant throughout the different time periods indicated, Cx46 message was up regulated up to 3 fold in response to TPA treatment. β-actin was used as a house-keeping gene. Quantitative real-time PCR data in B is plotted as the fold change in message over the control untreated HLEC message level. The asterisks indicate significantly different amount of message levels in comparison to the control ($p < 0.05$). Data is representative of three independent experiments.

3.3.6. Proteasome inhibitor MG132 blocks the depletion of Cx43 protein level

Several studies have shown that loss of Cx43 protein in response to TPA treatment is countered by proteasomal inhibitors (Qin et al., 2003; Leithe and Rivedal, 2004 and 2004b). To verify the involvement of proteasomal degradation pathway in the TPA-induced depletion of Cx43 protein level, HLECs were treated with vehicle (methanol) or the proteasomal inhibitor MG132 (10μM) for 30 min followed by co-incubation with 300nM TPA for the indicated time periods as illustrated in Fig. 3.7A. The TPA induced loss in the Cx43 protein level was completely counteracted by MG132 and, at the 3hr time point, significantly higher amount of Cx43 protein level over the control cells was detected. Under the treatment of MG132, Cx43 mostly remained in the P1 and P2 status at the time points investigated. Western blotting with the pS368Cx43 antibody showed that phosphorylation of Cx43 at the Ser368 caused by PKC was still intact in the presence of the proteasomal inhibitor and over time the pS368Cx43 form got accumulated in the MG132 treated samples. These data suggest that PKC-mediated phosphorylation of Cx43 at Ser368 residue triggers the proteasomal degradation of Cx43 as previously suggested (Leithe and Rivedal, 2004).

Interestingly, while Cx46 protein level increased in response to TPA treatment alone, pretreatment with MG132 blocked this up-regulation of Cx46 at the time points investigated (Fig. 3.7A and C). No significant change in the Cx50 protein level was detected. This suggests that up-regulation of Cx46 synthesis is possibly dependent on a decrease in Cx43 protein level. Pre-treatment with MG132 resulted in the detection of a slow-moving band for Cx46 indicating that it is possibly a phospho-Cx46 band which gets accumulated in the presence of the proteasomal inhibitor.

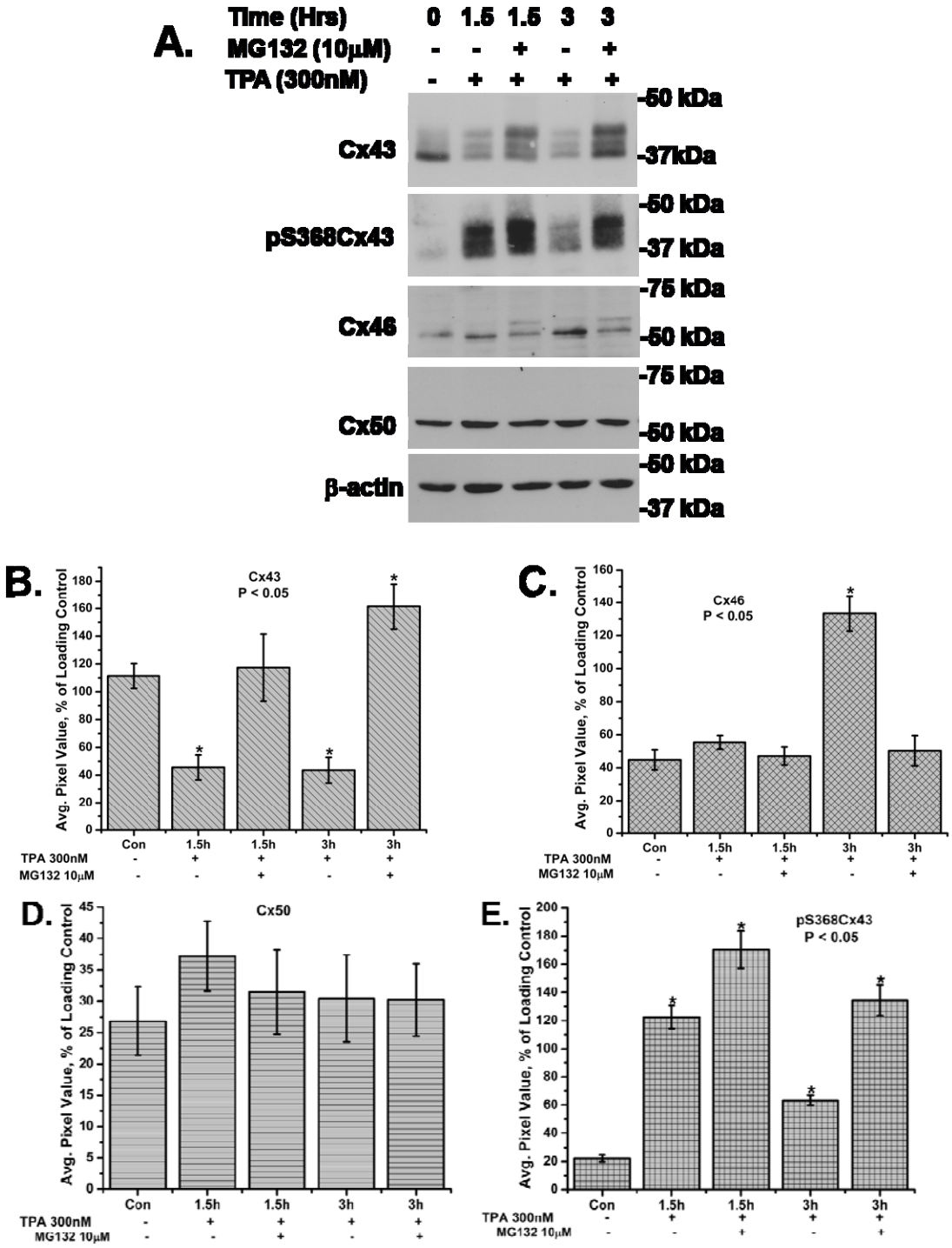

Figure 3.7 Effect of proteasomal inhibitor on TPA-induced down-regulation of Cx43 and up-regulation of Cx46. A. HLECs were treated with or without MG132 (10μM) for 30 min and coincubated with TPA (300nM) for the time points indicated. Equal amounts of whole cell lysates were analyzed by western blotting with anti-Cx43, phospho-ser368Cx43, Cx46 and Cx50 antibodies. β-actin was used as loading control. **(B)**, **(C), (D) and (E)** Quantitative comparison

of the detected protein levels of Cx43 (pixel intensity of multiple Cx43 bands detected were calculated together), Cx46, Cx50 and phospho-ser368Cx43 respectively in different treatments normalized to the levels of loading control, β-actin. The 0 hr treatment is regarded as a control. The asterisks indicate significantly different amount of protein levels in comparison to the control ($p < 0.05$). No significant change in the Cx50 protein levels was observed. Data is representative of three independent experiments.

3.4. Discussion

Internalization and degradation of gap junctions are highly regulated processes. Ubiquitination and proteasomal degradation of Cx43 in response to EGF and TPA treatment has been well established in the cultured rat liver epithelial cell line IAR20 (Leithe and Rivedal, 2004 and 2004b). In the present study, we show that Cx43 also undergoes a similar TPA-stimulated PKC-mediated internalization and degradation in the HLECs. Previously, we have reported the association of PKCγ isoform with Cx43 in response to TPA-treatment in HLECs (Akoyev et al., 2009). This report provides evidence that the PKCγ mediated phosphorylation of Cx43 on Ser368 is indeed the degradation signal for the proteasomal pathway.

However the upregulation of Cx46 in response to TPA treatment is the most novel finding of our study. TPA indeed has been reported to cause transcriptional up-regulation of Cx26 in a PKC mediated manner (Li et al., 1998). The upregulation of Cx46 message level in response to TPA treatment suggests a similar possibility and needs further investigation. Similarly, the involvement of PKC in the up-regulation of Cx46 needs further study.

According to our knowledge, this is the first instance of Cx46 being detected in the mitochondria of any cell type. Although our confocal microscopy and cell fractionation studies suggest the localization of Cx46 in the mitochondria, the presence of Cx46 in the organelles like endoplasmic reticulum (ER) and golgi-complex can't be ruled out at this point as no ER- or golgi-marker antibody has been used in our cell fractionation western-blotting to exclude the presence of ER or golgi proteins in the mitochondrial fraction. Nevertheless, it does appear that Cx46 is not localized to the cell membranes.

A sequence-alignment of the human Cx43, Cx46 and Cx50 (Fig. 3.8) revealed the highest sequence similarity among the two extracellular loop regions [37-76 (E1) and 178-208 (E2) in

Cx43; 41-76 (E1) and 174-201 (E2) in Cx46; and 47-76 (E1) and 174-204 (E2) in Cx50], whereas the highest variability was observed in the C-terminal tail (232-382 in Cx43; 223-435 in Cx46; and 228-433 in Cx50) and cytoplasmic loop (100-154 for Cx43; 98-152 for Cx46; and 100-150 for Cx50) sequences. This variability in the C-terminal and cytoplasmic loop region allows unique functional or regulatory properties for channels formed by different connexins (Hertzberg, 2000). Recent studies have identified a proline-rich motif (Pro^{277}-Pro^{284}) and an overlapping WW-binding domain ($S^{282}PPGY^{286}$) in the Cx43, and several serine and tyrosine phosphorylation sites primarily to the domain between Lys^{264}-Asn^{302} which are involved in the interaction with the ubiquitin ligase Nedd4 and a novel UbL (ubiquitin-like)-UBA (ubiquitin-associated) domain-containing Cx43-interacting protein (CIP75). Both Nedd4 and CIP75 have been shown to be involved in the regulation of ubiquitin-dependent degradation of Cx43 (Leykauf et al., 2006 and Li et al., 2008). The C-terminal consensus PY motif (*X*PP*X*Y) of Cx43 contains a nearby lysine residue ($S^{282}PPGYKLV^{289}$) similar to the extended PY motif sequence (*P*PP*XY XX*L) of the amiloride-sensitive epithelial sodium channel (ENaC) membrane protein, another Nedd4-binding protein. Ubiquitin is covalently conjugated to proteins at the ε-NH_2 of a lysine residue on the substrate protein (Leithe and Rivedal, 2007). The similarity of the ENaC PY motif and Cx43 PY motif raises the possibility of similar mechanism in Cx43 degradation and the nearby lysine residue is possibly a part of the ubiquitination signal (Berthoud et al., 2004; Lu et al., 2007). Although such a consensus PY motif (F^{274}PP*Y*Y^{278}) is present in Cx46 C-terminus region, a nearby lysine residue is missing, whereas the PY motif is completely absent in the Cx50 C-terminus. This could explain why Cx46 and Cx50 do not follow similar proteasomal degradation in response to PKC-activating TPA signal.

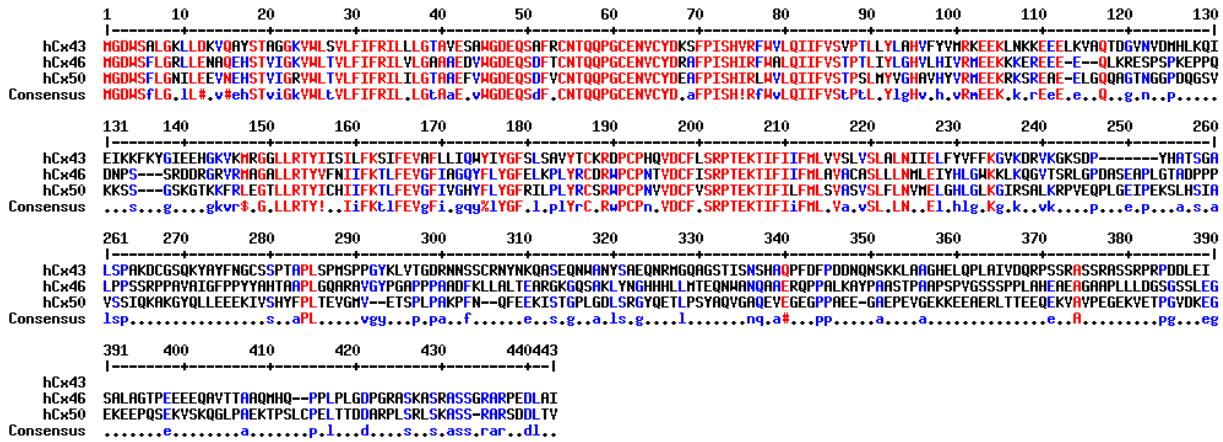

Figure 3.8 Protein sequence alignment of human Cx43, Cx46 and Cx50 proteins. Red letters are high consensus indicators and blue are low consensus indicators. Sequence alignment was done using the program Multalin (Corpet, 1988). The NCBI reference sequences are NP_000156.1, NP_068773.2 and NP_005258.2 for Cx43, Cx46 and Cx50 respectively.

Initially, gap junction proteins were thought to play their only role in gap junctional communication. But recently several studies have shown that connexin proteins as such can influence tissue homeostasis independent of their channel forming capabilities (Decrock et al., 2009). Recently, Cx43 has been shown to translocate from plasma membrane to the inner mitochondrial membrane upon ischemic preconditioning and helps in the survival of cardiomyocytes (Boengler et al., 2005; Rodriguez-Sinovas et al., 2006). So, the presence of Cx46 in the mitochondria needs further studies. Our lab has recently reported the expression of Cx46 in the breast tumor tissue and MCF-7 breast tumor cell line. GJIC is reduced in tumor tissue, but Cx46 in the breast tumor tissue was found to make the tumor tissue adapt and survive to the hypoxic nature of the tumor environment (Banerjee et al.; 2010). Cell fractionation of MCF-7 also revealed that presence of Cx46 in the mitochondrial fraction (Takemoto lab, unpublished data). Not much is known about the role of Cx46 in tissues other than its well established gap junctional function in the lens fiber cells. So, the upregulation of Cx46 in response to tumor-promoter TPA needs further research to find the novel functions of Cx46 independent of its channel forming capability.

3.5. References

Akoyev V, Takemoto DJ. (2009) ZO-1 is required for protein kinase C gamma-driven disassembly of connexin 43. *Cell Signal.* 19(5):958-67.

Akoyev V, Das S, Jena S, Grauer L, Takemoto DJ. (2009) Hypoxia-regulated activity of PKCepsilon in the lens. *Invest Ophthalmol Vis Sci.* 50(3):1271-82.

Banerjee D, Gakhar G, Madgwick D, Hurt A, Takemoto DJ, Nguyen TA (2010) A novel role of gap junction connexin46 protein to protect breast tumors from hypoxia. Accepted in *International Journal of Cancer*, In press.

Berthoud VM, Minogue PJ, Laing JG, Beyer EC. (2004) Pathways for degradation of connexins and gap junctions. *Cardiovasc Res.* 62(2):256-67.

Boengler K, Dodoni G, Rodriguez-Sinovas A, Cabestrero A, Ruiz-Meana M, Gres P, Konietzka I, Lopez-Iglesias C, Garcia-Dorado D, Di Lisa F, Heusch G, Schulz R. (2005) Connexin 43 in cardiomyocyte mitochondria and its increase by ischemic preconditioning. *Cardiovasc Res.* 67(2):234-44.

CORPET F. (1988) Multiple sequence alignment with hierarchical clustering. *Nucl. Acids Res.* 16 (22):10881-10890.

Das S, Lin D, Jena S, Shi A, Battina S, Hua DH, Allbaugh R, Takemoto DJ (2008). Protection of retinal cells from ischemia by a novel gap junction inhibitor. *Biochem Biophys Res Commun.* 373(4):504-8.

Das Sarma J, Meyer RA, Wang F, Abraham V, Lo CW, Koval M. (2001) Multimeric connexin interactions prior to the trans-Golgi network. *J Cell Sci.* 114(Pt 22):4013-24.

Decrock E, Vinken M, De Vuyst E, Krysko DV, D'Herde K, Vanhaecke T, Vandenabeele P, Rogiers V, Leybaert L. (2009) Connexin-related signaling in cell death: to live or let die? *Cell Death Differ.* 16(4):524-36.

Gaietta G, Deerinck TJ, Adams SR, Bouwer J, Tour O, Laird DW, Sosinsky GE, Tsien RY, Ellisman MH. (2002) Multicolor and electron microscopic imaging of connexin trafficking. *Science* 296(5567):503-7.

Goodenough DA, Goliger JA, Paul DL. (1996) Connexins, connexons, and intercellular communication. *Annu Rev Biochem.* 65:475-502.

Hertzberg, E. L. (2000). *Gap junctions*. Jai Press, Stanford, CT.

Koval M, Harley JE, Hick E, Steinberg TH. (1997) Connexin46 is retained as monomers in a trans-Golgi compartment of osteoblastic cells. *J Cell Biol.* 137(4):847-57.

Laird DW. (2006) Life cycle of connexins in health and disease. *Biochem J.* 394(Pt 3):527-43.

Lampe PD. (1994) Analyzing phorbol ester effects on gap junctional communication: a dramatic inhibition of assembly. *J Cell Biol.* 127(6 Pt 2):1895-905.

Lampe, P.D., Lau, A.F. (2000). Regulation of gap junctions by phosphorylation of connexins. *Arch. Biochem. Biophys*. 384, 205-215.

Lampe PD, TenBroek EM, Burt JM, Kurata WE, Johnson RG, Lau AF. (2000) Phosphorylation of connexin43 on serine368 by protein kinase C regulates gap junctional communication. *J Cell Biol.* 149(7):1503-12.

Leithe E, Rivedal E. (2004) Ubiquitination and down-regulation of gap junction protein connexin-43 in response to 12-O-tetradecanoylphorbol 13-acetate treatment. *J Biol Chem.* 279(48):50089-96.

Leithe E, Rivedal E. (2004b) Epidermal growth factor regulates ubiquitination, internalization and proteasome-dependent degradation of connexin43. *J Cell Sci.* 117(Pt 7):1211-20.

Leithe E, Rivedal E. (2007) Ubiquitination of gap junction proteins. *J Membr Biol.* 217(1-3):43-51.

Leykauf K, Salek M, Bomke J, Frech M, Lehmann WD, Dürst M, Alonso A (2006) Ubiquitin protein ligase Nedd4 binds to connexin43 by a phosphorylation-modulated process. *J Cell Sci.* 119(Pt 17):3634-42.

Li GY, Lin HH, Tu ZJ, Kiang DT. (1998) Gap junction Cx26 gene modulation by phorbol esters in benign and malignant human mammary cells. *Gene* 209(1-2):139-47.

Li X, Su V, Kurata WE, Jin C, Lau AF. (2008) A novel connexin43-interacting protein, CIP75, which belongs to the UbL-UBA protein family, regulates the turnover of connexin43. *J Biol Chem.* 283(9):5748-59.

Lin D, Takemoto DJ (2005) Oxidative activation of protein kinase Cgamma through the C1 domain; effects on gap junctions. *J Biol Chem.* 280:13682–13693.

Lin D, Barnett M, Lobell S, Madgwick D, Shanks D, Willard L, Zampighi GA, Takemoto DJ. (2006) PKCgamma knockout mouse lenses are more susceptible to oxidative stress damage. *J Exp Biol.* 209(Pt 21):4371-8.

Lai-Cheong JE, Arita K, McGrath JA. (2007) Genetic diseases of junctions. J Invest Dermatol. 127(12):2713-25.

Laird, D.W. (2005) Connexin phosphorylation as a regulatory event linked to gap junction internalization and degradation. *Biochim. Biophys. Acta.* 1711(2):172-82.

Lu C, Pribanic S, Debonneville A, Jiang C, Rotin D. (2007) The PY motif of ENaC, mutated in Liddle syndrome, regulates channel internalization, sorting and mobilization from subapical pool. *Traffic* 8(9):1246-64.

Mathias, R.T., Rae, J.L., Baldo, G.J. (1997) Physiological properties of the normal lens. *Physiol. Rev*. 77(1):21-50.

Meşe G, Richard G, White TW. (2007) Gap junctions: basic structure and function. *J Invest Dermatol.* 127(11):2516-24.

Musil LS, Cunningham BA, Edelman GM, Goodenough DA. (1990) Differential phosphorylation of the gap junction protein connexin43 in junctional communication-competent and -deficient cell lines. *J Cell Biol.* 111(5 Pt 1):2077-88.

Musil LS, Goodenough DA. (1991) Biochemical analysis of connexin43 intracellular transport, phosphorylation, and assembly into gap junctional plaques. *J Cell Biol.* 115(5):1357-74.

Nguyen TA, Boyle DL, Wagner LM, Shinohara T, Takemoto DJ. (2003) LEDGF activation of PKC gamma and gap junction disassembly in lens epithelial cells. *Exp Eye Res.* 76:565–572.

Oh SY, Grupen CG, Murray AW. (1991) Phorbol ester induces phosphorylation and down-regulation of connexin 43 in WB cells. *Biochim Biophys Acta.* 1094(2):243-5.

Qin H, Shao Q, Igdoura SA, Alaoui-Jamali MA, Laird DW. (2003) Lysosomal and proteasomal degradation play distinct roles in the life cycle of Cx43 in gap junctional intercellular communication-deficient and -competent breast tumor cells. *J Biol Chem.* 278(32):30005-14.

Rivedal E, Yamasaki H, Sanner T. (1994) Inhibition of gap junctional intercellular communication in Syrian hamster embryo cells by TPA, retinoic acid and DDT. (1994) *Carcinogenesis* 15(4):689-94.

Rodriguez-Sinovas A, Boengler K, Cabestrero A, Gres P, Morente M, Ruiz-Meana M, Konietzka I, Miró E, Totzeck A, Heusch G, Schulz R, Garcia-Dorado D. (2006) Translocation of connexin 43 to the inner mitochondrial membrane of cardiomyocytes through the heat shock protein 90-dependent TOM pathway and its importance for cardioprotection. *Circ Res.* 99(1):93-101.

Sanches, D. S., Pires, C. G., Fukumasu, H., Cogliati, B., Matsuzaki, P., Chaible, L. M., Torres, L. N., Ferrigno, C. R. A., Dagli, M. L. Z. (2009). Expression of Connexins in Normal and Neoplastic Canine Bone Tissue. *Vet Pathol* 46: 846-859.

Solan, J.L., Lampe, P.D. (2005) Connexin phosphorylation as a regulatory event linked to gap junction channel assembly. *Biochim. Biophys. Acta*. 1711(2):154-63.

Solan JL, Lampe PD. (2009) Connexin43 phosphorylation: structural changes and biological effects. *Biochem J.* 15;419(2):261-72.

Thomas MA, Zosso N, Scerri I, Demaurex N, Chanson M, Staub O. (2003) A tyrosine-based sorting signal is involved in connexin43 stability and gap junction turnover. *J Cell Sci.* 116(Pt 11):2213-22.

Zampighi GA, Planells AM, Lin D, Takemoto D. (2005) Regulation of lens cell-to-cell communication by activation of PKCgamma and disassembly of Cx50 channels. *Invest Ophthalmol Vis Sci.* 46(9):3247-55.

Chapter 4 - Protection of retinal cells from ischemia by a novel gap junction inhibitor

(This chapter has been published in *Biochem Biophys Res Commun.* (2008) 373(4):504-8 having Satyabrata Das, Dingbo Lin, Snehalata Jena, Aibin Shi, Srinivas Battina, Duy H. Hua, Rachel Allbaugh and Dolores J. Takemoto as authors, and reproduced with kind permission from Elsevier.)

4.1. Abstract

Retinal cells which become ischemic will pass apoptotic signal to adjacent cells, resulting in the spread of damage. This occurs through open gap junctions. A class of novel drugs, based on primaquine (PQ), was tested for binding to connexin 43 using simulated docking studies. A novel drug has been synthesized and tested for inhibition of gap junction activity using R28 neuro-retinal cells in culture. Four drugs were initially compared to mefloquine, a known gap junction inhibitor. The drug with optimal inhibitory activity, PQ1, was tested for inhibition and was found to inhibit dye transfer by 70% at 10 ıM. Retinal ischemia was produced in R28 cells using cobalt chloride as a chemical agent. This resulted in activation of caspase-3 which was prevented by PQ1, the gap junction inhibitor. Results demonstrate that novel gap junction inhibitors may provide a means to prevent retinal damage during ischemia.

4.2. Introduction

Retinal ischemia is a major cause of vision loss in various retinal diseases, e.g., diabetic retinopathy, glaucoma, and stroke (Osborne et al., 2004; Kamphuis et al., 2007; Leker and Shohami, 2002). The apoptosis of retinal neurosensory cells, which occurs during ischemia, is thought to be through open gap junctions, propagated by the ‘‘bystander effect” (Farahani et al., 2005).

Gap junctions are hydrophilic channels and/or hemichannels that allow the passage of both necessary metabolites and apoptotic signals from cell to cell (Thompson et al., 2006; Cusato et al., 2003; Lin et al., 1998; Neijssen et al., 2005; Giepmans et al., 2004). The gap junction ‘‘bystander effect” occurs when a dying cell delivers a cellular apoptotic signal such as high Ca^{2+} or ATP to an adjacent cell through open gap junctions which, in turn, causes spread of the death

signal (Farahani et al., 2005). The process is well-documented in brain ischemia (Velaquez et al., 2003; Contreras et al., 2004; Rossi et al., 2007). Retinal ischemia induces retinal cell death in a caspase-dependent manner (Singh et al., 2001).We have previously found that inhibition of gap junctions, in hippocampal HT22 cells, prevents oxidative cell death due to H_2O_2 through a caspase-3 pathway (Lin, D and Takemoto, 2007). It is apparent that proper control of gap junctions is essential for neural cell survival (de Pina-Benabou et al., 2005).

In the current study, we used cobalt chloride ($CoCl_2$) to induce a chemical hypoxia/ischemia condition in a rat retinal neurosensory cell line, R28. $CoCl_2$ has been shown to induce oxidative damage through the generation of reactive oxygen species (ROS) in a wide variety of cells (Guo et al., 2006) and has been recently reported to cause degeneration of mammalian retinal photoreceptor cells (Haraa et al., 2006). R28 cells offer a well-characterized population of precursors to multiple neuroretinal cell types to investigate ischemia-induced apoptosis.

In this study we determined the efficacy of a novel group of gap junction inhibitors which are based on primaquines. Previously the anti-malarial chloroquine drugs, such as mefloquine, have been reported to be potent inhibitors of the gap junction protein, Cx50 (Srinivas et al., 2005; Cruikshank et al., 2004). Based on simulated docking studies using this class of substituted quinolines, several structures were found to dock into the channel pore of Cx43. These drugs were synthesized and tested. The results suggest a novel class of gap junction inhibitors which can be used to prevent neural and retinal cell damage due to ischemia.

4.3. Materials and methods

4.3.1. Cell cultures

The rat retinal neurosensory R28 cells were cultured in DMEM (low glucose) (Invitrogen, CA) supplemented with 10% fetal bovine serum and 50 μg/ml gentamicin, 50 U/ml penicillin, 50 μg/ml streptomycin, pH 7.4, at 37^0 C in an atmosphere of 95% air and 5% CO_2.

4.3.2. Design and synthesis of primaquine-1 (PQ1).

In search of new inhibitors that inhibit gap junction intercellular communication (GJIC), we examined potential interactions of a number of substituted quinolines (code name PQs) with the partial crystal structure of the Cx43 hemichannel (Veenstra, 2003; Zucker and Nicholson,

2002) using Autodock computational docking software (Goodsell and Olson, 1990; Morris et al., 1996; Morris et al., 1998). In one of the minimum energy (-0.7 kcal/mol) bound structures, interactions (close contacts) between CF3 group of PQ1 and H–N of Leu144 of connexin (2.5 Å), OCH3 group of PQ1 and CH_2 of Phe81 of connexin (2.0 Å), and 3+ of PQ1 and $^{-}$O2C–Glu 146 of connexin were found. Consequently, we synthesized this class of quinolines and determined their ability to inhibit gap junction dye transfer. PQ1 was synthesized via a modification of the reported protocol (LaMontagne et al., 1982; LaMontagne et al., 1982; Lauer et al., 1946) starting from 4-acetaminoanisole. The detailed synthesis is described in Ref. Shi et al., 2008.

4.3.3. Cobalt chloride ($CoCl_2$) treatment-a chemical hypoxia model in R28 cells

Approximately 70% confluent retinal R28 cells were pre-incubated with PQ1 (10 μM, 40 min), followed by $CoCl_2$ treatments at 100, 200 and 500 μM for different time periods in a cell culture chamber (5% CO_2, room air, 37^0 C). Hypoxia induction was confirmed by testing the hypoxia-inducible factor 1-α (HIF1α) protein expression levels in nuclear extracts by Western blotting.

4.3.4. Gap junction activity assay

R28 cells were grown to 90% confluency on coverslips. They were treated with PQ1 at 10 μM for 40 min. A mixture of 1% each, in PBS, Lucifer yellow (LY) and Rhodamine Dextran (RD) (Molecular Probes, Eugene, OR) were added to the cells at the center of the coverslip. Two cuts across the coverslip were made to form a transient tear in the plasma membranes of the cells to permit dye entry into cells. Cells were incubated with 2.5 ll of both of the dyes for 20 min, then fixed in 2.5% paraformaldehyde, washed in PBS and examined by fluorescent microscopy using a Nikon C1 confocal microscope. For quantitation, the extent of dye transfer was calculated by counting the number of LY-labeled cells from the initial scrape with subtraction of RD-labeled cells, as a cell damage control, in the microscopic field. Four points per slide were photographed as previously described (Lin and Takemoto, 2005). The experiments were repeated six times, and data are means ±SEM.

4.3.5. Nuclear extracts

Following treatments with PQ1 and/or $CoCl_2$, R28 cells were scraped into cold phosphate-buffered saline, centrifuged and washed once in five packed cell volume equivalents of buffer A (10 mM Tris–HCl (pH 7.5), 1.5 mM $MgCl_2$, 10mM KCl) freshly supplemented with 0.5 mM dithiothreitol, 1mM sodium orthovanadate, 0.4 mM phenylmethylsulfonyl fluoride, and 10 μl/ ml of protease inhibitor cocktail (Sigma # P8340). Cell pellets were resuspended in 2.5 packed cell volume equivalents of buffer A and incubated in a pre-chilled Dounce homogenizer on ice for 10 min followed by homogenization by 20 strokes with a type B pestle (Aminova et al., 2005; Wang and Semenza, 1995). Nuclei were pelleted by centrifugation at 10,000g for 10 min, the supernatant was discarded and nuclei were resuspended in 3.5 packed nuclear equivalent volumes of buffer B (20 mM Tris–HCl (pH 7.5), 1.5 mM $MgCl_2$, 0.42 M KCl, 20% (v/v) glycerol) freshly supplemented with 2 mM DTT, 1mM sodium orthovanadate, 0.4 mM phenylmethylsulfonyl fluoride, and 10 μl/ ml of protease inhibitor cocktail. The suspension was rotated at 4^0 C for 30 min and centrifuged for 30 min at 14,000 rpm. The eluted nuclear proteins in the supernatant were collected and HIF1a protein levels were measured by Western blotting.

4.3.6. Western blot

Western blotting was performed as described previously (Lin and Takemoto, 2005). Anti-Cx43 was purchased from Fred Hutchinson cancer research center (#Cx43NT1), anti-HIF1α was purchased from Novus Biologicals (# NB100-105), and anti-caspase-3 (# 9661), phosphoCx43 (Ser368) (#3511S) were purchased from Cell Signaling Technology and anti-β-actin was purchased from Sigma (# A5441).

4.3.7. Apoptosis assay

Approximately 70% confluent R28 Cells in 25 cm^2 flasks were treated with PQ1 at 10 μM for 40 min followed by treatment with 500 μM $CoCl_2$ for different time periods to induce apoptosis. After this, cells were harvested and stained with Annexin V-FITC and propidium iodide (PI) according to the manu-facturer's protocol (BioVision # K101-100). Annexin V-FITC/PI binding was analyzed by flow cytometry using a BD FACSCalibur system and data was analyzed using the CellQuest software.

4.3.8. Statistical analyses

All analyses represent at least triplicate experiments. The statistical analysis employed in this paper is the Student's t-test. The level of significance (*) was considered at $p < 0.05$. All data are means ±SEM.

4.4. Results and discussion

4.4.1. Docking and synthesis of primaquine 1 (PQ1)

Since selective inhibition of gap junction intercellular communication with small molecules may potentially prevent cells from death during ischemic stroke, we used computational docking methods to search for chemicals that bind to the Cx43 gap junction hemichannel, based upon the partial crystal structure. After screening several classes of molecules, we focused on substituted quinolines based on their relative binding constants and bioactivities. Primaquine 1 (PQ1) analogs were synthesized via a modification of the reported protocol (LaMontagne et al., 1982; LaMontagne et al., 1982; Lauer et al., 1946) starting from 4-acetaminoanisole (Lauer et al., 1946). The succinic acid salt of PQ1 (structure shown in Fig. 4.1A) was prepared to provide water-soluble material for biological evaluation. Succinic acid alone does not show bioactivities.

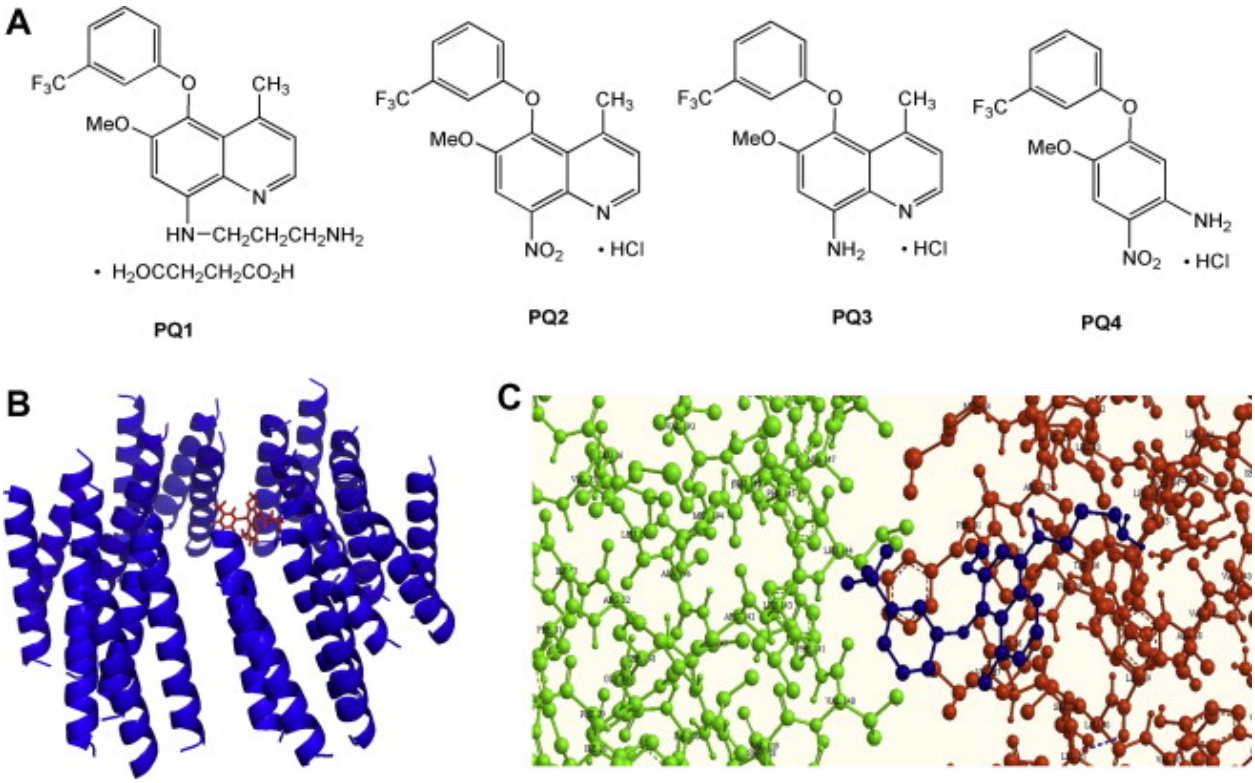

Figure 4.1Molecular formulas of PQs and computational docking. (A) PQ analogs were synthesized via a modification of the reported protocol (LaMontagne et al., 1982; Lauer et al., 1946). The succinic acid salt of PQ1 was prepared to provide water-soluble material for biological evaluation. HCl salts of PQ2, 3, and 4 were also made and they are soluble in water. Succinic acid alone does not show bioactivities. (B) Computational docking of gap junction hemichannel (the hexameric connexin is marked in blue) and PQ1 (marked in red). (C) Interactions between PQ1 (marked in blue) and two helical bundles of a connexin protein (marked in green and orange). (Synthesis and Docking studies of PQ compounds were done in Dr. Duy H. Hua's lab in the Dept. of Chemistry, KSU by S. Battina and A. Shi)

The interaction between the NH_3^+ group (under physiological conditions, N50-amino function of PQ1 exists as protonated form) of PQ1 with the carboxylate ion (negatively charged) of Glu 146 of the Cx43 may be significant. Docking studies are shown in Fig. 4.1B and C.

4.4.2. PQ1 inhibits gap junction activity in retinal R28 cells with similar efficacy when compared to mefloquine

During the synthesis of PQ1 several intermediates were tested and compared to mefloquine, a known gap junction inhibitor (Srinivas et al., 2005; Cruikshank et al., 2004). Gap junction dye transfer of Lucifer yellow was measured and results are shown in Fig. 4.2A and B. At 10 μM for 40 min, mefloquine (MQ) inhibited dye transfer by approximately 50% while PQ1, at the same dose inhibited dye transfer by 70%. The intermediates, PQ2 and PQ3 had poor inhibitory activity while PQ4 was similar to MQ. Since PQ1 had the greatest inhibitory activity and was water-soluble, this drug was further tested for protection from ischemia-induced apoptosis.

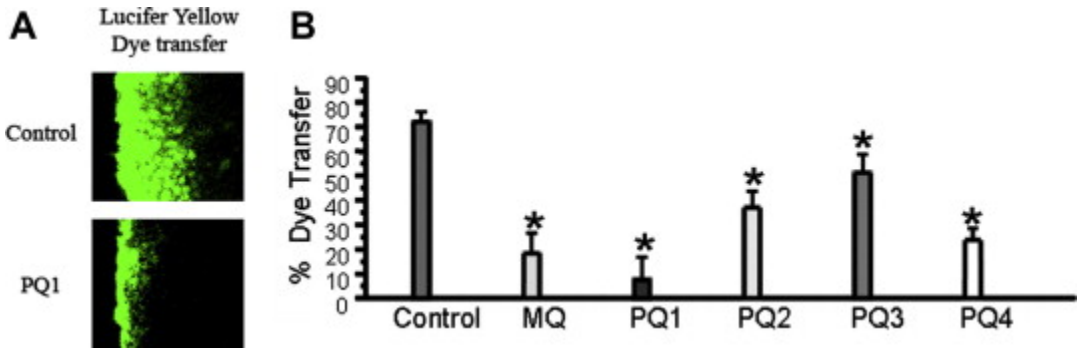

Figure 4.2 PQ1 inhibition of gap junction dye transfer activity in retinal neurosensory R28 cells in culture. R28 cells were grown in 6-well plates with coverslips. When cells reached 90% confluency, gap junction dye transfer activity was performed as described in Materials and methods. (A) The transfer of Lucifer yellow dye in the control and PQ1 treated cells. (B) Bar graph of percentage dye transfer in R28 cells after treatment with the different PQs and Mefloquine (MQ). Application of PQ1 significantly (*) inhibited gap junction activity. (Cell culture was done by Snehalata Jena and experiment performed by Dingbo Lin and Satyabrata Das)

4.4.3. PQ1 protects R28 cells from ischemic apoptosis induced by cobalt chloride ($CoCl_2$)

Next, we determined whether PQ1 inhibition of gap junctions could prevent retinal neurosensory R28 cells from apoptosis using a chemical ($CoCl_2$)-induced ischemia system as our model. As shown in Fig. 4.3A, $CoCl_2$ incubation at 500 μM for 24 h induced activation of

caspase-3. Pre-incubation of R28 cells with PQ1 at 10 μM for 40 min followed by co-incubation with $CoCl_2$ for additional 24 h blocked the activation of caspase-3 substantially. $CoCl_2$ at 500 μM caused stabilization of HIF1α in the nuclear extracts and this stabilization started as early as three hours after treatment (Fig. 4.3B). This confirmed induction of hypoxia. PQ1 alone did not cause activation or stabilization of caspase-3 or HIF1α, respectively. PQ1, $CoCl_2$ or a combination of both did not cause any change in the Cx43 gap junction protein levels or phosphorylation of Cx43 at residue ser368. Activation of caspase-3 and stabilization of HIF1α indicates hypoxia-induced apoptosis in $CoCl_2$ treated cells. Pre-treatment with PQ1 was able to prevent the activation of caspase-3 by $CoCl_2$.

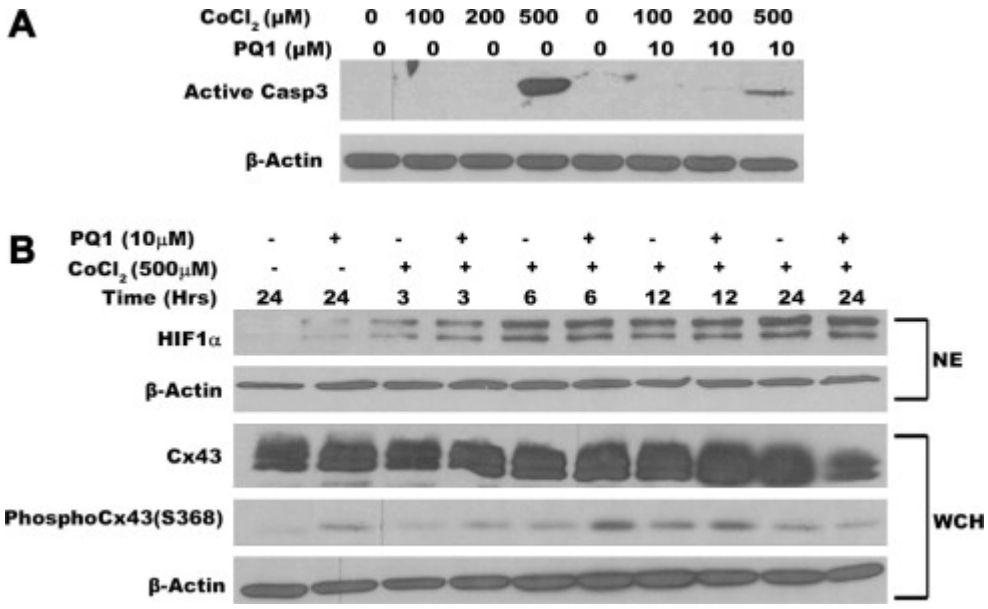

Figure 4.3 Protection of PQ1 from $CoCl_2$-induced hypoxia in R28 cells. (A) About 70% confluent retinal R28 cells were treated with 100, 200 and 500 μM $CoCl_2$ for 24 h with or without the pre-treatment of PQ1 (10 μM, 40 min) in a cell culture chamber (5% CO_2, room air, 37 °C). Caspase-3 activation was determined by Western blotting in whole cell homogenates (WCH). (B) HIF1α stabilization was measured in the nuclear extracts (NE) after treatment with 500 μM $CoCl_2$ at different time intervals with or without the pre-treatment of PQ1. $CoCl_2$ treatment stabilized HIF1α levels in the NE as early as after 3 h; PQ1 alone did not have any effect on HIF1α stabilization even after 24 h. Levels of Cx43 and phosphoCx43-Ser368 are measured in WCH. β-Actin is used as a loading control.

To confirm apoptosis, Annexin V-FITC/PI staining of cells was done. The early apoptotic stage is characterized by the cell membrane exposure of phosphatidylserine normally restricted to the inner cell membrane, which is recognized by Annexin V-FITC. The later phase of apoptosis is assessed by measuring the DNA labeling with the PI, an indicator of the cell membrane permeabilization. Once again, $CoCl_2$ at 500 μM for 24 h was found to cause significant apoptosis (Fig. 4.4A & B). Pre-treatment of R28 cells with 10 μM PQ1 for 40 min followed by incubation with $CoCl_2$ at 500 μM protected the cells significantly from undergoing apoptosis (Fig. 4.4). Treatment of cells only with 10 μM PQ1 did not cause any damage to the cells even after 36 h (Fig. 4.4C).

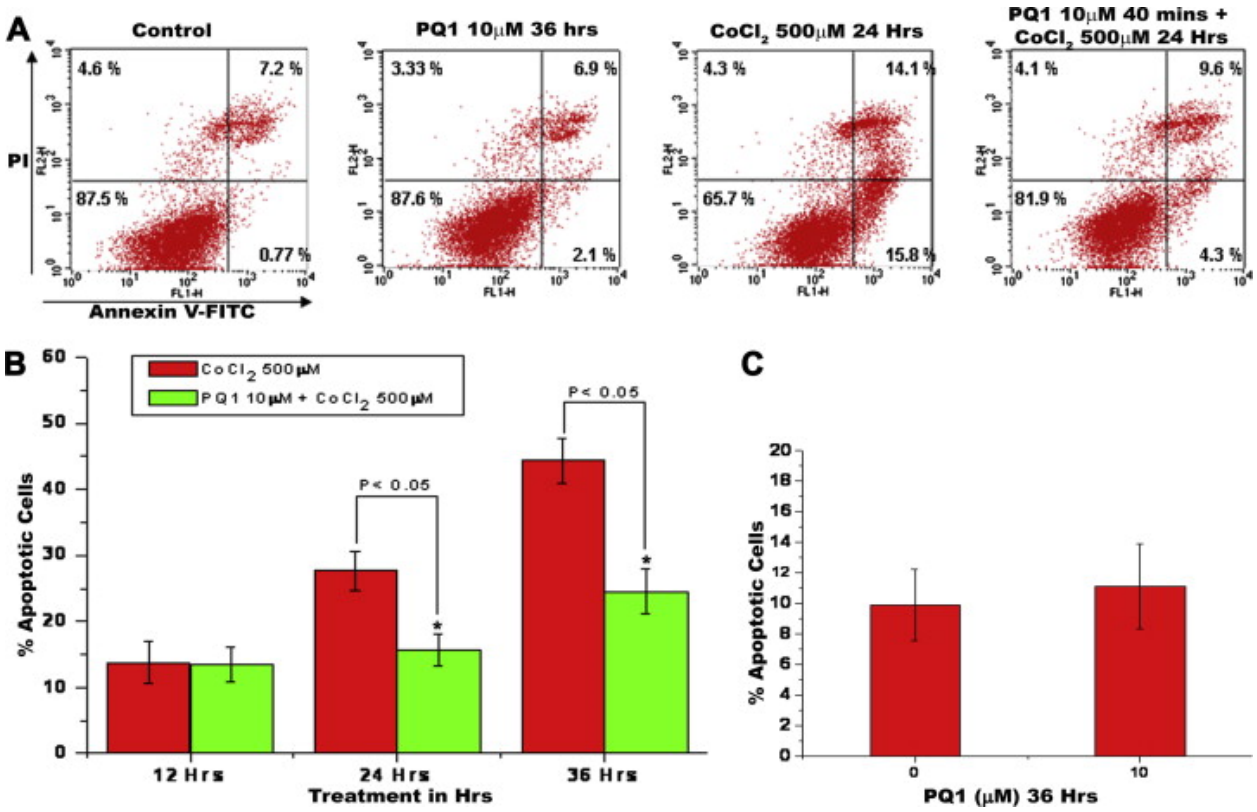

Figure 4.4 Apoptotis assay using the Annexin V-FITC Kit. (A) Representative flow cytometer images of R28 cells with different treatments of PQ1 and/or $CoCl_2$. The *y*-axis quantifies the number of cells stained with propidium iodine and the *x*-axis quantifies number of cells stained with Annexin V-FITC. (B,C) Histogram of % apoptotic cells after treatment with $CoCl_2$ and PQ1. The percentage of apoptotic cells represents cells that are Annexin V-FITC positive and both propidium iodide and Annexin V-FITC positive after different time periods.

These data suggest that inhibition of gap junctions by PQ1 protects cells from $CoCl_2$-induced ischemic apoptosis. This class of drugs could provide a novel method to prevent the damage which is known to occur during ischemic insult. There are very few known gap junction inhibitors. PQ1 is shown herein to be an excellent gap junction inhibitor which is not toxic and prevents retinal cell apoptosis.

4.5. References

Aminova, L.R., Chavez, J.C., Lee, J., Ryu, H., Kung, A., LaManna, J.C., Ratan, R.R. (2005) Prosurvival and prodeath effects of hypoxia-inducible factor-1(stabilization in a murine hippocampal cell line, *J. Biol. Chem*. 280 (5):3996–4003.

Contreras, J., Sanchez, H., Veliz, L., Bukauskas, F., Bennett, M., Saez, J., (2004) Role of connexin-based gap junctional channels and hemichannels in ischemia-induced cell death in nervous tissue, *Brain Res. Rev*. 47:290–303.

Cruikshank, S.J., Hopperstad, M. Younger, M., Connors, B.W., Spray, D.C., Srinivas, M. (2004) Potent block of Cx36 and Cx50 gap junction channels by mefloquine, *Proc. Natl. Acad. Sci*. USA 101 (33):12364–12369.

Cusato, K., Bosco, A., Rozental, R., Guimaraes, C.A., Reese, B.E., Linden, R., Spray, D.C. (2003) Gap junctions mediate bystander cell death in developing retina, *J. Neurosci*. 23:6413–6422.

de Pina-Benabou, M.H., Szostak, V., Kyrozis, A., Rempe, D., Uziel, D., Urban-Maldonado, M., Benabou, S., Spray, D.C., Federoff, H.J., Stanton, P.K., Rozental, R., (2005) Blockade of gap junctions in vivo provides neuroprotection after perinatal global ischemia, *Stroke* 36:2232–2237.

Farahani, R., Pina-Benabou, M.H., Kyrozis, A., Siddiq, A., Barradas, P.C., Chiu, F.C., Cavalcante, L.A., Lai, J.C., Stanton, P.K., Rozental, R. (2005) Alterations in metabolism and gap junction expression may determine the role of astrocytes as ‘‘good samaritans” or executioners, *Glia* 50:351–361.

Giepmans,B.N. (2004) Gap junctions and connexin-interacting proteins, *Cardiovasc. Res*. 62 (2) :233–245.

Goodsell, S.D., Olson, J.A., (1990) Automated docking of substrates to proteins by simulated annealing, *Proteins* 8:95–202.

Guo, M., Song, L.P., Jiang, Y., Liu, W., Yu, Y., Chen, G.Q. (2006) Hypoxia-mimetic agents desferrioxamine and cobalt chloride induce leukemic cell apoptosis through different hypoxia-inducible factor-1 a independent mechanisms, *Apoptosis* 11:67–77.

Haraa, A., Niwab, M., Aokie, H., Kumadad, M., Kunisadae, T. Oyamaa, T. Yamamotod, T., Kozawab, O., Moria, H. (2006) A new model of retinal photoreceptor cell degeneration induced by a chemical hypoxia-mimicking agent, cobalt chloride, *Brain Res*. 1109:192–200.

Kamphuis, W., Dijk, F., Bergen, A.A. (2007) Ischemic preconditioning alters the pattern of gene expression changes in response to full retinal ischemia, *Mol. Vis*. 13:1892–1901.

LaMontagne, M.P., Blumbergs, P., Strube, R.E. (1982) Antimalarials. 14. 5-(aryloxy)-4-methylprimaquine analogues. A highly effective series of blood and tissue schizonticidal agents, *J. Med. Chem*. 25 (9):1094–1097.

LaMontagne, M.P., Markovac, A., Khan, M.S. (1982) Antimalarials. 13. 5-Alkoxy analogues of 4-methylprimaquine, *J. Med. Chem*. 25 (8): 964–968.

Lauer, W.M., Rondestvedt, C., Arnold, R.T., Drake, N.L., Hook, J.V., Tinker, J. (1946) Some derivatives of 8-aminoquinoline, *J. Am. Chem. Soc*. 68:1546–1548.

Leker, R.R. Shohami, E. (2002) Cerebral ischemia and trauma-different etiologies yet similar mechanisms:neuroprotective opportunities, *Brain Res. Rev*. 39:55–73.

Lin, D., D.J. Takemoto, D.J. (2007) Protection from ataxia-linked apoptosis by gap junction inhibitors, *Biochem. Biophys. Res. Commun*. 362 (4): 982–987.

Lin, D., Takemoto, D.J. (2005) Oxidative activation of protein kinase Cgamma through the C1 domain. Effects on gap junctions, *J. Biol. Chem*. 280:13682– 13693.

Lin, J.H., Weigel, H., Cotrina, M.L., Liu, S., Bueno, E., Hansen, A.J., Hansen,T., Goldman, W.S., Nedergaard, M. (1998) Gap-junction-mediated propagation and amplification of cell injury, *Nat. Neurosci*. 1:494–500.

Morris, G.M., Goodsell, D.S., Halliday, R.S., Huey, R., Hart, W.E., Belew, R.K., Olson, A.J. (1998) Automated docking using a Lamarckian genetic algorithm and an empirical binding free energy function, *J. Comp. Chem*. 19:1639–1662.

Morris, G.M., Goodsell, D.S., Huey, R., Olson, A.J. (1996) Distributed automated docking of flexible ligands to proteins: parallel applications of AutoDock 2.4, *J. Comput. Aided Mol. Des*. 10 (4): 293–304.

Neijssen, J., Herberts,C., Drijfhout, J.W., Reits, E., Janssen, L., Neefjes, J. (2005) Cross-presentation by intercellular peptide transfer through gap junctions, *Nature* 43483–88.

Osborne, N.N., Casson, R.J., Wood, J.P., Chidlow, G., Graham, M., Melena, J. (2004) Retinal ischemia: mechanisms of damage and potential therapeutic strategies, *Prog. Retin. Eye Res*. 23: 91–147.

Rossi, D.J., Brady, J.D., Mohr, C. (2007) Astrocyte metabolism and signaling during brain ischemia, *Nat. Neurosci*. 10:1377–1386.

Shi, A., Nguyen, T., Battina, S., Rana, S., Takemoto, D.J., Chiang, P., Hua, D.H., (2008) Synthesis and anti-breast cancer activities of substituted quinolines, *Bioorg. Med. Chem. Lett*. 18:3364–3368.

Singh, M., Savitz, S.I., Hoque, R., Gupta, G., Roth, S., Rosenbaum, P.S., Rosenbaum, D.M. (2001) Cell-specific caspase expression by different neuronal phenotypes in transient retinal ischemia, *J. Neurochem*. 77:466– 475.

Srinivas, M., Kronengold, J., Bukauskas, F.F., Bargiello, T.A., Verselis, V.K. (2005) Correlative studies of gating in Cx46 and Cx50 hemichannels and gap junction channels, *Biophys. J*. 88 (3):1725–1739.

Thompson, R.J., Zhou,N., MacVicar, B.A. (2006) Ischemia opens neuronal gap junction hemichannels, *Science* 312:924–927.

Veenstra, D.R., (2003) Gap junction channel structure, *Recent Res. Devel. Biophys*. 2:65–94.

Velaquez, J., Frantseva, M., Naus, C. (2003) Gap junctions and neuronal injury: Protectants or executioners, *Neuroscientist* 95–9.

Wang, G.L., Semenza, G.L. (1995) Purification and characterization of hypoxia-inducible factor 1, *J. Biol. Chem*. 270 (3):1230–1237.

Zucker, S.N., Nicholson, B.J., (2002) Mutagenic approaches to modifying gap junction phenotype, *Curr. Drug Targets* 3:441–453.

Chapter 5 - Conclusions and Future Directions

The avascular lens tissue depends on an internal circulatory system to convect nutrients and carry out waste products, to and from the inner fiber cells respectively. Gap junctions are a critical component of this circulation system. The connexin proteins have a very high turn over rate, having half-lives less than 5 h, which helps in maintaining a balance and replacing the degraded gap junction channels. But in the lens core, the fiber cells have lost the ability to synthesize new proteins, so proper regulation of the gap junctions is even more important to maintain the lens homeostasis. PKCγ has been associated with the regulation of gap junction intercellular communication via phosphorylation of the connexins expressed in the lens. The first part of our study using the PKCγ KO mouse-model provided evidence that in the absence of PKCγ there is increased gap junction channel conductance both in the DF and MF suggesting the involvement of PKCγ in the regulation of gap junction channels. Detection of significantly reduced phosphorylation on serine residues in Cx43 and Cx46 indicates that the regulation is phosphorylation-mediated.

The involvement of PKCγ phosphorylation-mediated loss of Cx43 expression in the fiber cells was validated as Cx43 persisted into the DF in the absence of PKCγ KO lenses. Another reason for the expression of Cx43 in the DF could be the presence of nuclei in the KO lenses. Probably the synthesis of Cx43 is still continued and the expression of Cx43 is not lost in the DF even though they are undergoing degradation. Overexpression of Cx46 in cultured rabbit lens epithelial cells (N/N 1003A) has been found to intitiate the ubiquitinylation and eventual degradation of Cx43. In the current study, we found that inhibition of the proteasomal pathway in HLECs led to the accumulation of the Cx43 proteins and the TPA-mediated increase in Cx46 protein level did not happen in the presence of proteasome inhibitor. So, we hypothesize that the amounts of Cx43 and Cx46 proteins have a regulating effect on each other. The persistence of the extra Cx43 in the KO lense DF could therefore mediate an increased differentiation-dependent cleavage of the Cx46 resulting in the accumulation of the clipped versions of Cx46 detected in the KO lenses. This possibility of the regulatory effect of Cx43 and Cx46 protein levels on each other could be further pursued by knocking down the Cx43 protein level using Cx43-specific siRNA in HLECs and checking its effect on Cx46 protein level, and a similar experiment using Cx46-specific siRNA and checking its effect on Cx43 protein level.

Cx46 protein expression has been reported in the unusual tissues like the lens, cancer, ischemic and damaged tissue. This localization is concomitant with the specialized function of Cx46 in the lens. A low-sensitivity to change in pH and the ability to modulate gap junction activity upon formation of heterotypic channels enables the proliferation of intercellular communication despite the highly hypoxic and acidic conditions at the interior of the lens. This special ability may indicate that Cx46 bolsters cell survival in adverse microenvironments. Along with the up-regulation of Cx46 in response to the tumor-promoter TPA treatment reported in this study, up-regulation of Cx46 has also been observed in response to hypoxia in cultured lens epithelial cells in our lab. These observations indicate the up-regulation of Cx46 in stress conditions. TPA has been reported to cause up-regulation of Cx26 in a PKC-mediated manner. The involvement of PKC in the up-regulation of Cx46 observed in our study can be verified by using pharmacological PKC-inhibitors along with TPA.

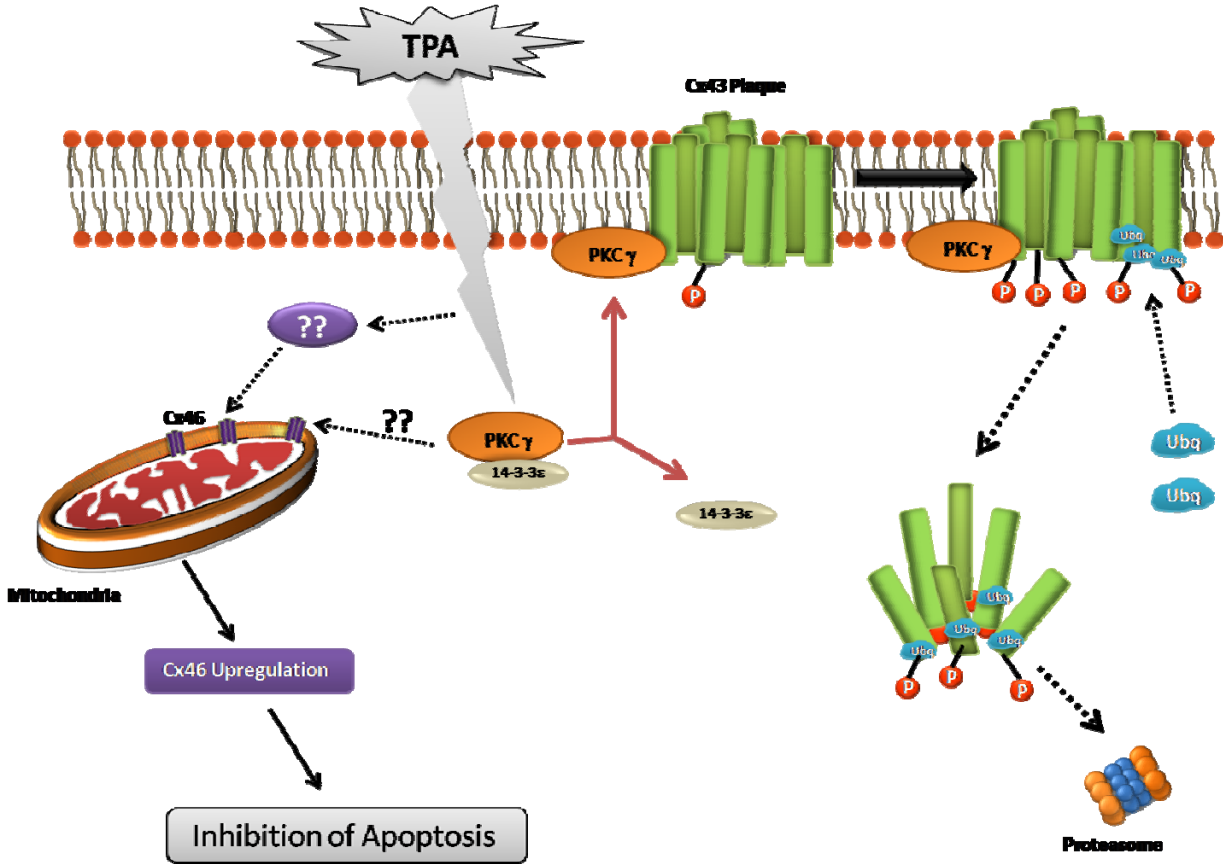

Figure 5.1 Model of antagonistic regulation of Cx43 and Cx46 by TPA treatment in HLECs. TPA-mediated activation of PKCγ leads to the phosphorylation, ubiquitination and subsequent proteasomal degradation of Cx43. Whereas TPA treatment leads to Cx46 up-

regulation by a PKC-mediated or other modulator-mediated way in the mitochondria which according to our hypothesis inhibits apoptosis.

While phorbol esters are capable of promoting motogenic or survival responses, many cell types undergo growth arrest or apoptosis in response to TPA-mediated PKC activation. Cx46 has not been reported to have non-gap junctional activity, so our suggested localization of Cx46 to the mitochondria would help reveal some novel functions for Cx46 when futher pursued. We hypothesize that the possible presence of Cx46 in the mitochondria has an anti-apoptotic/pro-survival activity in response to the TPA-induced stress which prevents the cells from undergoing apoptosis and once the effect of TPA subsides the Cx46 goes back to normal levels. In a broader sense, the finding of non-junctional activity of Cx46 would open a new area of study which would help explain the role of Cx46 in tumor tissue. Figure 5.1 summarizes our findings and hypothesis in HLECs.

Appendix A - Model of Gap Junction Coupling

"In spherically symmetric syncytial tissue, equations for radial current flow were derived by Eisenberg et al. (Eisenberg et al., 1979 in Chapter-1 References) and modified by Mathias et al. (Mathias et al., 1991 in Chapter-1 References). At sinusoidal frequencies approaching 1 kHz, the induced intracellular and extracellular voltages become nearly identical and are given by V = IR_s, where I is the injected current and R_s (Ω) is the cumulative series resistance between the point of voltage recording (*r* cm from the center), and the lens surface (*a* cm from the center). R_s is directly proportional to the parallel resistivity of the intracellular and extracellular compartments (R_P Ωcm).

$$R_S = \frac{1}{4\pi}\int_r^a \frac{R_P}{\rho^2}\,d\rho$$

$$R_P = \frac{R_i R_e}{R_i + R_e} \qquad (1)$$

The effective intracellular resistivity, R_i, is due mainly to the gap junctional coupling resistance whereas the effective extracellular resistivity, R_e, depends on the tortuosity and volume fraction of small extracellular clefts. In normal physiological conditions, R_e is much higher than R_i, therefore $R_P \approx R_i$. For simplicity and lack of contrary data, we assume that R_e is uniform, whereas we have measured that R_i changes at the DF to MF transition (defined as *r* = *b*). Integrating Eq. 1 gives:

$$R_S = \frac{R_{DF}}{4\pi}\left(\frac{1}{r} - \frac{1}{a}\right) \qquad b \le r \le a \qquad (2)$$

$$R_S = \frac{R_{DF}}{4\pi}\left(\frac{1}{b} - \frac{1}{a}\right) + \frac{R_{MF}}{4\pi}\left(\frac{1}{r} - \frac{1}{b}\right) \qquad r \le b \qquad (3)$$

where R_{DF} is R_i in DF and R_{MF} is R_i in MF. Eq 2 or 3 was curve fit to the R_S data to obtain values of R_{DF} and R_{MF}. Fiber cells are approximately 3 μm wide, so the coupling conductance per area of cell to cell contact was calculated as $1/(3\text{x}10^{-4}R_i)$."

[This model is quoted from Wang et al., 2009 (See References in Chapter-2)]

Appendix B - Supplemental Data for Chapter 3

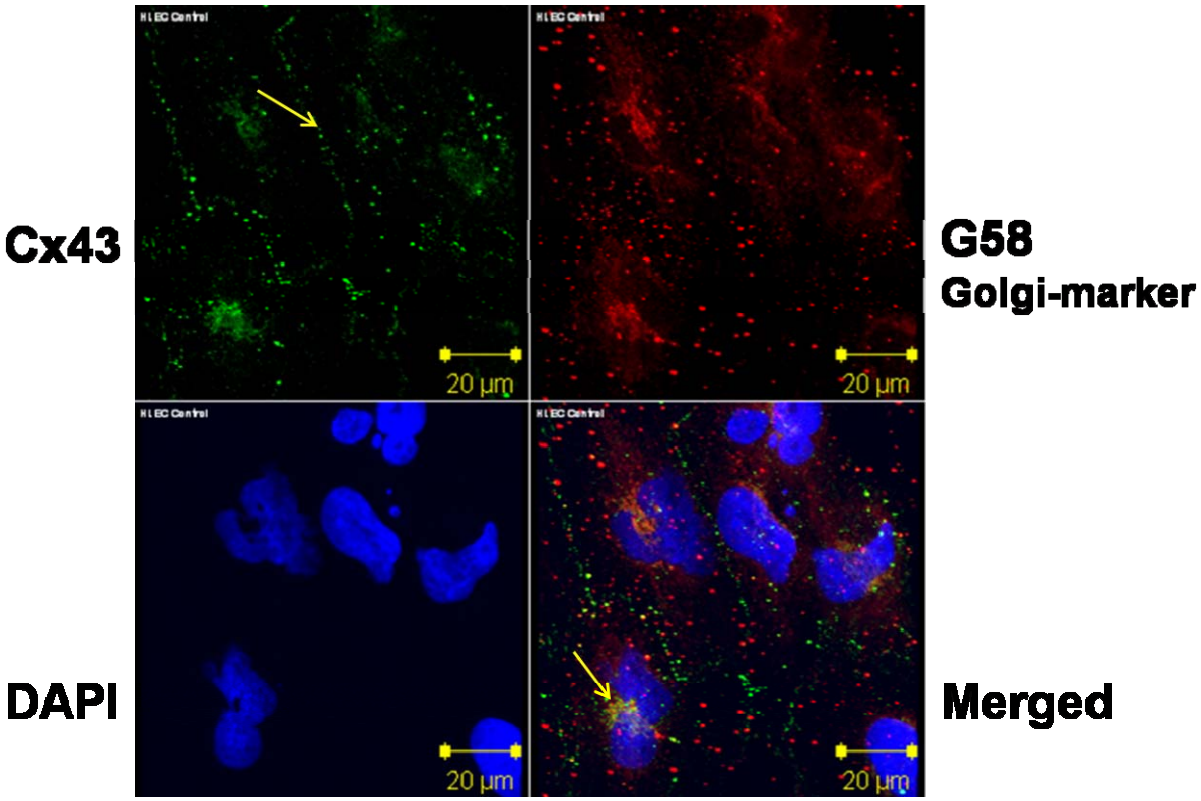

Figure S 1 Localization of Cx43 in HLECs. Control HLECs were immunostained with anti-Cx43 antibody (green, upper left panel) and anti-G58 (red, red upper right panel), a golgi-marker protein. DAPI (blue) was used to stain the nuclei. Cx43 was mainly detected as plaques (arrow in upper left panel) localized in the apposed membranes, whereas a cytosolic perinuclear distribution was also observed. The perinuclear stained Cx43 co-localized with the golgi-marker G58 staining (arrow in lower right panel) suggesting presence in the golgi-complex.

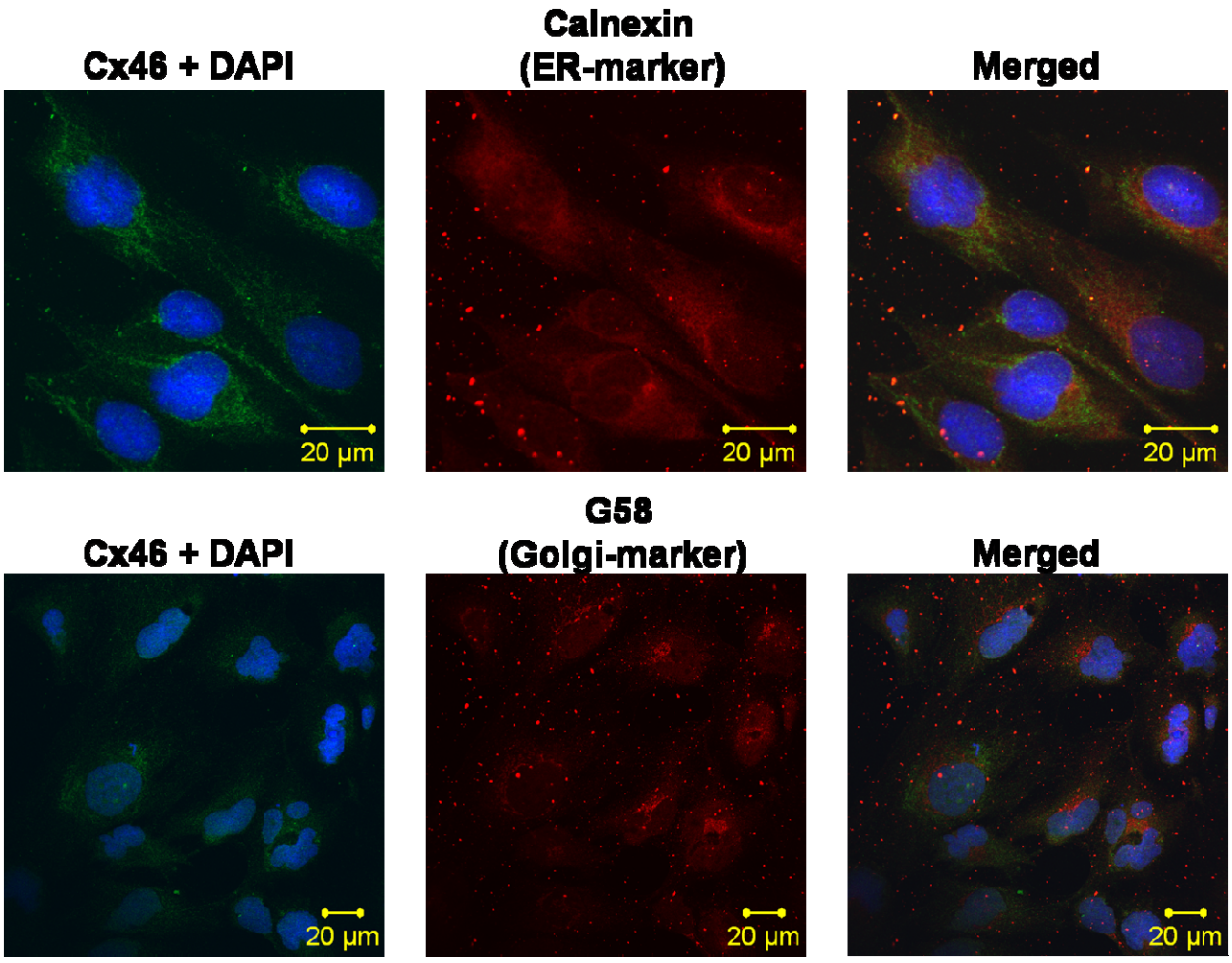

Figure S 2 Co-localization of Cx46 with endoplasmic reticulum (ER) and Golgi-complex marker proteins. Control HLECs were immunostained with anti-Cx46 antibody (green, upper and lower left panels) and anti-Calnexin (red, upper middle panel), an ER-marker protein or anti-G58 (red, lower middle panel), a golgi-marker protein. DAPI (blue) was used to stain the nuclei. Co-localization of Cx46 and Calnexin was not observed in the merged image (Upper-right panel). Similarly, Cx46 also did not co-localize with golgi-complex stained with golgi-marker protein G58 in the merged image (Lower right panel).